THE DRAG RESISTANCE OF BURNING DROPS

by

Swaminath Adi Arunachalam, B.Sc., (Fuel Tech.)(Banaras)
M. Tech.(Kharagpur)

Thesis submitted for Degree of
Doctor of Philosophy
in the Faculty of Engineering
of the University of London

Department of Chemical Engineering,
Imperial College,
London.

January, 1965.

ADDENDA AND ERRATA

Page No.		
iii	line 13	delete 'was', insert 'were'.
vi	IV.1.3	delete 'wake', insert 'side'.
vi	IV.2.2	delete 'in', insert 'on'.
viii	III.13	read .... 'schematic .....'
1	line 9	read .... 'accuracy'
13	line 1	read '..... $(80 < Re < 400)$'.
21	Fig. II.2	reverse 'ignited' and 'unignited'.
24	Bottom curve, fig. II.3:	$a = 91$ cm/sec^2.
30	Eqn. 2.2.1	read '.... $\frac{dm}{dt} = \frac{2k\pi d}{L}(T_g - T_s)$ '.
33	after eqn. 2.2.4. read	$\phi = \frac{\ln\left[1 + \frac{C(T_g - T_s)}{L}\right]}{C/L\ (T_g - T_s)}$
33	eqn. 2.2.5.	delete ' .... 2 ....'
37	line 20.	reference number for Bird is 36.
40	Fig. II.7	curves 1,2 correspond to left hand ordinate, and 3 to right hand ordinate.
41	after full stop in 4th line insert:	'The modified transfer number, B', of these two figures is related to the transfer number as shown in fig. II.7 '.
46	eqn. 2.3.1.	read - " $T_f - T_g = \frac{D\,\rho_{O_2}\,H\,p_{O_2}}{k\,r'\,P}$
49	in eqn. 2.3.5.	replace ' $m'_{O_2 g}$ ' by ' $m''_{O_2 g}$ '
82	line 15	read '..... ineffective with regard ....'
87	line 16	read '.... can receive an iris diaphragm ....'
94	line 10	replace 'adopted' by 'adapted'
98	line 7	delete 'the image of'
98	line 8	replace 'higher' by 'lower'
108	line 14	delete ' ... system'.
135	line 17	read 'drag coefficient'.
136	line 6	delete 'Spalding 3'.
136	line 16	delete '3'
150	line 6	replace ' C'_d ' by ' C'_{dm} '

Page No.

155		omit clause 2a.
156	5a	omit, '.... the low surface tension of the fuels' insert, ' the fuels wetted the outer wall of the capillary'
x	Symbols.	To the footnote on asterisks add "the dimensions of heat are ML^2/T^2.
xi	after line 11, insert	m''_{O_2} = mass fraction, dimensionless.
xiii	The dimensions for surface tension are M/T^2.	

ABSTRACT

An experimental study has been made of the drag resistance of burning drops.

Distance-time records of single freely falling drops of iso-pentane n-heptane and benzene, burning in cold, 100% oxygen atmospheres, were obtained. The records were obtained by a specially designed photographic technique and a technique for the measurement of time intervals between successive flashes of the repetitive flashing equipment. The drag coefficients and Reynolds numbers were obtained from the distance-time records by using a computer.

Experiments were conducted, mostly for drops < 2 mm. in size and in the Reynolds number range 90 to 300. The drop could support two types of flames, i.e. side flames and envelope flames. The drag coefficients for all fuels with side flames was less than the standard drag coefficient. The coefficients with envelope flames were higher than the standard value on the basis of approach properties, but were well below the standard value on the basis of the mean properties for the vicinity of the drop. The ratio of coefficients with and without combustion decreased with decreasing Reynolds numbers. It is believed that for burning drops, the effect of evaporation, which tends to decrease drag resistance, and the effect of increased temperatures, which increase the viscous forces, nearly cancel each other out in the experimental region studied.

ACKNOWLEDGEMENTS

The author wishes to thank Dr. P. Eisenklam for his invaluable guidance and supervision throughout this work.

The author also wishes to gratefully acknowledge the help of Dr. N. Dombrowski and Mr. Tyley of the electronics workshop in the development of the experimental technique. The kind help of Mr. J. Weston and Miss P.E. Taylor in the preparation of the thesis proved invaluable.

Thanks are also due to the Burmah Shell Company Ltd. who provided a grant through the Council of Scientific and Industrial Research, India, to support this work.

The author is grateful to Professor K.G. Denbigh for granting facilities to carry out research in the Department of Chemical Engineering and Chemical Technology, Imperial College, London.

CONTENTS

Abstract iii

Acknowledgements iv

Contents v

List of Figures vii

List of Tables ix

I INTRODUCTION 1

II LITERATURE SURVEY 9

II.1 Particle Dynamics 12
II.1.1 Steady isothermal flow over spheres theory 13
II.1.2 Recirculation - the sphere wake 16
II.1.3 Unsteady state motion of drops 22
II.2 Evaporation 30
II.2.1 Evaporation in moderate temperature media; stationary drops ... 30
II.2.2 Drops at motion relative to medium .. 31
II.2.3 Evaporation in high temperature media 33
II.3 Combustion of Liquid Fuels 42
II.3.1 Theory 45
II.3.2 Experimental studies 49
II.3.3 Experiments on the drag force on burning spheres .. 51

III EXPERIMENTAL PROGRAMME AND APPARATUS..... 59

III.1 Experimental Programme 64
III.2 Experimental Techniques and Apparatus 69
III.2.1 Combustion Chamber 70
III.2.2 The drop producer 74
III.2.3 Ignition 88
III.2.4 Photographic technique 91
III.2.5 The photographic apparatus 98
III.2.6 Synchronisation system 106
III.2.7 Development and measurements 108
III.2.8 The time monitoring system 109

IV EXPERIMENTAL RESULTS AND DISCUSSION 123

IV.1 Experimental Results 127
IV.1.1 Envelope flames - pentane 127

IV.1.2 Envelope flames - heptane-benzene 132
IV.1.3 Wake flames 133
IV.2. Discussion of Results 136
IV.2.1. Drag coefficients based on approach properties 136
IV.2.2 Study of the drag coefficients in the basis of mean properties 138
IV.2.3 Calculation of mean properties 140
IV.2.4 Comparison with theory 143
IV.2.5 The slope of the drag coefficient - Reynolds number curve for burning drops.. 148
IV.2.6 Comparison of burning rates 151
IV.2.7 Extrapolation to steady state conditions 152

V CONCLUSIONS 155

APPENDIX 1. CALCULATION OF DRAG COEFFICIENT AND REYNOLDS NUMBER A1.1

APPENDIX 2. STUDY OF SOURCES OF ERROR IN THE EXPERIMENTAL TECHNIQUE A2.1

APPENDIX 3. TABLES OF RESULTS A3.2

Symbols x
References xiv

LIST OF FIGURES

II.1	Angle of seperation of flow around a sphere.	21
II.2	Streamlines above a blunt wire.	21
II.3	Drag coefficient of accelerating spheres.	24
II.4	Drag coefficient of accelerating cylinders.	24
II.5	Drag coefficient of accelerating drops.	25
II.6	Mass transfer rates, boundary layer thickness and drag coefficients for a flate plate.	39
II.7	Relation between transfer number and modified transfer number	40
II.8	Variation of Nusselt number with transfer number.	39
II.9	Drag reduction for burning spheres (Lubanski)	53
II.10	Drag reduction for burning spheres (Khudyakov)	54
II.11	Drag coefficient of evaporating drops (Ingebo)	56
III.1	General view of apparatus	71
III.2	Schematic diagram of combustion system	72
IM.3	The Lane apparatus for drop production	76
IM.4	The drop producer. diagram	85
III.5	The drop producer. photograph	86
IM.6	Variation of drop postion with time	95
III.7	Layout of photographic system	96
III.8	View of mirror and combustion chamber	97

III.9	The Camera - side view	100
III.10	The Camera - rear view	101
III.11	Guide for plateholder movement	102
III.12	Synchronisation system	105
III.13	Schomatic diagram of recording system	112
III.14	System for storage and analysis of flashtube signals	114
III.15	Photograph of a drop with a side flame	121
III.16	Photograph of a drop with an envelope flame	121
IV.2	Drag coefficient of nonburning drops	129
IV.1	Drag coefficient of burning drops, envelope flame, pentane	128
IV.3	Drag coefficient of burning drops, envelope flames, heptane, benzene	131
IV.4	Drag coefficient of burning drops, side flames	134
IV.5	Drag coefficient of burning drops, approach properties, mean properties	141
IV.6	Predicted effect of evaporation on the drag coefficient. (Spalding)	144
IV.7	Variation of drag coefficient with transfer number (Muggia).	146
IV.8	Drag coefficient of drops, steady state	154

LIST OF TABLES

I	Variation of Transfer Number with gas composition	67
II	Variation of Transfer Number with gas temperature	67
III	Errors arising from short term changes in flashing frequency	A2.4
IV	Properties of fuels	A3.1
V	Position - time histories for non-burning drops	A3.3
VI	Position - time histories; heptane, benzene; envelope flames	A3.4
VII	Position - time histories; pentane; envelope flames	A3.7
VIII	Position - time histories; drops with side flames	A3.9

CHAPTER I.

INTRODUCTION.

Recent years have witnessed the spectacular growth of rocket engines and high speed aircraft. In such vehicles a high power/weight ratio of the propulsion system is of crucial importance. Therefore, the heat release rates in the combustion chamber must be very large, and there is a high premium on the precision of design. This leads to the need to burn fuels in the combustion chambers at the highest possible rates and at the same time to predict the various transfer coefficients with high accurancy.

In a typical bipropellant rocket engine, liquid fuel and oxygen are injected through an atomiser and the fuel drops either evaporate in the hot atmosphere with subsequent combustion of the vapour, or, under certain circumstances, burn with flames which surround the individual drops. After leaving the atomiser the drop undergoes a continuous decrease in size and moves with a varying relative velocity to the gas stream till it is completely consumed. For optimum design of such a rocket motor it is necessary to predict the ballistics of drops in a variety of circumstances, and thus the drag coefficients of drops under conditions of intense mass transfer must be known. A report describing

calculations of ballistics and vaporisation rates has been published by Priem[1].

There are many other practical situations where it would be useful to describe fluid flow past a dispersed phase in the presence of intense mass transfer, chemical reactions and steep property gradients. Catalyst regeneration, flow through reacting fixed and fluidised beds, the flow with combustion behind the baffle stabilisers in gas turbine power plants, and transpiration cooling are a few examples.

The drag coefficents of rapidly evaporating drops has not yet been studied adequately and most of the investigations dealing with the ballistics of such drops have used the standard drag coefficients, i.e., the coefficients for smooth spherical solid particles moving in the steady state without heat or mass transfer. However, due to a number of reasons it was expected that the drag coefficients for rapidly evaporating drops would be different from the corresponding standard values.

For burning drops, the fundamental theoretical problem of predicting the coefficients of mass, heat and momentum transfer have to be formulated in a manner different from that for drops with low rates of mass transfer.

Usually, the flow field is obtained from a solution of the Navier-Stokes equation or some simplification of this equation with the boundary conditions that, at the surface of the drop, the radial and tangential velocities are zero. At high mass transfer rates, one of these boundary conditions will be changed because the normal velocity of vapour leaving the drop could be in significant proportion to the main stream velocity. Further, due to chemical reactions, sources and sinks of heat as well as matter are distributed in the medium. While considering the heat balance over an element of space, along with the usual terms describing heat transfer by conduction and convection, allowance will have to be made for the transfer due to the enthalpy of the diffusing substance.

Theoretical solutions for flow with intense transfer across an interface have only been obtained for a small number of highly idealised systems. For example, Spalding[2] has studied the effect of evaporation on the laminar boundary layers for a flat plate in a longitudinal airstream, and the forward stagnation point of a sphere with a number of simplifying assumptions such as the existence of uniform properties throughout the fluid.

No such solutions are available for spheres but an idea of the magnitude of reduction of the film drag could be obtained from the fact that for the rates of evaporation

likely to prevail in the combustion of heptane in oxygen, the theoretical solutions for flat plates indicate a reduction of 80% in the drag coefficient compared to the standard value.

This reduction in film drag could be visualised as resulting from a thickening of the boundary layer and the consequent reduction in the velocity gradient due to bulk flow of vapour from the surface.

The form drag is also expected to be reduced as a consequence of combustion. The high flame temperatures cause gas expansion which would tend to "fill in" the low pressure region within the wake, and thus decrease the pressure difference between the regions upstream and downstream of the separation circle. Fluid movement around a body is further modified through a number of effects derived from combustion. It is known that evaporation affects the angle of boundary layer separation, and that the presence of the flame causes very steep property gradients. All these effects interact in a complicated way and their incorporation in a theoretical analysis of the drag force on drops involves immense difficulties.

The problem of the combustion rates of drops has been extensively studied, but most of the workers simplify the problem by postulating a spherically symetrical flame surrounding the drop.

Experimental results on the effect of combustion on the drag force on spheres have been reported by Spalding [3] Khudyakov [4] and Lubanski [5]. All these authors report reductions in the drag coefficient. The experimental systems consisted of supported spheres burning in air-streams and the Reynolds numbers were in the range 2000-10,000. However, in practical combustion systems, the drops are less than 1 mm in size and the Reynolds numbers are much less than 500 and, in rocket motors, the intensities of evaporation are much higher as combustion takes place in pure oxygen. Due to the differences in the flame/drop diameter ratios and the differences in the proportion of film drag to form drag, the results of the investigations in the high Reynolds number range cannot be easily extrapolated to the range relevant in practical systems. Ingebo [6] has reported values on the drag coefficient of heptane drops in a rocket motor, but studied the effect of evaporation and not combustion and the intensity of evaporation was not varied in his experiments. So far no definitive study has been reported on the drag coefficient of single small drops of fuel in free flight. This is probably due to the experimental and theoretical difficulties which would be outlined subsequently in

chapters I and III.

The object of this investigation was to study experimentally the drag force on single drops of iso pentane, n-heptane and benzene falling freely in cold oxygen rich atmospheres. The drops were mostly < 2 mm in size and the range of Reynolds number investigated was between 100 and 400 and it was hoped that this range would correspond closely to that obtained in practical combustion systems. It was decided to use single drops in order to avoid interference from a number of other variables associated with drop clouds. The use of oxygen rich atmospheres was prompted by two reasons; a) high oxygen concentrations were considered likely to yield the largest magnitude differences from the standard drag coefficients, and thus illustrate the effect of evaporation at the highest intensities; b) control of the oxygen percentage is an easy method of varying the intensity of evaporation over a wide range.

The drag coefficients were calculated from the drop size, the distance-time data and the knowledge of the properties of the undisturbed atmosphere in the combustion chamber. The distance-time records of the falling drops and the sizes were obtained by a specially designed

photographic technique.

It was found that over the range of Reynolds numbers studied, the drag coefficients of drops associated with flames which completely enveloped them were slightly higher but very near the standard values, and that the ratio of the drag coefficients of burning drops to the corresponding standard coefficients decreased with Reynolds number. For pentane, variation of the oxygen content in the atmosphere from 65% to 100% did not lead to appreciable changes in the drag coefficient.

The reason for the high drag coefficient values in comparison with expectations of large reduction from the standard values can be attributed to the fact that the drag coefficients and Reynolds numbers were calculated on the basis of the properties of the undisturbed medium while the actual properties in the immediate vicinity of the drop were very different from those of the undisturbed medium and changed steeply over short distances. It is believed that two large magnitude effects nearly cancel each other out, i.e., intense vaporisation from the surface tends to lower the drag coefficient while the high temperatures accompanying combustion increase the viscous forces.

It was found that one of two different types of

flames was associated with the drop, depending on the ignition conditions, the drop size and the oxygen percentage of the atmosphere. Apart from the flames which envelope the drop, which have already been mentioned, one could also obtain a flame which did not envelope the drop, but was almost attached to it at some lattitude on its surface. Such flames are referred to here as 'side flames' and when such flames were downstream of the equator, the drag coefficients were over 30% below the corresponding standard values. This decrease is believed to be caused by the large expansion of gases following combustion near the drop surface and could be visualised as a consequence of a "thrust effect".

CHAPTER II

LITERATURE SURVEY.

CHAPTER II.

The object of this survey is to take stock of existing theoretical and experimental information with a relevance to the problem under study.

There are only a few publications with direct relevance to the subject of this investigation. There have been no experimental investigations reported so far on the drag coefficients of burning single drops and most of the publications on burning spheres have been concerned with high Reynolds numbers and with a type of flame different from that of this investigation. Most theoretical investigations tend to discuss the problem under highly idealised conditions. In view of the state of developement of the subject, it was felt that all the fundamental aspects of the subject must be reviewed.

Before the effect of combustion on the drag force could be evaluated, it is necessary to study the process of combustion itself. Combustion is a special case of evaporation. The various phenomena of particle dynamics in isothermal flow without mass transfer need to be known before knowledge can be extended to flow with combustion.

Therefore, this chapter is devided into three parts. Flow at low Reynolds numbers, Stokes and Oseen approximations, recirculation and unsteady flow are discussed

under 'particle dynamics'. Evaporation in both moderate and high temperature media and the effect of evaporation on the drag force are discussed in the second section. The third section is concerned with combustion of drops and includes a review of experimental investigations of the effect of combustion of the drag force.

II-1. Particle Dynamics.

A sphere travelling in motion relative to a fluid experiences a drag force. It is customary to correlate data on fluid resistance by using a parameter called the "drag coefficient" which is defined by the following relations.

$$F = \frac{1}{2} C_d \rho_g A v^2 \quad \ldots\ldots\ldots 1.1$$ where,

F = drag force,

C_d = drag coefficient, dimensionless,

ρ_g = density of the fluid,

A = projected area of the body,

v = relative velocity of the body.

The drag coefficient was first used by Lord Rayleigh to present graphically the data on fluid resistance for a variety of solid sphere-fluid combinations with the drag coefficients and Reynolds numbers as the coordinates. The phenomena of fluid resistance are complex and no simple relationship can be used to express the relation between fluid flow and the force on a spherical particle. However, the experimental findings of several investigators have been assembled in the form of the familiar steady state drag coefficient vs Reynolds number curve. Empirical expressions are also available for restricted Reynolds number ranges. For the approach Reynolds number range relevant to this

investigation, (80 Re 400), the Langmuir[7] expression is the best approximation.

$$C_d\ Re/24 = 1+0.197\ Re^{0.63} + 2.6\times10^{-4}\ Re^{1.38} \qquad 2.1.2.$$

where Re = Reynolds number, given by $dv\rho_g/\mu$

where d = diameter of the sphere,

and, μ = viscosity of the medium,

Very few theoretical derivations of the drag coefficient are available.

II.1.1. Steady isothermal flow over spheres - theory.

The evaluation of the drag coefficient depends on a solution of the Navier-Stokes equation. This equation describes the movement of an element of fluid under the action of viscous and pressure forces. In vector form, the Navier-Stokes equation states:

$$D\vec{v}/Dt = \vec{F_1} - (1/\rho)\,\mathrm{grad}P + \nu\nabla^2\vec{v} \qquad 2.1.3.$$

where $D\vec{v}/Dt$ is the total derivative of the velocity vector $\vec{v}$, with respect to time t, and $\vec{F_1}$ represents the body force, p the pressure, and ν, the kinematic viscosity. The continuity equation states:

$$\mathrm{div}(\rho\vec{v}) = -\partial P/\partial t \qquad 2.1.4.$$

It is well known that the solution of the full

Navier-Stokes equation presents almost insuperable mathematical complexity due to the non-linear terms. Therefore solutions have been obtained only for a few cases where this equation could be simplified. The first such solution was that by Stokes for very low Reynolds numbers. The solution was facilitated by ignoring the inertial terms in the Navier-Stokes equation:

$$\text{grad}p = \nu \nabla^2 \vec{v} \qquad 2.1.5.$$

This relation is solved with the boundary condition that fluid velocity with respect to the particle is zero at the particle surface and equals the mainstream velocity at large distances from the surface. The following drag relation is obtained:

$$F = 3\pi d\mu v \qquad 2.1.6.$$

This drag force is actually made up of two components - (a) the skin or film drag, due to shear, and, (b) the drag due to pressure distribution over the sphere, the form drag. These two are in the constant ratio 2:1 according to the Stokes solution. However, the solution derives from an assymptotic approximation to the Navier-Stokes equation when $Re \to 0$. In comparison with experimental results, it is found that the Stokes relation for the drag force is valid up to Reynolds numbers of the order of 0.1. At higher Reynolds numbers, the

drag coefficient as well as the proportion of form drag are higher than those predicted by Stokes.

The next improvement was due to an approximation proposed by Oseen. The inertia terms were assumed to be important only at large distances from the sphere where the velocity approaches that of uniform flow. The resulting linearised equation is:

$$\vec{v}_\infty \text{ grad } \vec{v} = -\frac{1}{\rho}\nabla p + \nu \nabla^2 \vec{v} \qquad 2.1.7.$$

Goldstein[8] obtained the complete solution for the Oseen approximation and the expression for drag coefficient is:

$$C_d = (24/Re)\left(1 + \frac{3}{16} Re - \frac{19}{1280} Re^2 + \frac{71}{20480} Re^2\right) \qquad 2.1.8.$$

This expression is in agreement with experimental results at a Reynolds number of 1, but are in excess by 10% at Re = 10.

Pearson and Proudman[9] obtained separate infinite expansions of the stream functions for regions close to and far away from the sphere, referred to as the Stokes and Oseen expansions respectively and employed a matching procedure to obtain a relation for the drag coefficient:

$$C_d = (24/Re)\left\{1 + \left(\frac{3}{16}\right)Re + \left(\frac{9}{160}\right)Re^2 \log Re\right\} \qquad 2.1.9$$

Kawaguti[10] used an empirical method known as

the Galerkin method to obtain the forms and the constants of stream functions for the Reynolds number range 10 to 80. This is not a purely theoretical method since the selection of the form of the stream function involves comparisons with experimental data. However he was able to obtain drag coefficients as well as stream functions which agree with experimental results and for reasons which will emerge in chapter IV, Kawaguti's method might well be a starting point for a theoretical study of the drag force on burning drops.

Kawaguti's work represents the upper limit of Reynolds numbers for which theoretical solutions are available.

II-1.2. Recirculation - the sphere wake.

In an infinite non viscous fluid, a sphere in motion relative to the fluid should not affect the fluid in any other way than that of instantaneous displacement and hence the flow should exhibit symmetry about the equator. However all fluids are viscous and approach such symmetry only at very low Reynolds numbers. As the relative velocity increases, the divergence from symmetry about the equator increases and a point is reached when the streamlines appear to leave the surface of the sphere at

some latitude upstream to the rear stagnation point. The rear stagnation point is the rearmost point on the sphere in the direction of relative movement of the sphere. These lines converge some distance from the sphere enclosing a region of 'dead fluid'. The fluid in this space is actually circulating within its boundaries to give a torroidal eddy, the surface of which moves at a speed close to that of the surrounding fluid.

It was pointed out in chapter I that form drag could form a significant proportion of the total drag, and also that it was influenced in a manner different from that by which combustion affects film drag. The literature relevant to the wake and the influence of combustion on the wake will be reviewed in this section.

There seems to be little agreement in literature[11,12,13,14] regarding the wake configuragation behind a sphere moving in a real fluid and the Reynolds number at which recirculation sets in. But it can be assumed that for isothermal, non-evaporating sphere - fluid systems, such formation begins at some Reynolds number below 50 and hence a wake could exist in the present investigation.

It is believed that separation is initiated in

the following manner: as a sphere moves relative to the fluid, at very low Reynolds numbers, flow is identical about the equator of the sphere. Near the sphere surface, fluid velocity is zero near the forward and rear stagnation points and maximum across the equatorial circle. The static pressures are, correspondingly, maximum at forward and rear stagnation points and minimum along the equator. But as the Reynolds number increases viscous forces tend to retard the motion of the fluid in the boundary layer adjacent to the sphere surface. On the upstream side, this retarding force does not change the character of the motion because the pressure gradient acts in the direction of motion. On the downstream side of the equator, an element of fluid near the surface will be subjected to friction at the sphere surface as well as an "adverse" pressure gradient, i.e. a gradient acting against the direction of motion. As the Reynolds number increases, the pressure gradient increases and at a certain point the fluid is brought to rest near the sphere surface and a slow backflow begins - the forward boundary layer stream leaves the surface of the sphere and the latitude at which this happens is known as the point of separation.

The eddy circulating downstream to the separation

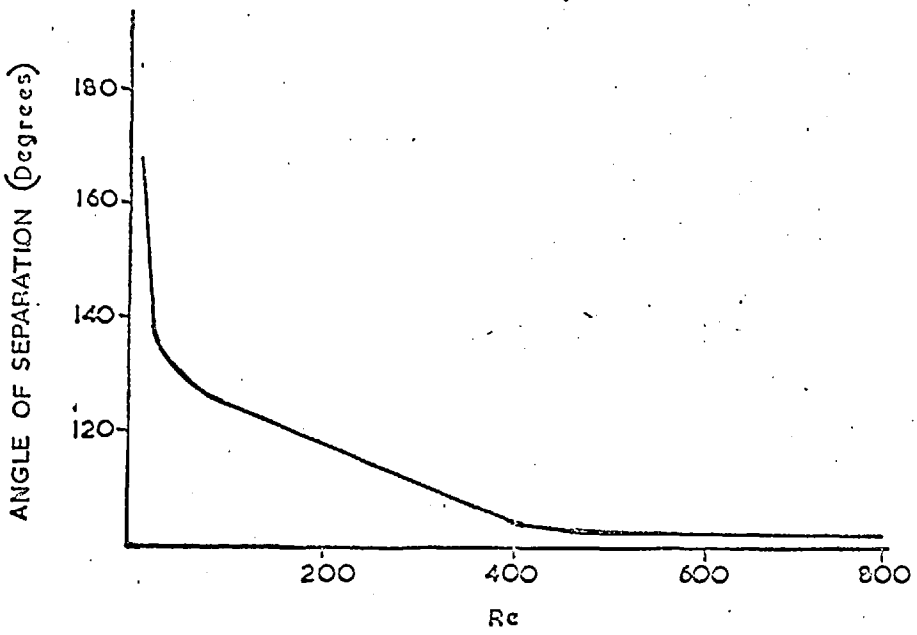
point is termed the 'wake'. A number of experimental studies have been reported on the formation and subsequent behaviour of the wake[12], but their findings are not consistent. In this connection, it has been pointed out by Garner[14] that dynamic similarity cannot be obtained by specification of the Reynolds number alone. A typical value for initial wake formation is a Reynolds number of 24, which was reported by Taneda[15]. The angle between the forward stagnation point and the separation circle increased with the Reynolds number and reached a value of 72° at Re = 450. Garner[14] also obtained similar results, and his findings are reproduced in fig.(II.1.)

As the Reynolds number increases the fixed ring vortex grows in size and also decreases in stability and Taneda[15] reported that at a value of Reynolds number of 130, its tail begins to oscillate. The oscillations become more severe, until, at a value called the "lower critical Reynolds number", it detaches from the fluid system adhering to the body of the sphere and streams away at velocity lower than the relative fluid velocity. Again there is no agreement regarding the Reynolds number at which this occurs, and figures ranging from 200 to 1000 have been quoted.

It was pointed out in chapter I, that a part of

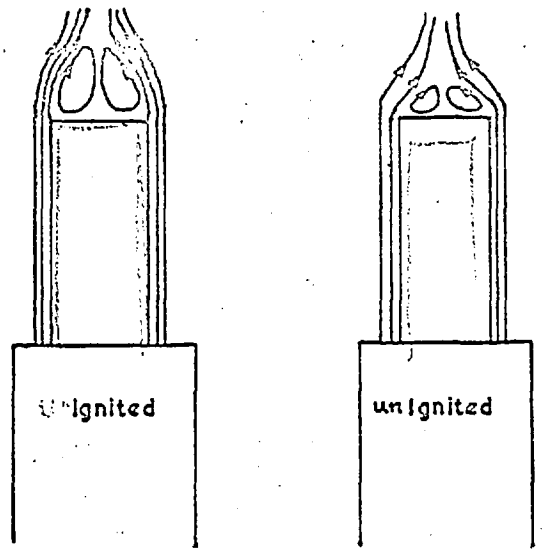
drag reduction in the presence of combustion was probably a consequence of the reduction in form drag due to the expansion of gasses following combustion. Most of the available information on wake flow pattern refersto the adiabatic wake, i.e., the wake in which no heat transfer takes place between various points in the wake and there is no chemical reaction. The theoretical problem in predicting the drag correction under conditions of form drag preponderance is one of predicting the pressure field in the rear half of the sphere with a vortex attached to it, when the elements of fluid circulate through the flame front or along it. It will be noticed that a similar situation is obtained behind baffle stabilisers with the difference that the gases are premixed in the baffle case. It has been recognised that combustion can exert a profound influence on the ~~value~~ nature of flow as the fluid is no longer baratropic, i.e. the density of fluid is no longer a function of pressure alone.

Only a limited amount of work has been done on the flow behind baffle stabilisers. Lewis and von Elbe[16] observed that the flow about the end of a blunt wire when it was acting as a stabiliser for a V-flame was quite different from ~~that for~~ adiabatic flow. The principal change was the decrease in the size of eddies behind the



ANGLE OF SEPARATION OF FLOW AROUND A SPHERE (ref 14)

Fig II. 1



STREAM LINES ABOVE A BLUNT WIRE
(Ref. 16)

FIG. II.2

obstacle. This is illustrated in fig.II.2. Hotell, Scurlock and Williams[17] have reported that the most important influence of the flame was in inhibiting the shedding of vortices and extending the stable recirculation regime. It has been stated earlier that vortex shedding occurs at the "lower critical Reynolds number", which could be anywhere between 200 and 1000. Once vortex shedding occurs, the flame will cease to be stabilised continuously behind the baffle. Hotell concluded that vortices do not shed from the rod stabilisers during combustion at Reynolds numbers far in excess of the conventional 'lower critical Reynolds numbers.'

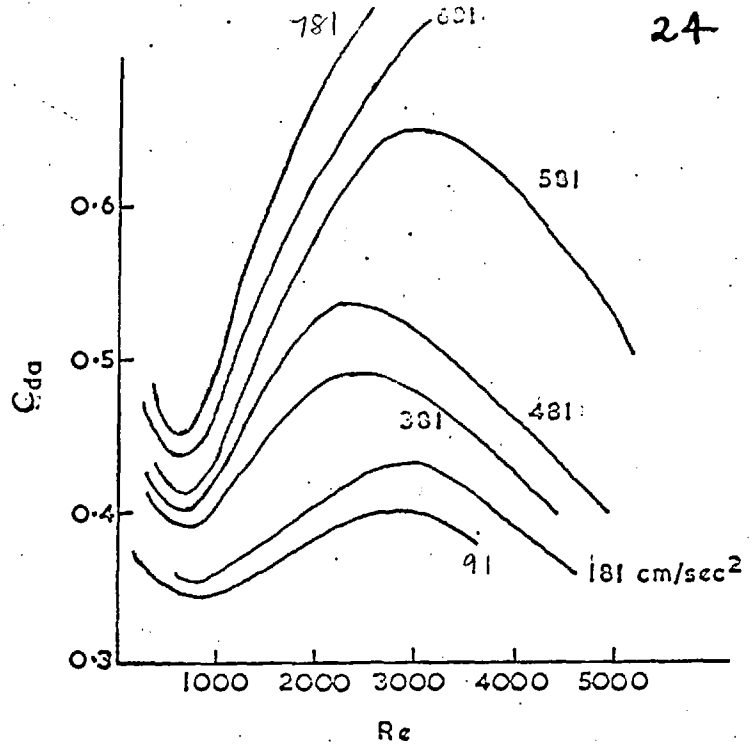
II-1.3. Unsteady state motion of drops.

In this investigation, the movement of the drops was unsteady, i.e. a constant velocity was never attained. Even when the drops were small and had an initial size which indicated a smaller distance for the attainment of terminal velocity than was under observation by the camera, drop movement was still unsteady due to the change in drop diameter.

It is known that acceleration could affect the drag coefficient of drops and therefore it is necessary to evaluate and separate the influence of acceleration so

that the effect of combustion could be accurately interpreted. In this section, the effect of acceleration would be reviewed with a view to assessing its importance under the conditions of this investigation.

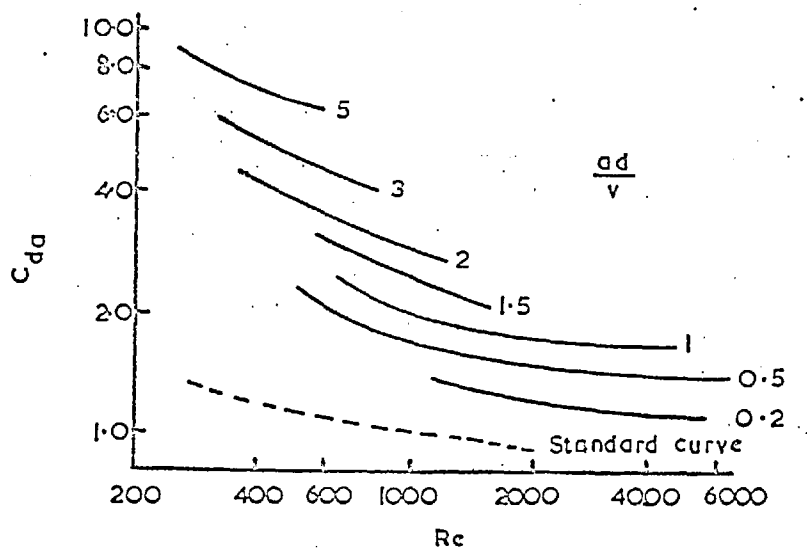
The conventional drag coefficient, expressed as a function of Reynolds number alone has been known to fail in predicting the ballistics of particles and drops undergoing acceleration or deceleration.[18,19]. It has been observed[19] that eddy formation in the rear of spheres undergoing acceleration would occur at lower Reynolds numbers than those for spheres in steady motion. Thus, the form drag would be increased. Lunnon[20] carried out investigations on the drag force on accelerating bodies and found that the drag coefficient increased with acceleration, depending on its magnitude. Lunnon's data, replotted by Gauvin, are shown in fig. II.3. He explained the increase of resistance as a consequence of the rapid change of streamlines in time, which would be favourable to the production of eddy motion. If such is the case, deceleration should also cause an increase in the drag coefficient. In the case of drops injected into combustion chambers, the relative velocity decreases as the drops travel forward in the chamber and simultaneously, they would also be decreasing in size.



DRAG COEFFICIENT OF ACCELERATING SPHERES

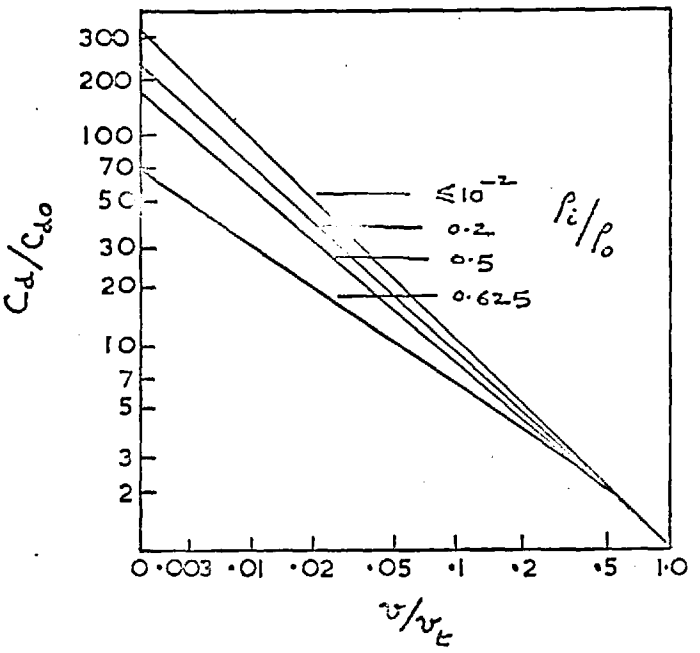
(Lunnon) Ref 20

FIG. II.3



DRAG COEFFICIENT OF ACCELERATING CYLINDERS (ref 21)

Fig II. 4



DRAG COEFFICIENT OF ACCELERATING DROPS

(Gilliland & Hughs) Ref 23.

FIG. II.5

Therefore, the rate of change of streamline pattern in the neighbourhood of the drop would be intensified and thus the effect on the drag coefficient would be larger.

Keim[21] has studied the acceleration drag for bodies with shapes such as circular discs moving in the same direction as their axis and hence under a high form drag condition. The curves obtained by Gauvin from his data are reproduced in fig. II.4. The magnitude of acceleration, the relative velocity and the body dimension are the parameters incorporated in this figure. The Reynolds number range was between 200 and 1000. A study of this figure reveals that the drag coefficients of drops of 1mm diameter, subjected to accelerations less than 1 g would be affected significantly only at very low relative velocities. This is ~~roughly~~ not the region considered in the present investigation and therefore, it may be assumed that the data obtained need not be corrected for acceleration.

Gauvin[18] has stated that even the rate of change of acceleration would affect the drag coefficient since the experiments with constant and varying accelerations gave different results. It is also believed that an increase in wake turbulence caused by increasing Reynolds numbers or by surface roughening would decrease the influence of acceleration on drag.

While the evidence so far presented shows an increase of drag coefficient with acceleration, Ingebo[22] has has reported a decrease in the drag coefficient for accelerating drops. He investigated the drag force on drops at accelerations between 10,000 and 25,000 ft/sec^2, at Reynolds numbers between 5,400, and drop sizes of 20 to 120 . He obtained the relation $C_d = 27/Re^{0.84}$ 2.1.10

He reported that rapid acceleration gave instantaneous drag coefficient values between those at steady state and those indicated by Stokes law, and that when accelerations and velocity differences were low, the unsteady state drag coefficients were identical with steady state drag coefficients. In his investigation, the dependancy of the drag on the magnitude of acceleration was not quantitatively studied and the difference in the direction of the acceleration effect from that reported by Lunnon has not been explained. The data for solid and liquid spheres was correlated by the same formula.

Data on the influence of acceleration on drag coefficient have also been reviewed by Gilliland and Hughes.[23] They used the mathematical solutions for the case of very slow, or "creeping flow" which were summarised by Bassett[24]

and plotted values of C_d/C_{do}, where C_d is the drag coefficient corresponding to velocity v, and C_{do} is the steady state drag coefficient corresponding to the terminal velocity v_t, for a number of values of ρ_i/ρ_o, where suffixes 'i' and 'o' denote the inner and outer phases (fig.II.5). Due to mathematical difficulties, calculations could not be carried out for values of $\rho_i/\rho_o > 0.625$. For values of $\rho_i/\rho_o > 0.625$, Hughes and Gilliland expected that C_d/C_{do} should rapidly approach unity. In this investigation ρ_i/ρ_o was 3 orders of magnitude larger than 0.625.

II.2. Evaporation.

II.2-1 Evaporation in moderate temperature media - stationary drops.

The evaporation of drops into low temperature media in the absence of convection can be described by the expression:

$$dm/dt = \frac{2\,k\,d\,(T_g - T_s)}{L} \qquad 2.2.1$$

where, m = mass of drop

k = conductivity of the vapour-gas mixture,

L = Latent heat of evaporation,

T = temperature

suffixes g and s refer to the ambient gas and the drop surface respectively.

This equation applies to steady state evaporation. But, as the drop diameter changes, evaporation can never be perfectly steady. In the unsteady state, the evaporation is lowered according to the relation[26]

$$dm/dt = \left\{dm/dt\right\}_o \left\{1 - \sqrt{\frac{m'_s - m'_g}{\rho_l}}\right\} \qquad 2.2.2.$$

where m' = the mass concentration of vapour.

and, $\left(\frac{dm}{dt}\right)_o$ indicates the steady state evaporation rate.

However, it can be shown that when $m'_s << \rho_l$ evaporation can be considered to be quasistationary and relation (2.2.1)

is applicable when the concentration and temperature gradients are small.

II.2-2 Drops at motion relative to the medium.

A large amount of experimental information is available for the evaporation of drops at movement relative to the fluid, ~~again~~, under conditions of mild temperature gradients. While theoretical prediction is possible under certain circumstances for the region of the drop surface upstream to the separation circle, analysis of the region downstream to it is extrmely difficult and only experimental evidence is available.[14] Frössling[35] has obtained local evaporation rates from the sphere as a function of the angle between the line joining point concerned with the drop centre and the axis of flow and found that the Sherwood number decreased from the forward stagnation point down to the separation circle and then increased again, and that the average rate of evaporation from the forward region and the wake region could be taken to be in the ratio 10:1. He correlated data for the evaporation of water, aniline and naphthalene into airstreams at room temperature over a Reynolds number range between 2 and 750 and obtained[27]:

$$Nu_m = 2 + 0.55Re^{\frac{1}{2}}Sc^{\frac{1}{3}} \qquad 2.2.3$$

where Nu_m = Sherwood number

Sc = Schmidt number.

In practical combustion systems, the instantaneous relative velocities obtained for a drop depend on its size and velocity history and the drag force The evaporation rate would be a function of the relative velocity. It is often assumed that small drops aquire stream velocity very soon after injection and therefore could be described by equations for evaporation rate without convection.

While discussing the evaporation in turbulent aerosols, Fuchs[28] has pointed out that "Since pulses of turbulence which completely entrain the drops clearly have no effect on their rate of evaporation, and since the degree of entrainment rises with the increase in the ratio of the Lagrange period of oscillation to the time of mechanical relaxation of drops, while the energy of pulsation falls with decrease in their period, it is obvious that the effect of turbulence on the rate of evaporation must increase with the drop size." This comment has a bearing on the importance of the knowledge of drag coefficient in sprays. In view of the statement by Fuchs, it is obvious that the drag coefficient would influence the increment in burning rate due to turbulence and that a reduction in the drag coefficient would cause an increase in the burning rates.

II.2.3 Heat and momentum transfer in high temperature Media.

Considering drop evaporation without free convection first, the difference from the situation which could be described by equation 2.2.1 is that the sensible heat acquired by the vapour after leaving the drop surface could be in significant proportion to the latent heat and the evaporation rate for drops is indicated by:

$$\frac{dm}{dt} = \frac{2\pi K d}{L} (T_g - T_s) \phi \qquad 2.2.4.$$

where $$\phi = \frac{\ln \left[1 + \frac{C(T_g - T_s)}{H}\right]}{\frac{C}{L} (T_g - T_s)}$$

where C is the specific heat of vapour. As the temperature difference $(T_g - T_s)$ increases, the parameter ϕ decreases and therefore the evaporation rate decreases in relation to that predicted by equation 2.2.1. The evaporation rate under forced convection can be obtained from:

$$\frac{dm}{dt} = \frac{2\pi k d}{L} (T_g - T_s) \phi Nu_H \qquad 2.2.5.$$

where Nu_H is the Nusselt number for heat transfer.

Ranz and Marshal[29] have found a relation for Nu for water drops over a range of Reynolds number 0 to 200 and air temperatures between 80·F and 400·F:

$$Nu_H = 2.0 + 0.6\, Re^{\frac{1}{2}} Pr^{\frac{1}{3}} \qquad 2.2.6$$

At very high mass transfer rates, the bulk flow of vapour leaving the interface affects the various property profiles. A fully theoretical evaluation of mass transfer rates would involve a knowledge of the flow pattern through the solution of the Navier Stokes equation or a simplification of this equation with the boundary conditions that the velocity at and normal to the interface is zero. But at high mass transfer rates, one of the boundary conditions is that there is a finite normal velocity.

Attempts have been made to evaluate the influence of bulk flow of vapour on the friction factors, heat transfer and mass transfer coefficients by predicting 'correction factors'.

$$\theta_v = C_d^*/C_d, \theta_T = h^*/h, \quad \theta_{AB} = h_m^*/h_m$$

where θ = the correction factor.

C_d = drag coefficient

h = heat transfer coefficient.

h_m = mass transfer coefficient.

Subscripts v, T and AB indicate corrections for momentum, heat and mass transfer coefficients.

* indicates the high mass transfer case.

Such correction factors have been obtained for a few simple cases. It is worth noting that the coefficients for low mass transfer rates too have been obtained theoretically only for a few idealised cases.

The correction factors have been obtained mainly on the basis of three theoretical approaches - film theory penetration theory and boundary layer theory.

Film theory: Lewis and Chang[30] applied film theory to interphase transfer of both species of a binary mixture at high mass transfer rates. Ackerman[31] applied film theory to heat transfer in the presence of rapid mass transfer. Colburn[32] and Drew confirmed Ackerman's analysis and applied the results of the two earlier works to rapid condensation of mixed vapours. Mickeley[33] extended the subject to momentum transfer in constant pressure systems. Considering laminar steady flow along a plane surface and assuming that the transport properties μ, the viscosity, k the conductivity and D the diffusivity are constant in the neighbourhood of the drop and ignoring homogenous chemical reactions, viscous dissipation and radiant heat transfer,

the correction θ_v was obtained by Mickeley:

$$\theta_v = \frac{i}{e^i - i} \quad \ldots\ldots 2.2.6.$$

where i is a quantity called the rate factor and is given for the system under consideration by the relation:

$$i = \frac{N_A M_A}{\frac{1}{2}\rho_g V_\infty C_{d,loc}} \quad \ldots\ldots 2.2.7.$$

where,

N_A = molar flux of diffusing substance,

M_A = molecular weight of diffusing substance,

$C_{d,loc}$ = drag coefficient, local, uncorrected.

According to this theory, mass transfer of components A ~~and B~~ into the stream decrease the transfer coefficients and transfer from the stream increases the transfer coefficients.

The limitation of this theory is that the dependence of ρ_g, v_x and T (pressure, local velocity along main axis of flow, temperature) is purely one dimensional. Hence it is not readily applicable to flow around spheres and is of interest mainly for flow in such cases as channels, with fully developed profiles. Pressure gradients along the

wall have been ignored and therefore the theory cannot be applied to flows with form drag.

Another assumption whose validity is doubtfull is that the film thickness is unaffected by mass transfer.

Penetration theory. Higbie[34] has applied penetration theory to prediction of mass and heat transfer coefficients as influenced by the mass transfer rate. This theory assumes a flat velocity profile near the interphase, and is thus applicable mainly to the liquid phase and as such is not of interest in the study of liquid drop combustion.

Boundary layer theory: In both film and penetration theories, the effect of v_x, the local velocity in the mainstream direction on the concentration and temperature profiles was suppressed. Further, they were only applicable to fully developed flow. The boundary layer theory of simultaneous mass, heat and momentum transfer takes these into account and is therefore preferred under conditions such as pipe entrances. The works of Mickeley, Stewart, Chambre and Young, Schlichting and others are incorporated in the book on "Transport Phenomena" by Bird[36] et al. The Prandtl boundary layer equations are solved exactly and θ, the correction factor is obtained as the ratio of "dimensionless gradients at the wall".

$$\theta = \frac{\pi'(0,\Lambda,K_b)}{\pi(0,\Lambda,0)} \qquad 2.2.8$$

where K_b is the dimensionless mass flux at the wall and Λ, a dimensionless physical property ratio, equal to one in the case of momentum transfer.

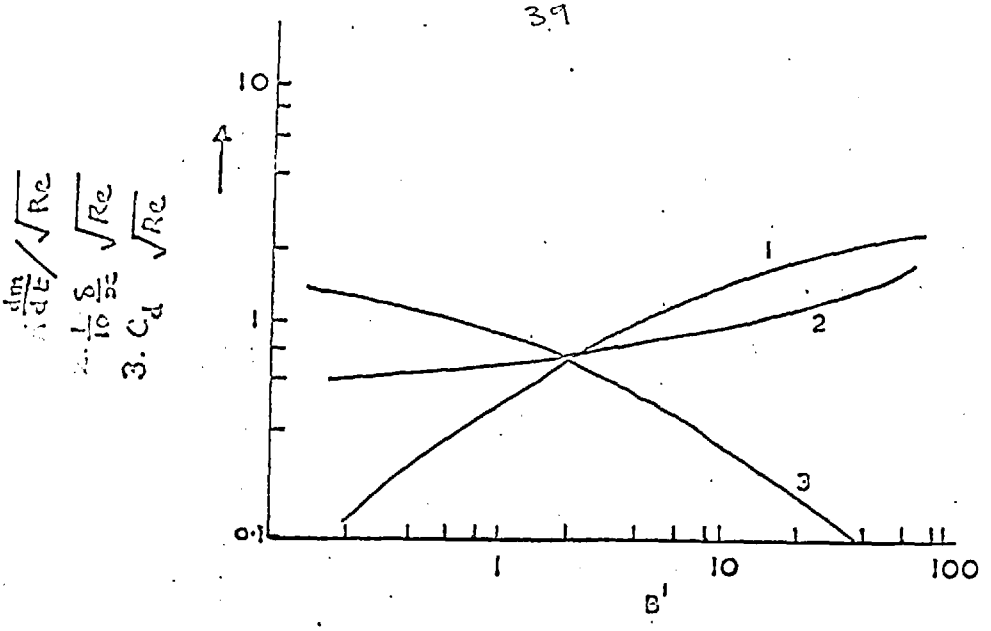
$$K_b = (2v_{yo}/v_\infty)\sqrt{(v_\infty x)/\nu} \qquad 2.2.9$$

where v_{yo} = normal vapour velocity at surface
x = position coordinate, in X direction.

values of $\pi'(0,\Lambda,K_b)$ for various values of K_b and Λ have been computed by and presented in tabular form by Bird, et al[36]

By all three methods of attack, a decrease in the various transfer coefficients is indicated for mass transfer to the gas stream and an increase for mass transfer towards the liquid phase.

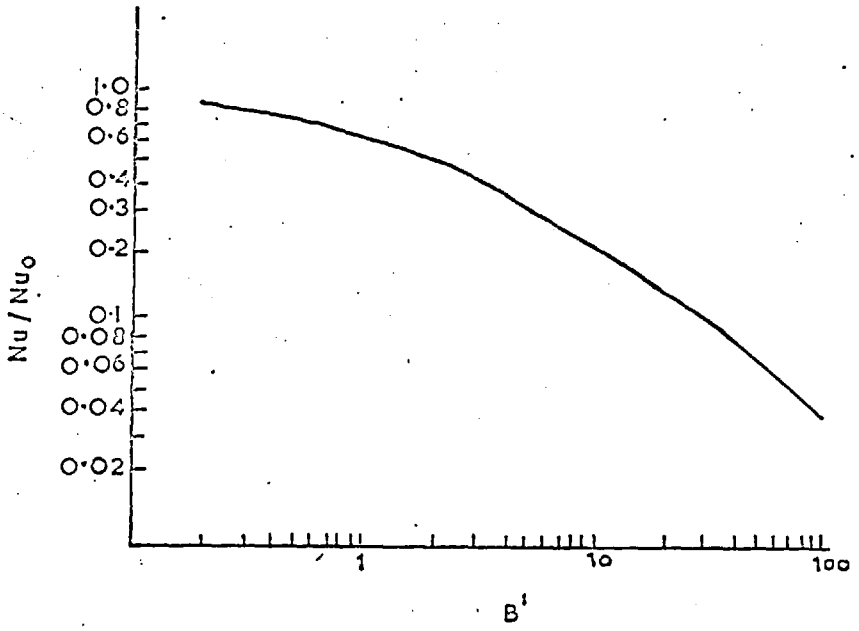
Spalding[37] has computed the effect of mass transfer on the drag coefficient for flat plates and the forward stagnation point of spheres in laminar airstreams. He used for his analysis a driving force called the "transfer number". For evaporation, the transfer number is given by the relation: $B = \frac{C_p (T_g - T_s)}{L}$ 2.2.10



B'. MODIFIED TRANSFER NUMBER

MASS TRANSFER RATE, BOUNDARY LAYER THICKNESS AND DRAG COEFFICIENT, FLATE PLATE (Ref. 2)

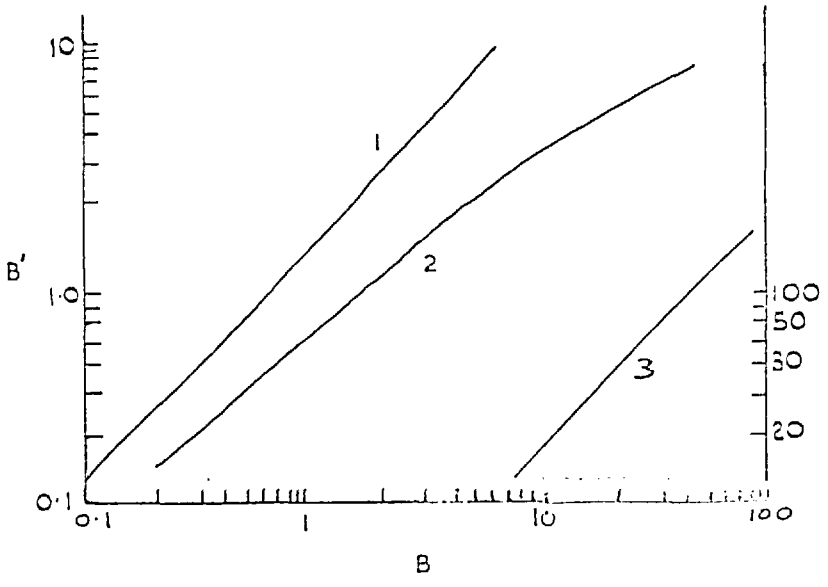
FIG II·6



B'. MODIFIED TRANSFER NUMBER

REDUCTION OF NUSSELT NUMBER BY MASS TRANSFER (Ref. 2)

FIG. II.8



B'- MODIFIED TRANSFER NUMBER

RELATION BETWEEN B AND B'.
1 - FLAT PLATE;
2,3-SPHERE STAGNATION POINT
(Spalding) Ref. 2.

FIG. II.7

His results for the variation of the drag coefficient, mass transfer rates and the ratio of Nusselt numbers with and without mass transfer are reproduced in figs. II.6 and II.8. It can be shown that the transfer number for the combustion of pentane in oxygen is of the order of 34 (TableI) and for this transfer number, the ratio of drags with and without mass transfer is of the order of 0.1, i.e. there is a 90% decrease in the drag coefficient. It can be seen from fig. II.8 that the Nusselt number is also reduced by the same magnitude.

All of the work considered in this section so far has been on heat and mass transfer to and from plane surfaces. The only publication at present available which theoretically calculates the drag coefficient for an evaporating sphere is that by Muggia[38]. He investigated the flow around a spherical evaporating drop at low Mach and Reynolds numbers and when the drop temperature was invariant. He extended Oseen's theory of the field around a spherical solid to the case of an evaporating sphere, and determined the variations of velocity, temperature, pressure, enthalpy and concentration of the vapour in the field around the drop. He then calculated the evaporation rates and drag force exerted by the stream on the drop. His theory is based on steady flow and is

valid only when the velocity variation of the drop is not high. Further, his approximations correspond to those for a spherical solid and would not hold at Reynolds numbers over 1. As it was noticed earlier, the Oseen theory for flow around a spherical solid is true only upto Reynolds numbers of the order of and therefore only for a small part of the Reynolds number regime in droplet combustion.

His predictions, expressed in terms of the transfer number, B and the Reynolds number are:

Evaporation:

$$\frac{dm}{dt} = 8\pi\mu r \frac{B}{4}\left(\frac{4 + Re}{2 + B}\right) \qquad 2.2.11$$

Drag coefficient:

$$C = \frac{24}{Re}\left[\frac{2 + B}{2 + \frac{3}{4}B - \frac{3}{16}Re\,(2+B)} - \frac{B}{3}\left(\frac{4+Re}{2+B}\right)\right] \qquad 2.2.12$$

His results are discussed further in Chapter IV

II.3 Combustion of Liquid Spheres.

First, the state of theory on the combustion of liquid spheres will be examined and then some experimental investigations will be mentioned. This will be followed by a more detailed review of available papers in the drag of burning surfaces.

When a liquid drop burns, fuel is evaporated from the liquid interphase and diffuses to the flame front, while oxygen moves from the atmosphere to the flame front. The rate at which the drop burns is determined by the heat transfer from the flame front to the liquid surface. The flame is a diffusion flame in most cases and chemical processes are assumed to occur so rapidly that burning rates are solely determined by mass and heat transfer rates. Spalding[39] and Graves[40] consider a two film model for combustion of liquid fuel. One film separates drop surface from flame front; a second separates flame front from surrounding atmosphere. Combustion is thus a process in a system of three spheres when there is no natural or forced convection.

As there is always a large density difference between combustion products and cold air, natural convection cannot be eliminated except in the absence of gravity. Under this condition the flame is spherical and completely envelopes the drop. As the relative velocity between drop and medium rises, the flame lengthens and at a certain point known as the 'extinction point' breaks away from the forward stagnation point of the sphere and is sustained in the lagging half of the sphere. Such a flame is called a wake

flame. The transition from envelope to wake flames has been studied by Spalding. The velocity at which extinction occurs was shown to be proportional to the drop diameter. For hydrocarbon fuels burning in atmospheric air, Spalding arrived a value of $v/d = 100\ sec^{-1}$. The wake flames could be divided into two types, the first being known as the 'closed wake flame' when the flame is of the diffusion type, and, the second, 'open wake flame' which is obtained at very high Reynolds numbers and is premixed. In this investigation, the closed wake flame was obtained even when the velocity was well below the extinction velocity and the flame could be attached at any lattitude to the drop. Therefore, all flames which do not completely envelope the drop are called side flames.

II.3.-1. Theory.

Most theoretical investigations on combustion of drops assume a model with spherical symmetry. Combustion is considered as a special and complicated case of evaporation.

It has already been shown that at Reynolds numbers above one, the solutions of the Navier Stokes equation is very difficult. At high Reynolds numbers one can use the boundary layer approach. This postulates the existance of a boundary layer which is very thin compared to the body dimensions. One value quoted for the lower limit of Reynolds numbers for spheres for the boundary layer approximation to be valid, is 1000.[42]

Thus, we find that a purely theoretical analysis of convective mass transfer involves knowledge of flow patterns and an analysis of drop combustion presumes an understanding of evaporation. Correlations using various dimenionless groups would need a large amount of experimental data which are not available at present for high intensity evaporation and combustion with forced convection. Therefore, all theoretical treatments of combustion involve a one dimensional model. The further assumptions are: (a) the various transport properties are uniform throughout the gas-vapour medium in the vicinity of the drop; (b) there is no reaction any-

where except in an infinitely thick flame front.

(c) the effect of radiation is negligible.

Using the equation for oxygen diffusion in the region outside the flame, the stochiometric ratio, and the equation for heat transfer outwards from the spherical flame surface, one could obtain the flame temperature -

$$T_f - T_g = \frac{D \rho_{O_2} H \rho_{a_2}}{12 \pi' P} \qquad 2.3.1$$

where D = diffusion coefficient.

H = lower heat of combustion of fuel,

π' = stochiometric ratio

and suffixes f and g refer to flame and gas at an infinite distance from the drop.

ρ_{O_2} = partial pressure of oxygen.

Spalding has calculated flame temperatures for kerosine drops when there is no dissociation.[39] Graves[40] took dissociation into account and calculated flame temperatures for isoatane drops, assuming that ρ_{O_2} is small. It was found that the flame temperatures were higher than the corresponding adiabatic flame temperatures. This was because of the fact that there is no net flow of inert gas through the burning zone and oxygen is preheated to the combustion temperature by the reaction products.

Godsave[43] has obtained the temperature gradients at the surface of a drop which is surrounded by a flame.

$$\frac{dT}{dR} = \frac{E(T_f - T_s)}{e^{-E/r_f} - e^{-E/r_s}} \quad \frac{e^{-E/r_s}}{r_s} \quad \ldots\ 2.3.2.$$

where, suffixes f and s stand for flame and drop resp.ly,

$$E = \left(\frac{dm}{dt}\right) C/4\Pi k$$

When E is increased, keeping the other quantities constant, the temperature gradient at the drop surface is decreased. Burning rates can be calculated by using the equations for heat and mass transfer in the region between the drop surface and flame front. Godsave's burning rate equation for a drop at its boiling point, is:

$$\frac{dm}{dt} = \frac{\log_{10}\left[1 + \frac{C(T_f - T_s)}{L}\right]}{0.4343\ \frac{C}{4\Pi k}\left(\frac{1}{r_s} - \frac{1}{r_f}\right)} \quad \ldots\ 2.3.3.$$

For calculations of burning rate, Godsave used the flame and drop radii which had been experimentally found. Graves[40] has theoretically obtained the ratios of flame and drop radii. For osooctane drops he obtained a ratio of r_f/r_s of 18.5. For nearly the same conditions Godsave experimentally found a ratio of 3. The difference is

supposed to arise from the effect of natural convection. Therefore, the influence of forced convection could easily be seen to make the application of the theory very difficult. Godsave has calculated the Nusselt Number for burning drops.

$$Nu_H = \frac{2E}{r_s} \frac{1}{e^{E\left(\frac{1}{r_s} - \frac{1}{r_s}\right)} - 1} \quad \ldots\ 2.3.4.$$

Spalding[44] has investigated the combustion of liquid fuels. He uses a transfer number for liquid fuels which is given by the relation:

$$B = \frac{m_{o2,g}^{1} H/r^{1} + C(Tg - Ts)}{L} \quad \ldots\ 2.3.5.$$

The drop surface temperature could be assumed at the boiling point of the fuel. In this investigation the transfer number is used as a convenient index of the intensity of combustion.

III. 3.2 Experimental Studies

(i) Natural Convection

Experiments in the burning time of droplets have been carried out by Godsave who suspended the droplet on filaments and measured the rate of decrease in size photographically. Similar experiments have been done by Kumagai and Kimura[45] and Kumagai and Isoda.[46] Bett[47] has studied the

combustion of freely falling single drops and small drop clouds produced from spinning disc atomisers.[45] These authors generally correlated their results in terms of λ, an "Evaporation Constant" given by

$$d^2 = d_o^2 - \lambda t \qquad 2\cdot3\cdot6$$

where t is the time after ignition and d is the drop diameter, subscript o indicating the initial diameter. For the case of pure spherical envelope flame combustion, can be related to the transfer number by the relation:

$$\lambda = \frac{8k/c \ln (1+B)}{\rho_1} \qquad 2\cdot3\cdot7$$

In all these studies, it was found that d^2 varies linearly with time. From these considerations, it was concluded that the essential features governing the rate of combustion of single drops (not in motion relative to atmosphere) were understood.[48]

(ii) Droplets in Motion

Spalding[59] has studied the combustion from flat plates, cylinders and spheres in airstreams. He believed that, in general, combustion rates can be predicted from existing heat transfer data by the relation:

$$\frac{dm}{dt}\frac{1}{4\pi r^2} = h/c \ln (1+B) \qquad 2\cdot3\cdot8$$

His data for both flat plate and sphere combustion

with natural convection were well correlated by the flate plate derivations[37] described earlier. He has also discussed transient effects[50] such as the heating up of the drop during combustion and the rise of transfer number with time for drops which are mixtures of compounds of various boiling points..

II.3.3 Experiments on the drag of burning and evaporating bodies.

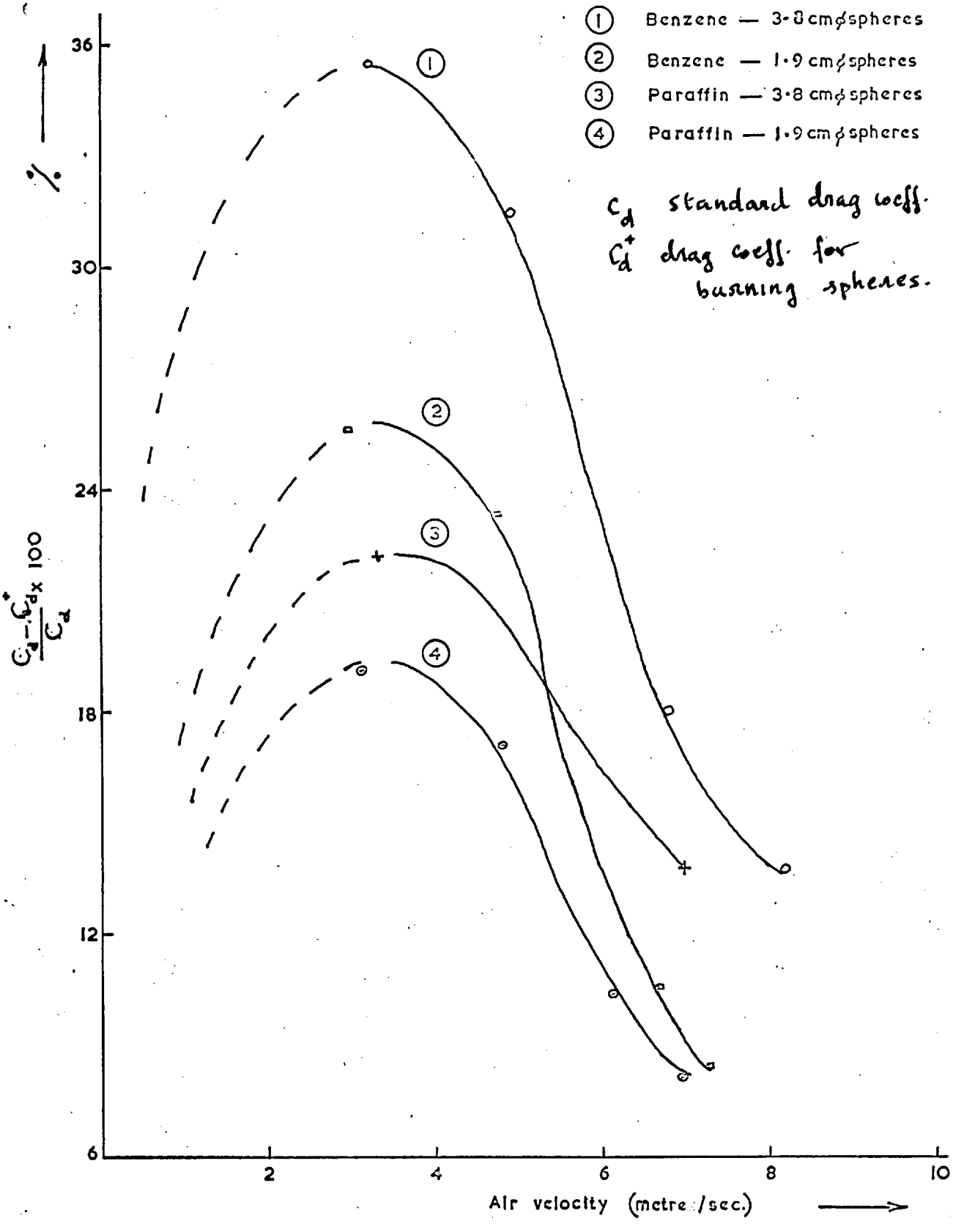
A very limited amount of experimental work isavailable on the drag of bodies when combustion or intense evaporation takes place.

Lubanski[5] measured the drag reduction by combustion on liquid spheres made up of cotton wool soaked in liquid fuel. His experimental system consisted of a sphere suspended at the end of a string in a wind tunel. From a knowledge of the deflection of the sphere and its mass, one can calculate the drag on the sphere. He found the deflection less in the case of combustion, thus directly proving the drag reduction due to combustion. The spheres he used were of 38mm and 19mm dia and the fuels used benzole and paraffin. His curve for drag reduction are reproduced in fig.II.9. It is noted that the reduction is lower with benzene than with paraffin, that a larger diameter ball suffered the greater percentage of drag reduction and that the reduction with air velocity was

maximum at about 3

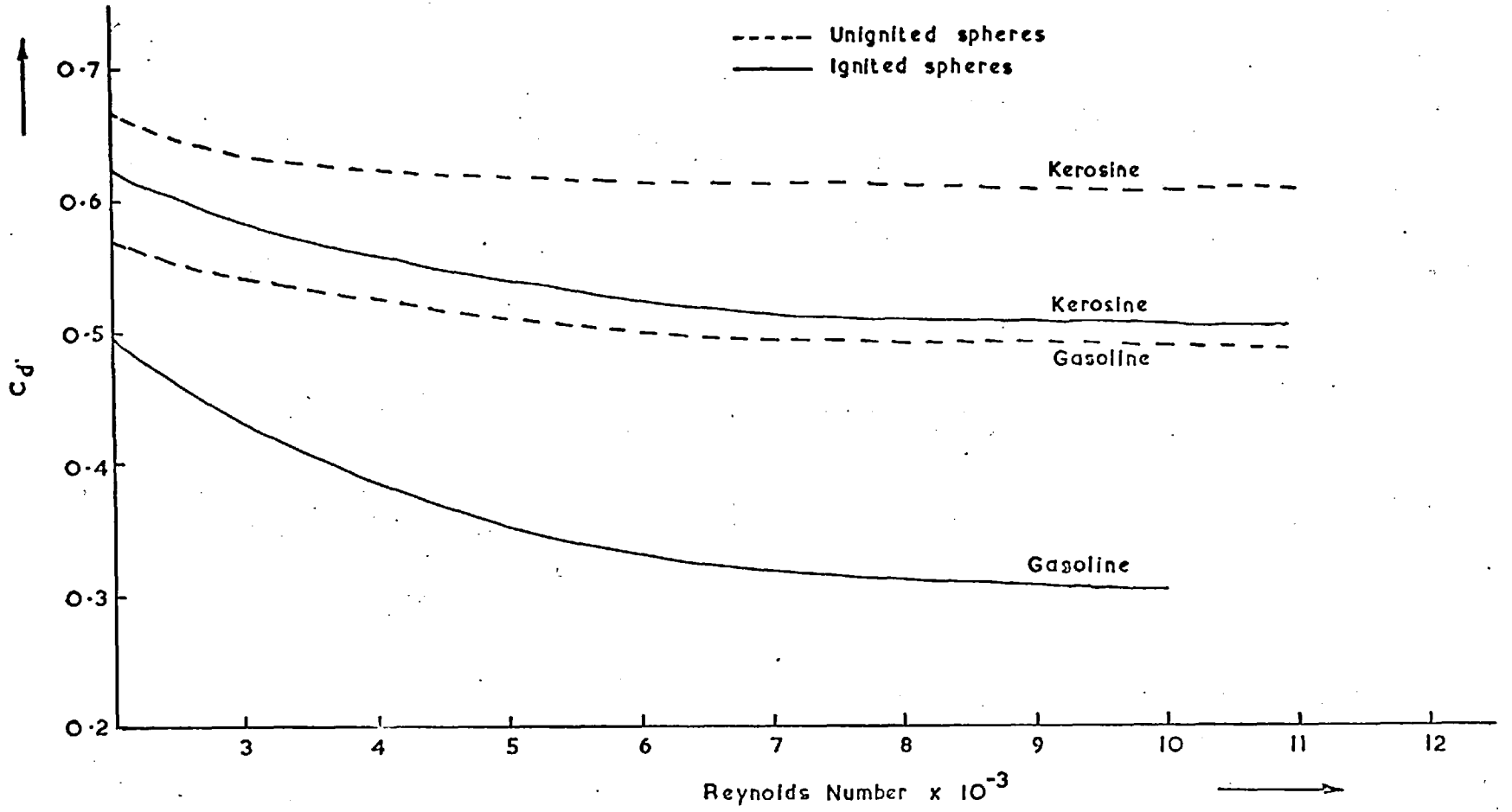
metres per second.

As can be seen from fig. II.9, the degree of reduction of drag from the standard value decreases with the stream velocity. Lubanski explained this as a consequence of natural convection. When the stream velocity is reduced, the flame tends to lift up and therefore reaction tends to act at an angle to the horizontal. The horizontal component is therefore reduced and hence the degree of drag reduction. The Reynolds numbers were of the order of 4000. He suggested the following reasons for drag reduction: (a) Streamlining of the turbulent wake and the 'filling up' of the wake. (b) As a greater part of the evaporation occured from the rear half of the sphere with respect to the direction of air flow, there could be an appreciable net reaction from the vapour leaving the drop, (c) Reduction of velocity gradient at drop surface due to evaporation. He also suggested that the reduction could be due to a number of periodic explosions down stream to the sphere. He argued that the wake behind the sphere was very turbulent and consisted of a series of eddies which could conceivably cause discontinuous combustion. He further submitted that every jet, when ignited, makes a noise, and that this increases with jet velocity and that discontinuous combustion could be a reason for the noise.



DRAG REDUCTION FOR BURNING SPHERES (Lubanski) Ref 5

FIG. II-9



DRAG REDUCTION FOR BURNING SPHERES (KhudyaKOV) Ref. 4

FIG. II.10

Khudyakov[4] measured the drag force on supported spheres in a wind tunnel. Fuel was effused through the porous sphere and the drag force was measured directly with a flat spring. The range of Reynolds numbers investigated was 2000 to 11,000. His curves for drag with and without combustion are reproduced in fig. II.10. The reasons for the difference in the curves for the unignited sphere for gasolene and kerosine are not known. He found that the pressure in the wake region was higher when a flame was present relative to the pressure for a non burning sphere. He also found that the flame was attached to the sphere even at velocities of the order of 24 metres/sec. The ratio v/d in this case was about 1700 sec^{-1}. ~~Thus~~ The experiments were conducted well above the extinction velocity of 100xd which was quoted earlier in this chapter. Thus, Khudyakov's results correspond to a wake flame.

Bolt[47] studied the combustion rates of drops falling freely in a combustion chamber. Incidentally to his combustion rate measurements, he also obtained the time interval taken by the drop to fall through known intervals. These values were used to calculate the drag coefficient of drops and the results are shown in fig. II-11

Ingebo[6] measured the drag coefficients and evaporation rates of ethanol drops in a rocket motor. He did not report the effect of combustion on a particular drop,

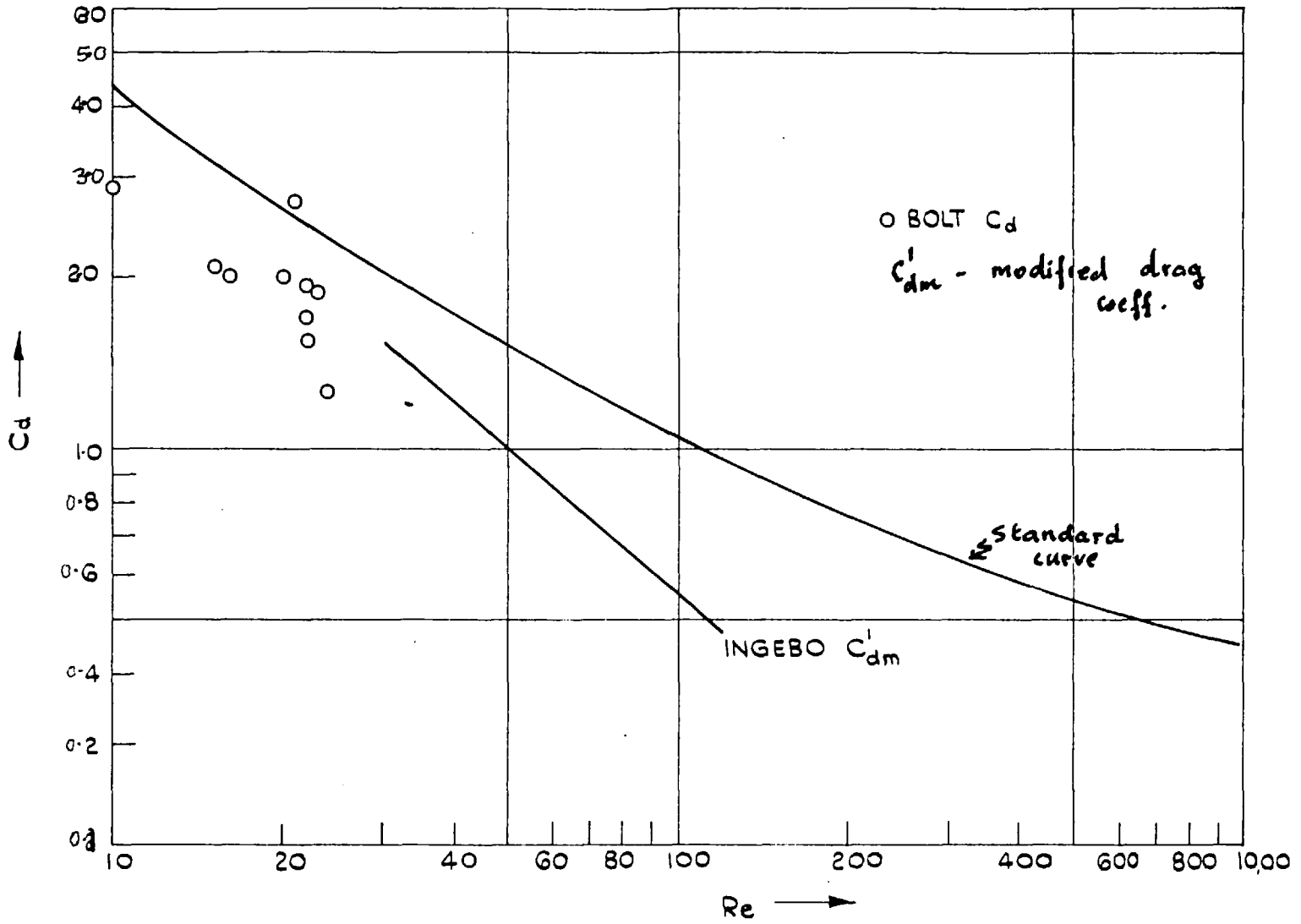


FIG. II. 11. DRAG CO-EFFICIENT OF EVAPORATING DROPS.

(Refs. 6; 47)

but reported his results for the whole spray in terms of the evaporation rates and drag coefficients of the area median drop. His results for the drag coefficient are shown in fig. II-11 He concluded that heat transfer coefficients, and drag coefficients for burning sprays based on the area median drop size agreed with those for non-burning drops. The drop sizes were of the order of 100 μ and the relative velocities were about 80 fps. Therefore, one obtains a ratio v/d = 240,000! Even at high temperatures and oxygen concentrations, it is doubtful whether the drop could be 'burning' with attached flames at such relative velocities.

His data are difficult to interpret due to the interference from other drops, the variation in combustion or evaporation rate along the chamber and due to the fact that the whole spray is represented by the area median drop.

Spalding[51] reported drag coefficients slightly lower than the standard value for burning surfaces and confirmed that the pressure in the wake region is higher than that in the isothermal wake.

CHAPTER III

EXPERIMENTAL PROGRAMME AND APPARATUS.

CHAPTER III

It was pointed out in chapter I that most of the investigations reported so far on the drag force on burning surfaces were concerned with direct measurement of drag force on supported spheres in airstreams. The experimental arrangements of Lubanski[5], Khudyakov[4] and Spalding[3] have been mentioned in chapter II. Such systems only permit measurement of drag force at Reynolds numbers of the order of thousands.

The drawbacks of such systems are: (a) as high velocity streams of gas are used, only a limited range of transfer numbers could be studied, i.e., those very near the value corresponding to atmospheric air, (b) the ratios of flame to drop diameter are different from those relevant in drop combustion, (c) the proportion of form drag to film drag is higher than for drop combustion, (d) it might be difficult to study the effect of envelope flames because this demands that the airstream velocities be below the extinction velocity and direct measurements are facilitated by a high drag force, i.e., high relative velocities.

The main reason for the use of such experimental systems is that it is difficult to obtain accurate measurements of the ballistics of small drops in free flight. Gauvin[52], for instance, has stated that "since it is easier

to measure the velocity of a fluid than a particle, a solution to the drag coefficient problem was sought by somehow measuring the force on spheres suspended in a laminar fluid stream". Khudyakov has also commented on the difficulty of obtaining accurate data on the velocity history of drops.

However, at the beginning of this investigation, it was hoped that with the proposed photographic technique which would be described subsequently, it might be possible to obtain very precise size-time and distance-time records of drops as small as 50 μ . An experimental program was envisaged in which curves of drag coefficient against Reynolds number would be obtained for a wide range of Reynolds numbers and for transfer numbers ranging from 5 to 30. It was found later that the full scope of the photographic system could not be realised due to the mutual interaction of the various parts of the experimental system, i.e., the photographic system, the illumination system, the igniter and the drop producer.

Ingebo[6] has experimentally studied the drag coefficient of drops in a rocket motor. But his investigation was on drop clouds and not single drops and his observations were with respect to a steady process and he had no problems of synchronising his observational apparatus to his process. The only photographic investigation of single falling drops

in controlled atmospheres is that by Bolt.[47]

He obtained the diameter history of drops using three camera stations and a sophisticated synchronisation system. The difficulties in applying his system for the purpose of obtaining ballistics is that one camera station is needed for each observation while a large number of observations are required for precise acceleration measurements. It was found in this investigation that position data for 5 points in time was rather inadequate for the purpose of obtaining accurate polynomial approximations to the distance-time function described by the drop.

For drag coefficient measurements, great accuracy in knowledge of the time between successive drop positions is required. This is because such measurements require the second derivative of the position histories of drops while for combustion rate experiments, only the first derivative of the drop size history is required. Even for combustion rates, only few investigations have been reported with drops in flight.

Thus, the major difficulties in obtaining the experimental data in this investigation were (a) the need to observe accurately the diameter and position histories of drops over a distance of 3' with a single camera (b) the need to synchronise the fall of the drop with the operation

of the camera, and, (c) the need to have very precise knowledge of the duration between conseoutive light flashes.

III.1 Experimental Programme

The experimental programme consisted mainly of the study of the drag force on single drops of pentane, heptane and benzene burning with envelope flames, falling freely in quiescent oxygen atmospheres over a Reynolds number range between 100 and 400. The free fall of burning pentane drops was also studied in oxygen-nitrogen atmospheres with 65% and 75% oxygen.

Results were also obtained for wake flames of drops of all these fuels for a variety of oxygen atmospheres, but no definitive study was made as such flames were unsteady and the theory of drops burning with wake flames was much less advanced than that of envelope flames.

This overall programme was pursued for the following reasons:

(a) Use of freely falling drops

It is possible to study the combustion rates of small supported drops. But it is not possible to directly measure the minute drag force on supported burning drops. Therefore, it was decided to obtain data on the ballistics of drops falling freely and infer the drag force from such data.

(b) Use of drops

The investigations reported so far on the drag force on burning surfaces refer to supported spheres and cylinders at Reynolds Numbers of the order of thousands. As such values are far in excess of those obtained in practical combustion and as data from these investigations cannot be extrapolated to lower Reynolds Numbers due to the different ratios of form drag to film drag, it was desirable to directly measure drag force on drops, even though the experimental work was much more difficult in view of the transient nature of the experimental process.

A further reason was that atmospheres with very high oxygen percentages were to be used, and it was not practical to obtain steady streams with such oxygen contents in a wind tunnel.

(c) Use of single drops

It was decided to study single drops rather than streams or clouds as such a study would obviate complications associated with drop clouds, such as interference between drops, non-uniform atmospheres, etc. One fact in favour of experiments with clouds is that methods for producing clouds of particles of known size are more developed than methods of single drop production.

(d) The cold atmosphere

As the main independent variable in the problem under study was the intensity of combustion , it was decided to vary the intensity in a series of experiments and obtain curves of drag coefficients-Reynolds numbers for each intensity of combustion, characterized by the parameter "Transfer Number". (See Chapter II for a definition of "Transfer Number".) This procedure could have been achieved by using atmospheric air and a hot experimental chamber, as described by Bolt[47], or, by varying the oxygen percentage in the experimental chamber, or, a combination of both. It can be seen from tables I and II, that a greater range of Transfer Numbers could be obtained by variation of oxygen percentage than was possible by temperature control alone. Thus, to obtain an adequate range of Transfer numbers, one had to vary the oxygen percentage, with or without the use of a hot chamber.

The use of a hot chamber involves problems of temperature non-uniformity and control within the chamber, natural convection, the relative inflexibility of the heavy chamber, and the possibility of erratic drop trajectory within the chamber.

Table I. Variation of Transfer Number with Oxygen Percentages in the Gas mixture

entane, introduced at 15°C, Gas temperature - 15°C.

Percentage O_2 (by mass)	Transfer Number
23	8.56
50	18.76
75	28.07
100	34.43

Table II. Variation of Transfer number with temperature of the Gas mixture

pentane, introduced at 15°C. Atmospheric Air.

Air Temperature °C.	Transfer Number
15	8.56
100	8.76
200	9.075
300	9.35
400	9.63
500	9.90
600	11.17
700	11.45

An additional factor entering into the choice of the type of chamber is the 'extinction velocity' of a burning drop. With the information available it was not possible to predict extinction velocities with any accuracy for small drop sizes, high temperatures and enriched oxygen atmospheres.

A hot chamber would permit higher extinction velocities than a cold one for identical oxygen concentrations, but the degree of advantage could not be foreseen and it was, therefore, decided to use a cold chamber.

(e) The Reynolds number range over which experiments were carried out was between 100 and 400. At higher Reynolds numbers, drops become non-spherical, and it was difficult to evaluate the drag coefficient accurately with the sharpness of drop images that could be obtained. At Reynolds Numbers below 100, it was difficult to reproduce the trajectories to the increased accuracy demanded for small drops by the photographic system.

(f) Experiments were conducted in conditions of free fall. It was obviously desirable to be able to impose arbitrary velocities on drops, instead of studying them only under the velocities obtained due to gravity alone. Such experiments would have involved the use and control

of airjets through the nozzle in which the drop was being produced. It was found that the use of such airjets prevents the realization of reproducible trajectories.

(g) The range of oxygen percentages used could not be extended below 65 as it was not possible to stabilize envelope flames at lower oxygen percentages. Within the 65% - 100% range experiments were not conducted at a larger number of intervals as it was found that the drag coefficients did not vary significantly over this entire range.

III.2 Experimental Techniques and Apparatus

The experimental system consisted of single burning drops falling through cold, stationary oxygen enriched atmospheres.

To measure the drag coefficient of a drop under this system, it is necessary to obtain accurate distance-time records and 'size-time' records of the drop.

This object was achieved by using a photographic system. By this system, a number of silhouettes of a burning drop, were obtained, all on one plate, corresponding to several instants in time, as the drop

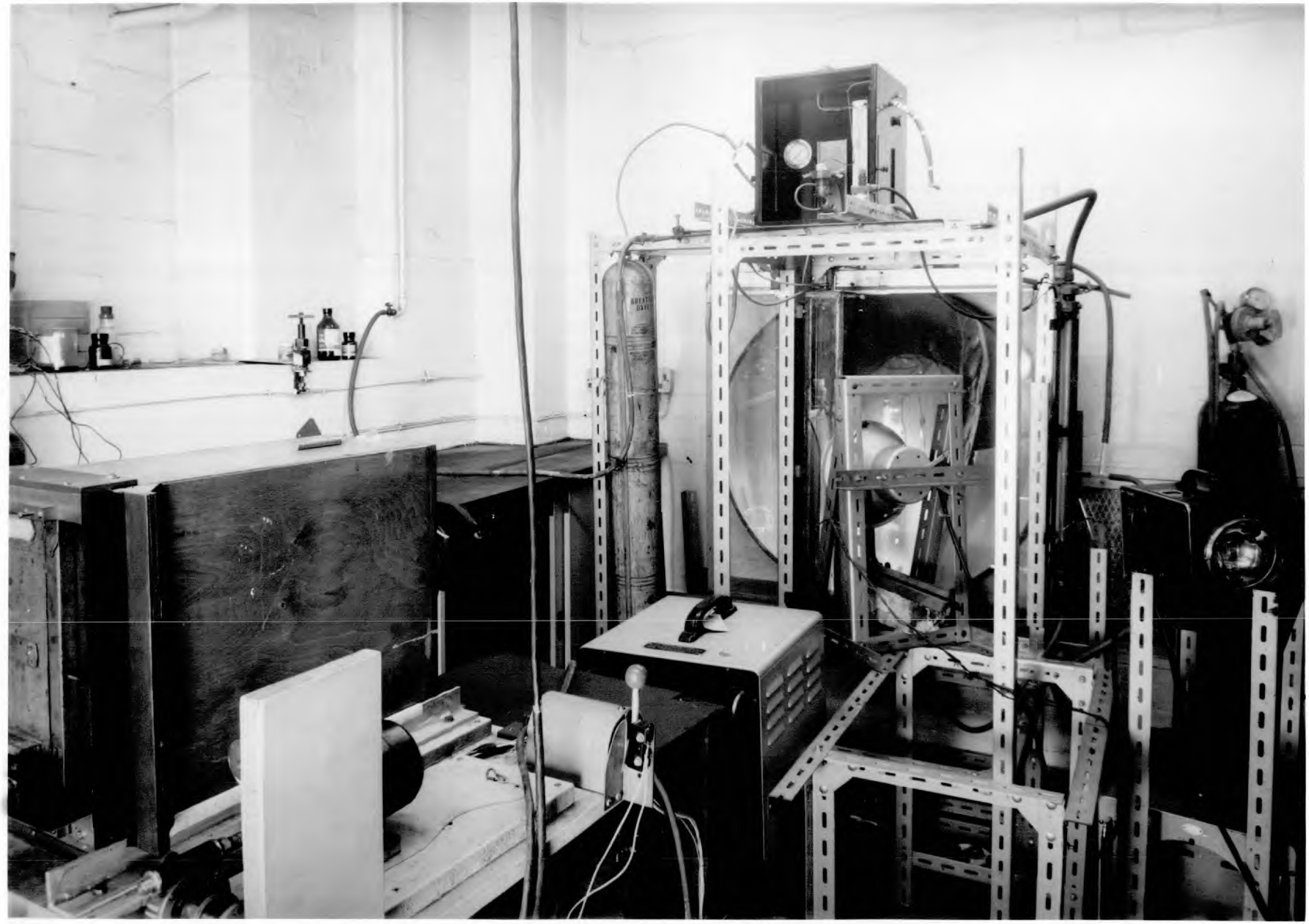
fell freely in a chamber containing a controlled atmosphere. The positions of drop images on the plate were accurately measured by using a travelling microscope. The illumination was by a flash tube operated by a Dawe Stroboflood unit and triggered by a Strobo flash. Single drops were produced by a microburrete apparatus. The drops fell through an ignition tube in which town gas was burned in an oxygen enriched atmosphere and then through a slow transverse current of oxygen into the experimental chamber.

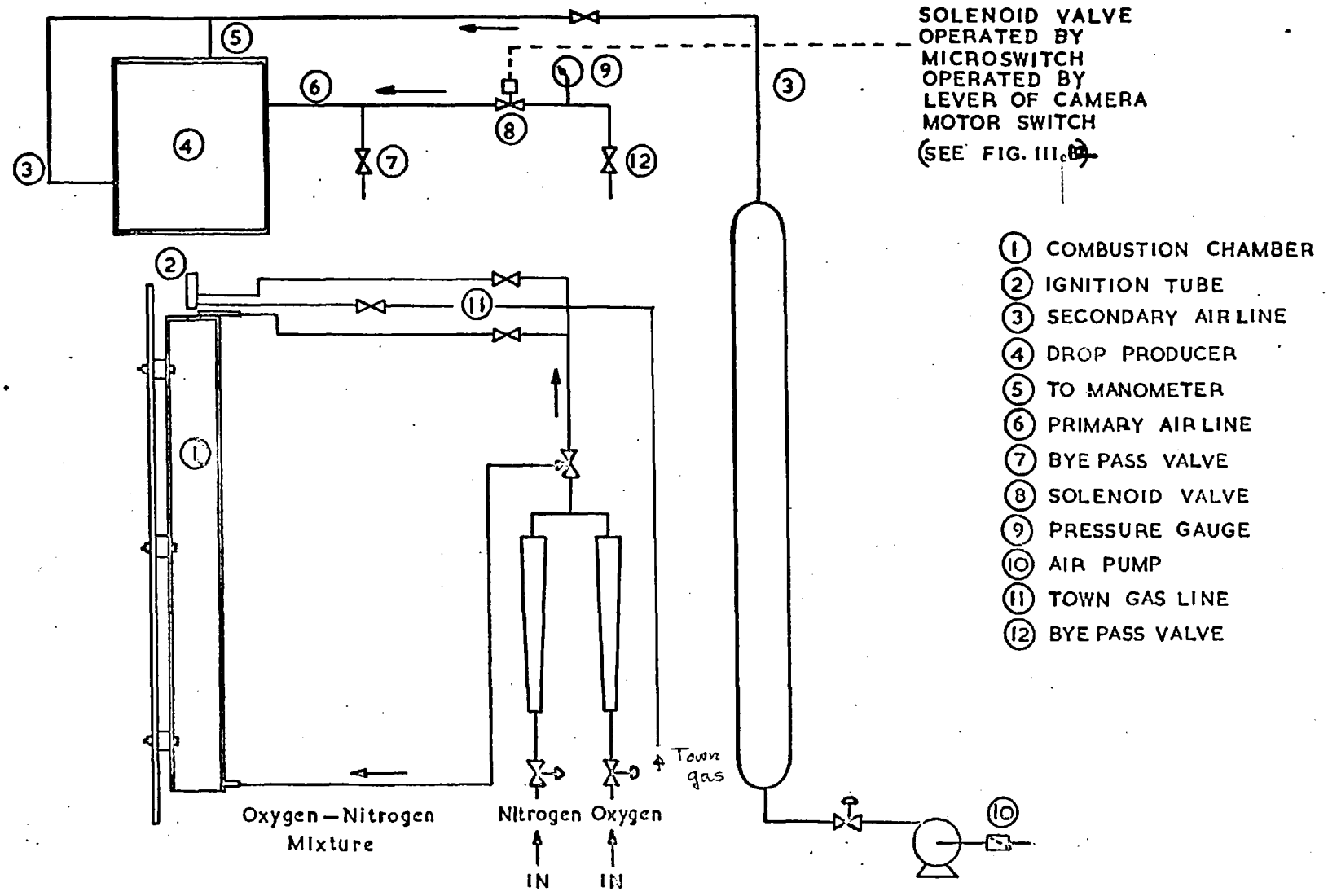
III.2.1 The combustion chamber

The combustion system comprises of the drop producer, the ignition tube and the combustion chamber. They were arranged in the manner shown in Fig. III.2.

The chamber is of dimensions 3' x 4" x 3". It consists of a skeleton made of brass angles and covered on two opposite sides and the top and bottom by brass strips and on the other two sides by optical grade plate glass. An opening of dimensions 2" square is cut into one of the brass sides and covered with gummed paper during the experiments and served as an explosion vent.

III.1 General view of apparatus





SCHEMATIC DIAGRAM OF COMBUSTION SYSTEM

FIG. III. 2

The sides exposed to the camera consist of optical grade glass plates of area 3' x 3" and $\frac{1}{4}$" thick. The plates are held against the side of the frame by means of two short brass angles at the top and bottom. The gaps between the glass and the side of the frame are sealed by strips of plasticine running along the entire length of the chamber.

The top and bottom of the chamber are covered with brass plates of area 5" x 4" and $\frac{1}{8}$" thick with a $\frac{3}{8}$" diameter hole in the centre. Originally it was intended to permit the drops to fall through and out of the chamber by this arrangement. Subsequently, due to difficulties in control of drop trajectory and in the operation of shutters that were intended to open the chamber only for the duration of drop fall, the use of shutters was discontinued and the bottom hole was closed up and the top hole was always left open. A layer of silica cement was spread on the bottom plate to prevent the ignition of the brass strip or the plasticine which was used for sealing the chamber. In view of the very rich oxygen atmosphere which was used in most experiments, ignition does sometimes occur on contact with the burning drop.

The chamber was bolted on to a wooden board. The board was in turn bolted on to two vertical handy angle sections in a manner which permitted control of the vertical level of the chamber and also its inclination.

The controlled atmosphere is admitted through tubes at the bottom of the chamber. The arrangements for feeding the controlled atmosphere to the chamber are shown in Fig. III.2.

III.2.2 The drop producer

It was required to produce small single drops. It was originally intended to conduct experiments with drops as small as 50 microns in diameter.

The apparatus finally adopted for drop production was similar to a microburette apparatus described in an unpublished report by Abberton[53]. Experiments were first conducted with the drop producing apparatus of a type due to Lane[54]. Since the Lane apparatus is the earlier one and is based on the same principle, its description will be given.

The Lane apparatus used airflow around the drop forming at the end of a capillary to augment the downward pull of gravity. When a hypodermic needle is charged with liquid, the liquid drains out of the tip under the force of gravity, but remains attached to the tip by surface tension force. The drop is detached from the tip when the weight of the drop overcomes the surface tension force. The weight of the drop thus formed is given by the relation:

$mg = 2\Pi r_t T' f(r_t/a)$ where,

r_t = radius of the tip,

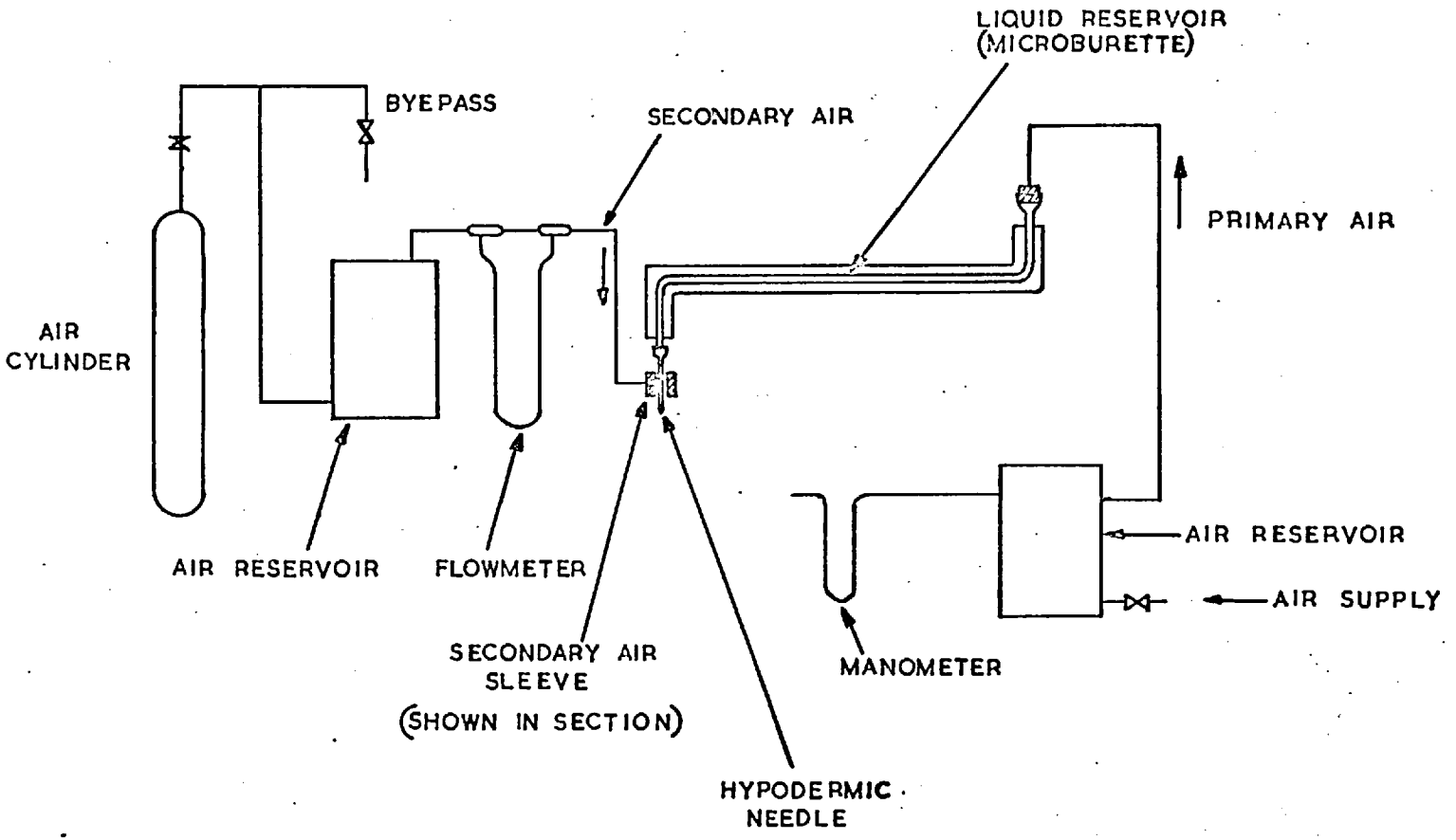
T' = surface tension of the liquid,

$a^2 = 2T'/\rho_l g$ = capillary constant of the liquid,

ρ_l = density of the liquid.

Harkins and Brown[55] have published experimentally determined values of the function $f(r_t/a)$ for a series of values of r_t/a and these values could be used to calculate the size of drops produced by any given capillary tip and a liquid of known surface tension and density.

Lane calculated that under the conditions of applicability of Harkins and Brown relationships, spherical drops of Apiezon oil of 1 mm diameter would call for a capillary tip of external radius of 0.01 mm.



THE LANE APPARATUS FOR PRODUCTION OF DROPS

FIG. III. 3

As it was then impossible to use capillaries of this diameter, he devised an apparatus in which the gravitational pull was augmented by the drag force exerted by the air stream around the drop. The Lane apparatus is shown in Fig. III.3.

The Lane apparatus employed a hypodermic needle attached to the end of a burette with two right angle bends to facilitate the maintenance of a uniform hydrostatic head, and airflow through a nozzle coaxial with and around the hypodermic needle. The burette was charged with the fuel which flowed through the hypodermic needle at a rate depending on the hydrostatic head and the pressure applied to the liquid reservoir. The experiments with the Lane apparatus showed that over the range of drop sizes of interest to this investigation both (i) the instant of drop shedding, and, (ii) the trajectory of the drops could not be easily controlled. An important requirement in this investigation was that it should be possible to direct the drop vertically downward for a distance of about 5'.

The Abberton apparatus which was finally used, operated on the same principle as the apparatus already described, but was more advanced in the following two details :

(i) Finer capillaries were used, thus making possible the production of drops of a required size with much lower nozzle air velocities, and,

(ii) the nozzle diameter was larger and controllable and it was easier to centre the capillary in the nozzle.

The rate of liquid flow out of the capillary is controlled by the pressure of primary air applied to the liquid reservoir, and the drop size by the capillary tip diameter and the velocity of secondary air at the nozzle. It was felt that this apparatus would allow production of drops down to 50 μ in diameter and also a clear control over the frequency of drop production and the trajectory.

The Abberton apparatus was developed for micro-biological research. When used in conjunction with the igniter, the fuels, and synchronization system and the photographic arrangement of this investigation, it was found that the full potential of the apparatus in terms of smallness of drop size could not be realized. The complete system could only be used for the study of drops with an initial size of not less than about 500 μ. The reasons for this limitation are as follows:

(1) As pointed out earlier the photographic system dictates that the drop should fall a distance of about 5' without a transverse movement in excess of $\frac{1}{4}$". When secondary air supply was used, it was very difficult to achieve such precision of trajectory. Even though the reproducibility of trajectory was better than with the Lane apparatus, it was still inadequate. Therefore, the use of secondary airflow for drop size control was abandoned and reliance was placed solely on the use of capillary tips of various degrees of fineness. Therefore, the lower limit of drop size attainable was considerately raised.

(2) Another factor which raised the size of smallest drops attainable was the very low surface tension of the liquids used which invalidated the application of the Harkins and Brown relation quoted earlier for drop size. The only dimension of the capillary tube that entered this relation was the external radius of the tip. This relation rests on the assumption that a growing drop would only wet the tip of the capillary and not the side. The liquids used in this investigation were pentane, heptane and benzene, with surface tension values of 15, 20 and 29 dynes/$_{cm}$ respectively at 20°C in contact with air, compared to 74 dynes/$_{cm}$ for water.

Therefore, these liquids had a much greater tendency to spread. On inspection, it was found that the liquid flowing out of the capillary tip did not accumulate at the tip, but crept up on the outer surface of the capillary, and accumulated in the form of a ring some distance above the tip. Therefore, the size of drops shed would correspond to a complex relation and would be a function of capillary tip diameter, liquid flow rate and the outer profile of the capillary tube.

Attempts were made to suppress such liquid spreading by coating the outer wall of the tube with a number of materials of low surface energy. It was found that even a material with as low a surface energy as that for 'Fluon' did not suppress spreading with heptane, and therefore, surface chemical means of drop size control could not be used, and the drop sizes were larger than would be indicated by the Harkins and Brown relations if one used the tip diameter.

Further, as the drop size depended on the profile of the capillary tube and not just the tip, and no two tubes were identical, the results with two tubes with the same tip diameter were not the same and the synchronization system had to be set up by trial and error for each capillary tube.

(3) After leaving the capillary tip, the drops fell through an ignition tube traversed by hot combustion products. This current of hot gases caused the drops to deviate from a vertical trajectory and the deviations did not occur in a reproducible fashion. As the degree of deviation increased with the decrease in drop size, work with very small drops was not convenient.

(4) The nature of the synchronization system further discriminated against the study of small drops. The system to synchronize movement of the plateholder with the time of fall of the drop rested on the assumption that after the application of primary air pressure to the capillary, a drop will be detached from the tip in a reproducible time interval. The time intervals permissible were between $\frac{1}{4}$ and 1 second. As the fuels used were very volatile, their rate of evaporation from the tip was comparable to their rate of flow from the capillary at the setting for small drops and not reproducible. Therefore, the time lag between the application of primary air pressure and drop shedding was not exactly reproducible, and the synchronization system became unreliable.

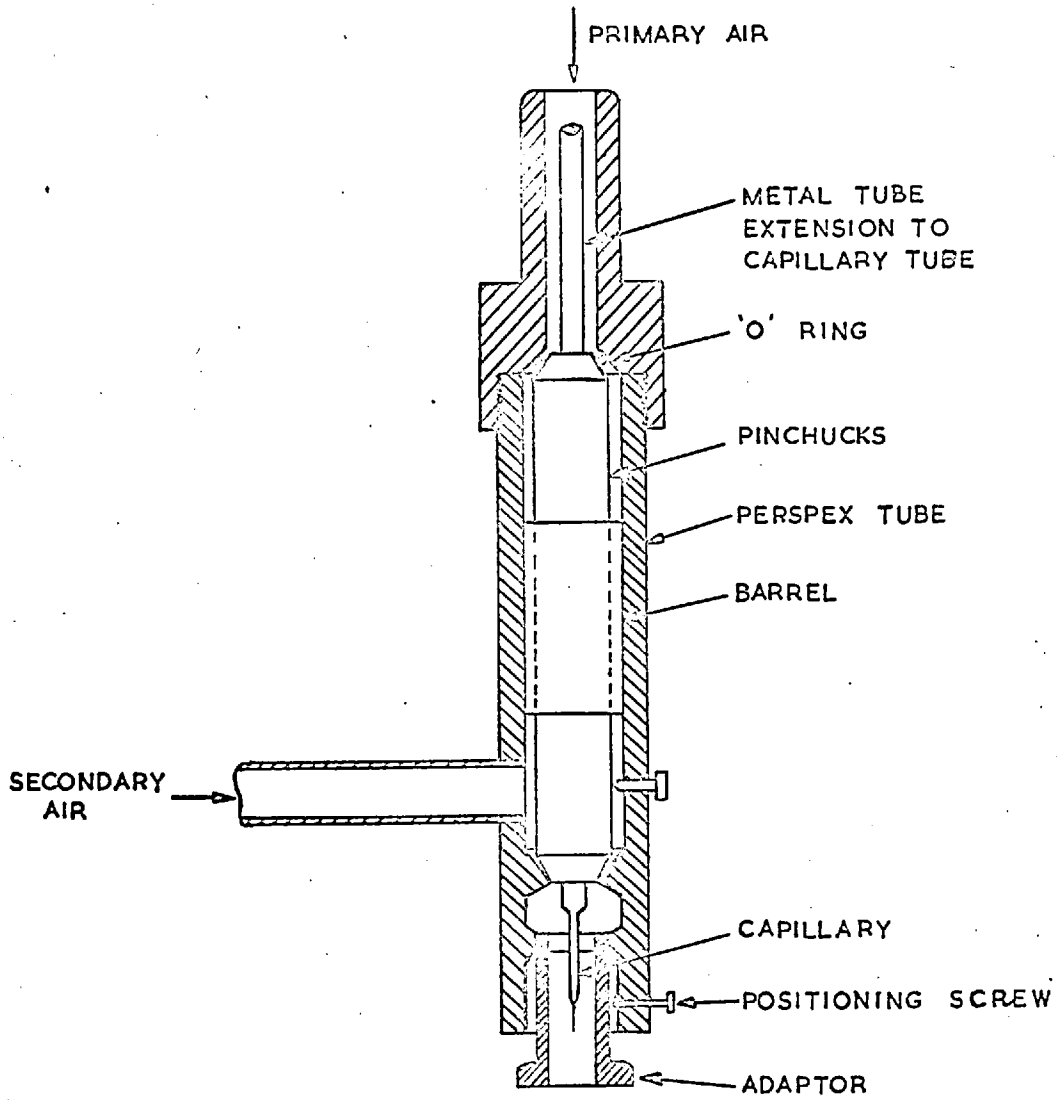
The production of small drops also called for very fine capillaries and these tended to get clogged up and change their pressure drop characteristics very soon after installation and invalidate the synchronization system.

(5) The capillary tip diameters for the production of 100 micron drops of pentane are of the order of 10 microns. Apart from clogging difficulties, such capillaries were extremely fragile and this made their use very difficult. Because of the high volatility of the fuels, and the resulting evaporation from tip, moisture condensed on to the region of the tube near the tip, and this made the fineness of the tube ineffective the regard to drop size. The condensed dew had to be frequently wiped off the capillary tip and this could not be done safely for very fine capillaries.

(6) While the tendency to deviate from a desired trajectory increased with reduction of drop size, precise adherence to such trajectories became more important for small drops, from the point of view of photography to record the drop size accurately.

Thus, the overall drop producer - igniter - photographic system for the production of burning drops falling with a vertical trajectory was inexact in operation. The system became increasingly difficult to operate successfully with decrease in drop size and the smallest drop size which could be studied was 500 μ. Even above this drop size and throughout the range of drop sizes, only a small proportion of plates exposed were successful. The capillaries needed frequent replacement due to breakage and clogging and, for each drop size, a different capillary had to be employed. Each new capillary called for setting up of the primary air pressure and the synchronization system by trial and error photographically.

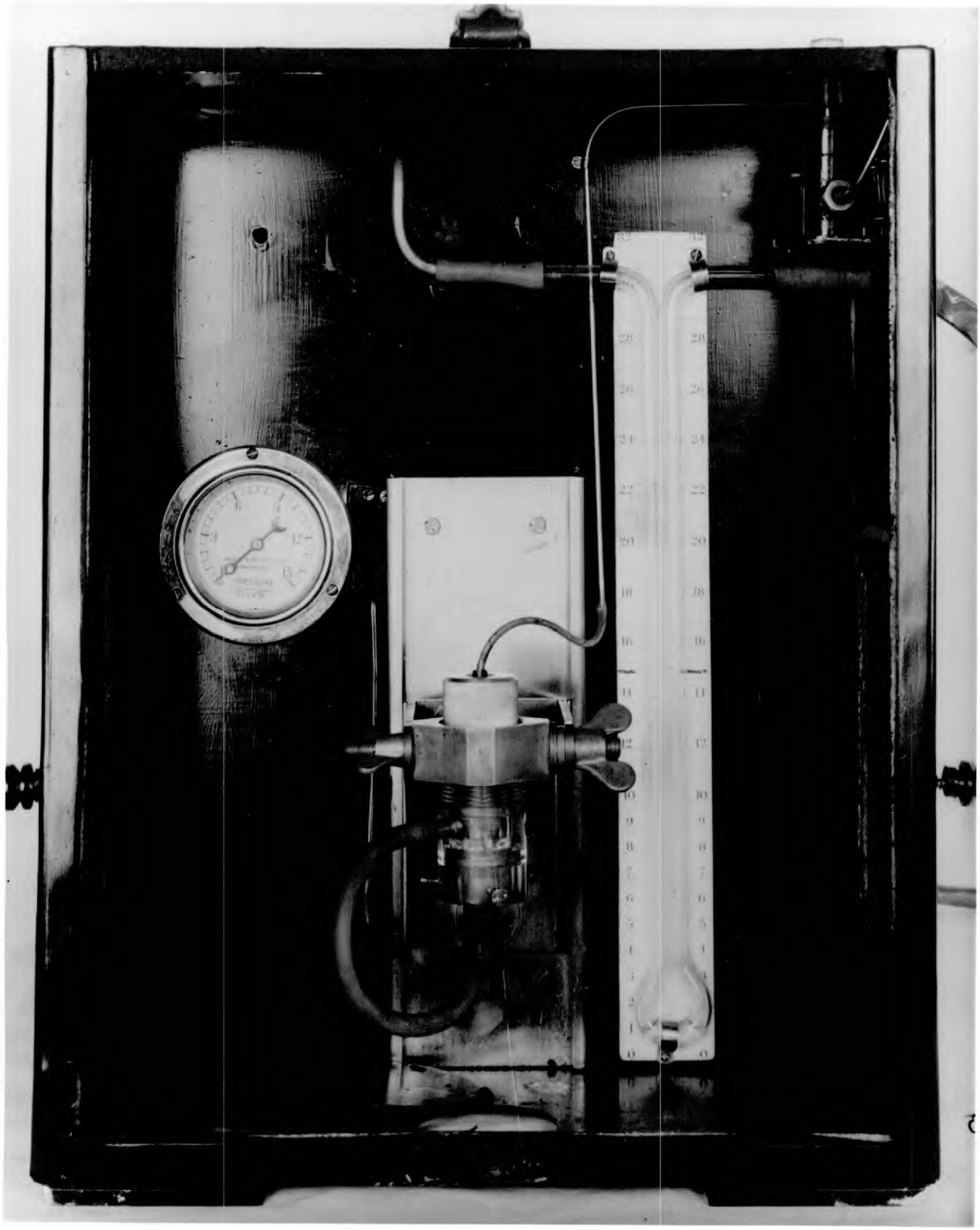
The drop producer is shown in Fig. III.4 and III.5. The drop producer moves vertically in a guide built in a steel supporting box which houses the primary and secondary air control arrangement, the pressure gauge for primary air, and a manometer for secondary air. The air flow for the drop producer is schematically depicted in Fig. III.2.



THE DROP PRODUCER

FIG. III. 4

III.5 The drop producer. Photograph.



The capillary is held in place by two pin chucks screwed on to a barrel as shown in Fig. III.4. The pin chuck device fits inside a perspex tube with a very small clearance and rests on shoulders in the tube. A primary air attachment can be screwed on to the perspex tube. The lower part of the perspex tube is sealed from the primary air supply by an 'O' ring placed between the top pin chuck and the primary air attachment.

Secondary air enters the perspex tube through a side tube and passes down towards the capillary tube through holes cut into the shoulder support for the pin chucks. An adaptor can be loosely screwed into the bottom of the perspex tube and then accurately positioned by means of three screws placed around the circumference of the perspex tube. The adaptor can receive on iris diaphragm which enables control of the size of opening of the secondary air orifice around the capillary. The capillary is made by drawing out a glass tube in a micro-electrode puller of the type marketed by C.F. Palmer (London) Ltd.

Use of metal extensions to capillary tube

The glass capillary tubes were found to have a very small storage capacity for liquids, necessitating frequent recharging and were also very fragile. Therefore, it was found desirable to insert the short capillary tubes in a brass tube 7" long and seal the gap between the brass and capillary tubes with Araldite. This provided for larger time intervals between charging and greater ease in handling of the capillaries. Due to the very small bore of the capillaries, they clogged up very easily. A length of cotton thread inserted and packed inside the capillary served as a rudimentary filter.

III.2.3. Ignition

Ignition of drops before entry to the chamber was achieved as the drops fell down an ignition tube in which town gas was burned in an enriched oxygen atmosphere.

Initially it was decided to obtain an ignition device which would not disturb the drop trajectory. It was felt that a simple way of achieving this would be to use the repetitive sparks from the electrode of a high frequency sparking unit of the type used for vacuum testing.

The model T2 high frequency tester manufactured by Edwards High Vacuum Limited was used in the preliminary experiments. It was found that large drops (> 2 mm) could be ignited by this method, but not small drops.

The spark gap was very small and the spark was weak and, therefore, the drop had to travel precisely across the spark for satisfactory ignition. As it was difficult to control drop trajectories correct to fractions of a millimeter, this method of ignition had to be abandoned. Large drops had a greater probability of travelling across or, in the neighbourhood of, the spark gap and further left behind a trail containing a greater volume of gas and therefore ignition was easy.

The next arrangement used was an ordinary horizontal gas flame with a tube discharging a jet of oxygen immediately below and parallel to the gas jet.

The drops were successfully ignited by this arrangement, but as the work progressed, it was found that the flame did not completely envelope the drop. As the wake flame on the drop was unsteady in the sense that the position of the flame on the drop progressively changed as the drop travelled down, and as such unsteadiness could not be studied in a controlled fashion, it was decided to study mainly the influence

of envelope flames on the drag coefficient.

To facilitate this, a high intensity igniter was finally employed. The igniter consisted of a vertical steel tube 3" long and placed with the same axis as that for drop fall (Fig. III.2) and the igniter was traversed by the products of combustion of town gas and oxygen in a counter current fashion with respect to drop travel.

It is believed that falling drops were ignited in the following manner after their passage through a flame from a horizontal burner: the drop is subjected to high temperatures for a very short period and only a small amount of vapour is produced and a flame is obtained in the region of maximum vapour concentration, i.e., the wake behind the drop. The flame thus attached to the drop causes an increase in vapourization in its immediate neighbourhood and, therefore, the flame progressively diverges away from the rear stagnation point of the drop till it completely envelopes the drop. This process indicates that if the drop were to be subjected to high temperature conditions for a long enough period, envelope flames could be attained before the drop leaves the igniter.

This reason led to the use of an igniter which ensured that the drop will fall for about 3" in conditions of high temperature and oxygen concentrations. This was adequate for the production of envelope flames.

The igniter tube was of brass $\frac{3}{4}$" diameter and 3" long and was attached to the top of the combustion chamber by two brass angles. A clearance of $\frac{1}{2}$" was allowed between the bottom of the igniter tube and the top of the combustion chamber to prevent the atmosphere in the combustion chamber from being disturbed by the current of burning gases in the igniter. During an experiment, a slow traverse current of oxygen is passed across this gap to prevent the extinction of the burning drop leaving the igniter before it enters the oxygen-rich atmosphere in the combustion chamber, oxygen and town gas are fed to the igniter and burn inside. Envelope flames and side flames are shown in figs. III.15 and III.16.

III.2.4. Photographic Technique

The bulk of the work done on the drag force on bodies in relative motion to fluids used experimental techniques in which the object was attached to some form of force measuring device with the fluid streaming past the body in a wind tunnel and the object was stationary during an experimental observation.

Only a few investigations deal with freely falling drops due to the obvious reason that a transient process is more difficult to study. Khudyakov [4] measured the drag force on burning spheres wetted by fuels and attached to a leaf spring in a wind tunnel. With regard to the study of burning drops, he commented "Experimental investigation of actual drop in flight is difficult to achieve as it is impossible to make the necessary observations and measurements during its short duration in flight".

But such study has become possible since the development of electronic and photographic techniques for the study of movement. It was desired to study drop fall over a distance of about 3' and, therefore, a conventional cinematographic technique would be unsuitable because the large field/image ratio precludes measurements of drop size and position with sufficient precision.

An experimental technique for studying the combustion rates of freely falling drops was reported by Bolt [47]. The falling drops intercepted a light beam and caused a photomultiplier to actuate a flash-lamp. A camera with an open shutter received the drop image as a silhouette in a bright background provided by the flashlamp.

He had three such camera-flash tube stations and the time intervals for the fall of the drop between successive stations was obtained from an electronic arrangement which acted on the photomultiplier signals.

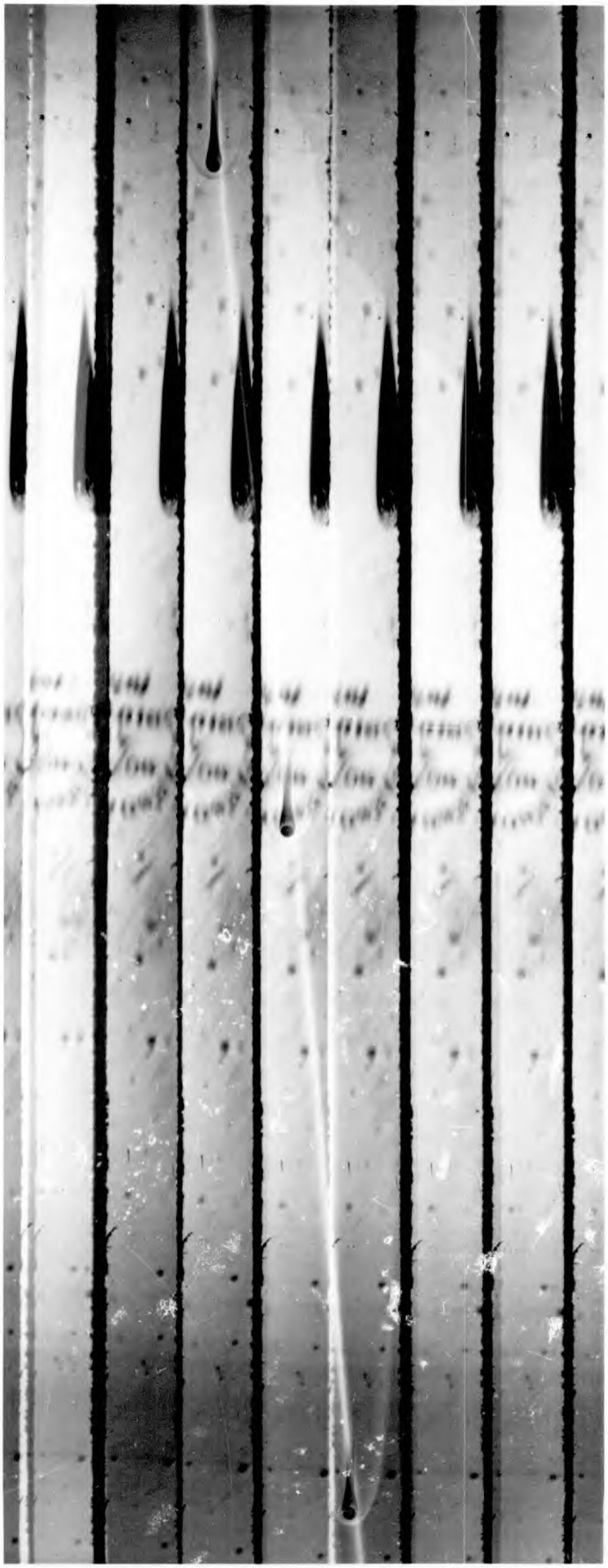
In the present investigation, it was desired to study the size and position history of the drop over its fall through 3' divided into a large number of stages so that the values of velocities derived from positions would be more nearly instantaneous than average. Therefore, an arrangement similar to that of Bolt would have become very elaborate as one camera station was required for each drop position.

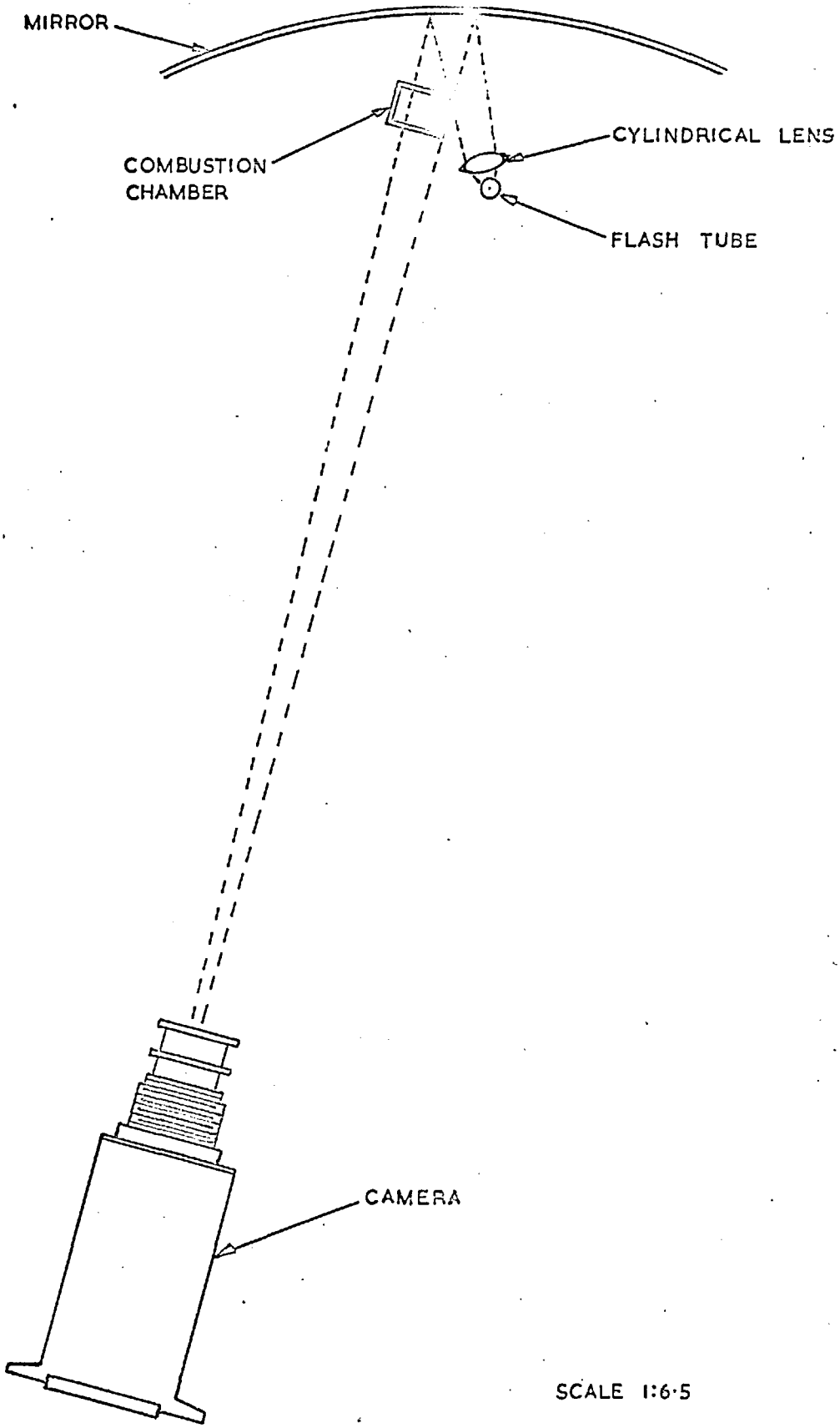
After a period of unsuccessful trials with another photographic technique, a shadowgraphic technique was developed which permitted the recording of the position and size history of the drop over its 3' fall in a single run. Repetitive illumination was employed in conjunction with a camera which was used, in effect, as a drum camera. To obtain a shadowgraph, the camera is focussed on the plane of drop fall and the camera 'sees' a silhouette of the drop against the bright background.

In normal shadowgraph work, the bright background consists of the light from a flashtube which is focussed by a condenser in such a way as to illuminate the exposed plate. This enables the maximum intensity to be derived from a given light source. The light bundle converging from the condenser covers the field to be photographed and is normal to it.

In the present investigation, such a technique had to be adopted for the study of a 3' long plane of drop fall. This was achieved by arranging for a 3' diameter searchlight mirror to focus on to the camera lens the reflected image of the spark from a flashtube. The mirror, camera, flashtube and the combustion chamber are laid out in the plan as shown in Fig. III.7. Fig. III.1 shows a general view of the entire apparatus. The camera was masked so that the plate was exposed to the process through a vertical slit of dimensions 10" x $\frac{1}{8}$". Fig. III.8 shows a close-up view of the mirror, the combustion chamber and the illumination unit.

III.6 Variation of drop position with time.

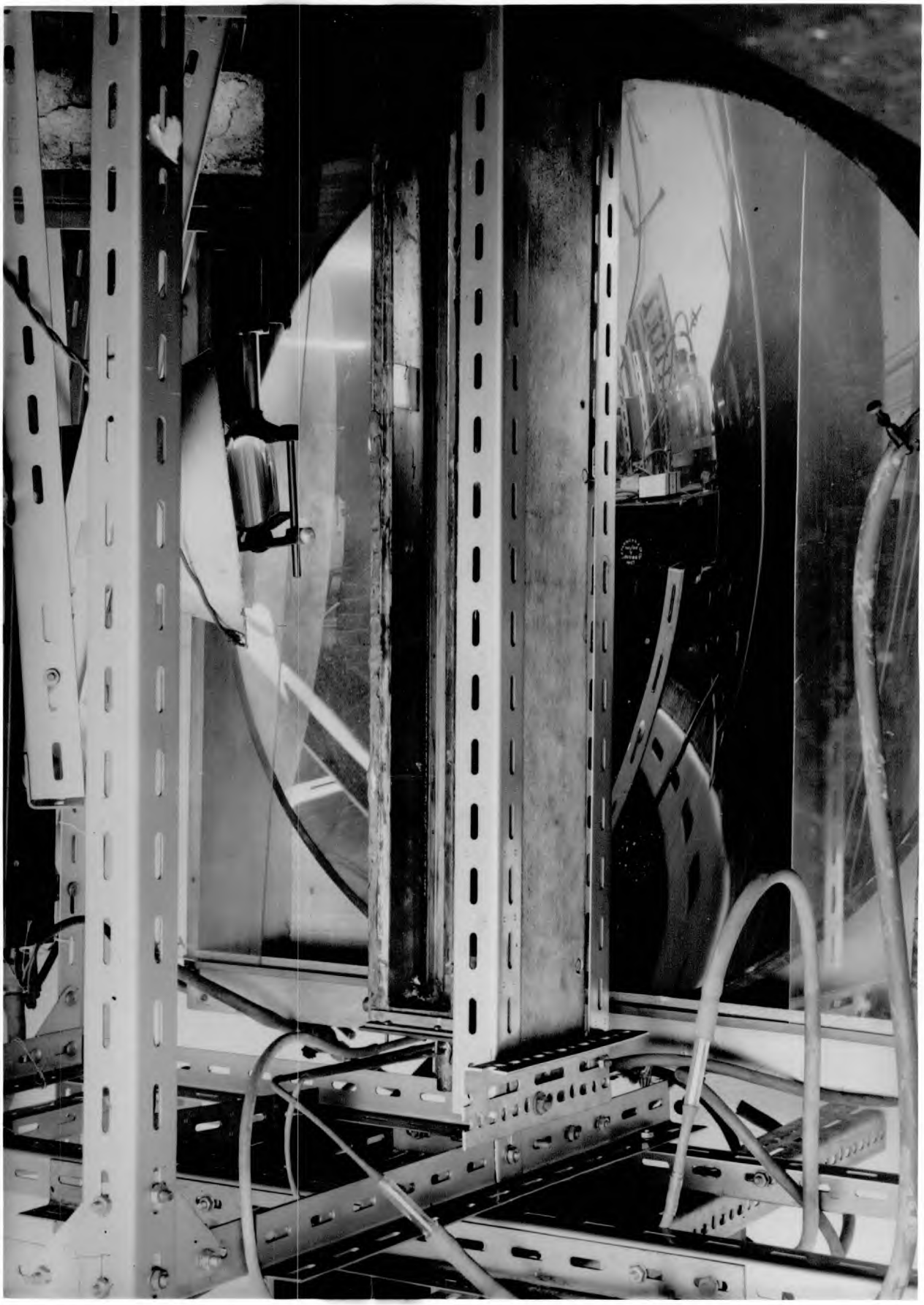




LAYOUT OF PHOTOGRAPHIC SYSTEM

FIG. III.3

III.8 View of mirror and combustion chamber.



By this method, for each light pulse, a narrow strip corresponding to the path of drop fall, was exposed on the plate, the drop image appearing as a bright circle against a dark background. The plate was moved horizontally during exposure and, therefore, a number of such strips were exposed, and the image of the falling drop appears in progressively higher positions as one proceeds from the first to the last strip in the order of exposure. Fig. III.6 shows one such distance-time record. 10" x 4" photographic plates were used and the magnification was about 0.3. Therefore, it was calculated that approximately 2½' could be studied. In fact, it was only possible to obtain information over a distance of 1½' because of certain limitations to obtaining a bright background to the drops over larger distances.

III.2.5 The photographic apparatus

The photographic system is shown in General Layout in Fig. III. 7

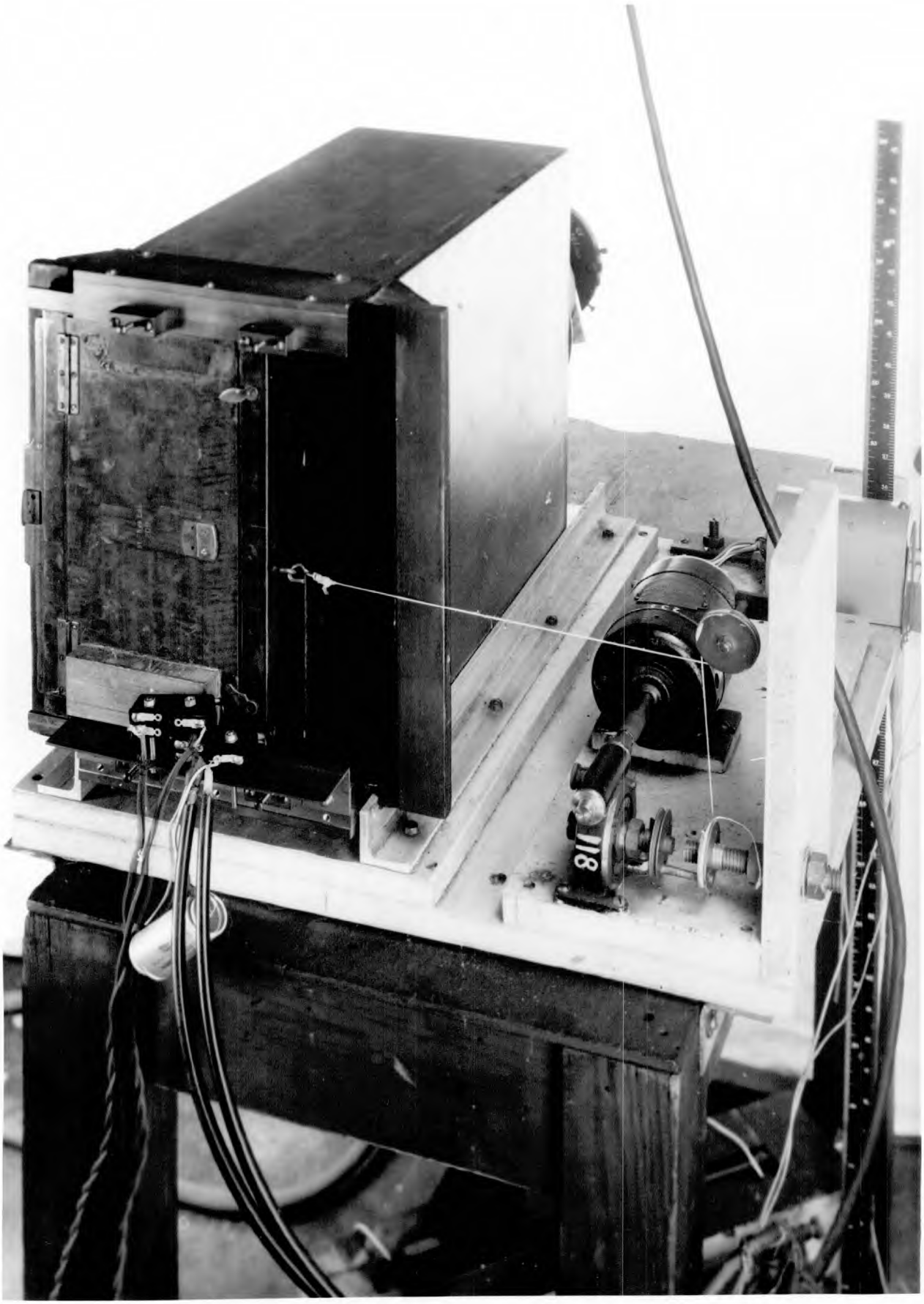
The illumination is provided by a Mazda F.A.5 flashtube connected to the capacitor of the Dawe Stroboflood, type 1201E. The Stroboflood is triggered by a Dawe Strobaflash of type 1200D.

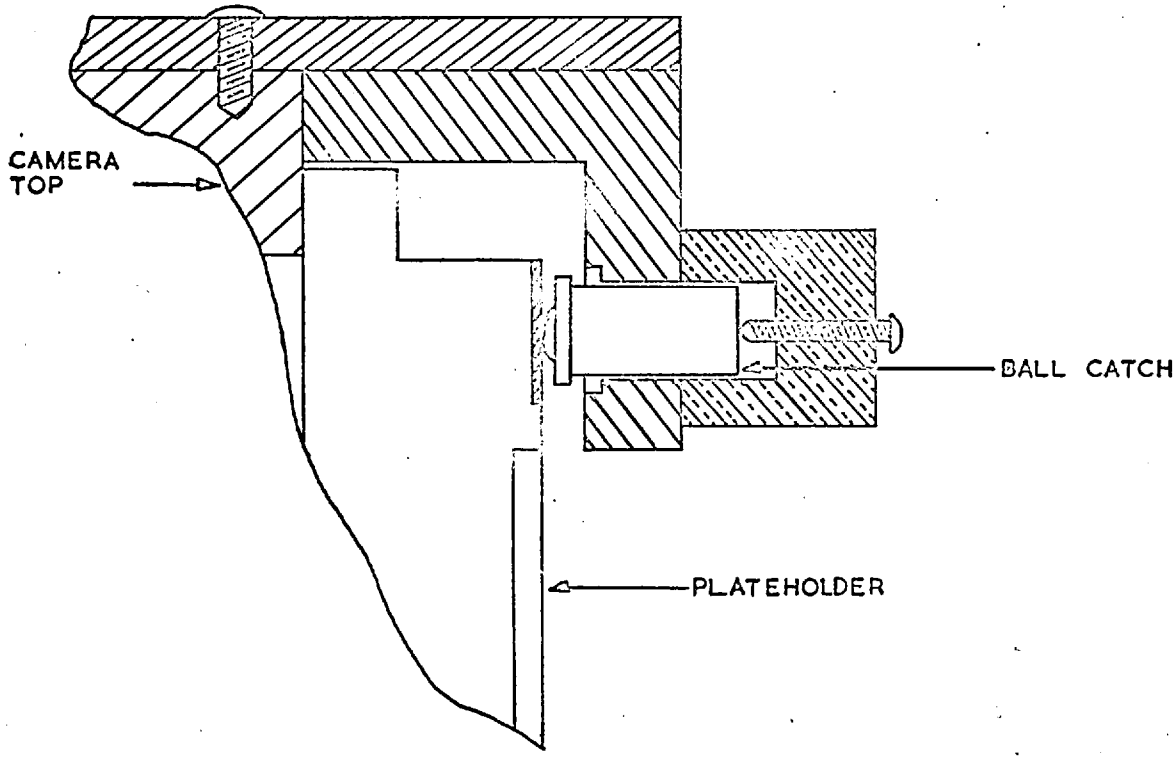
A cylindrical lens is used to narrow the light from the flashtube and project it in the form of an elipse with a vertical major axis on to a 3' diameter searchlight mirror. The mirror condenses the light into the camera lens. The line of drop fall is through this converging light beam. The camera lens is focussed on the plane of drop fall. The flashtube, the mirror and the camera lens are all in the same horizontal plane.

In practice, it was found difficult to illuminate the entire plate when working with $\frac{\text{image}}{\text{object}}$ magnifications of 0.3 and apertures of the order of f/16. This was so because the mirror did not condense the image of the flash in the form of a point, but rather more into complex shapes with dimensions of the order of inches. The maximum intensity and coverage of the path of drop fall could only be obtained by trial and error. This is probably due to the fact that the mirror was originally intended to provide a parallel beam of a light from a source close to it rather than to provide a small image of a source further away.

FORWARD
238

III.10 The Camera - rear view.


8/11



GUIDE FOR PLATEHOLDER MOVEMENT

(SIDE ELEVATION)

FIG. III. II

The Camera

The camera consists of a wooden box measuring 11" x 5" x 15" with a metal sleeve screwed on to its front. The sleeve is threaded inside and holds a brass extension containing the lens mount. (See Fig. III.9). A parfaca wide angle lens of focal length 14" is used.

The rear face of the camera is modified to make it, in effect, and drum camera. The rear face is extended in width to render the unmasked plateholder lightproof at its extreme points of travel. Attachments are made at the top and bottom to serve as guide arrangements for movement of the plateholder (See Fig. III.11)

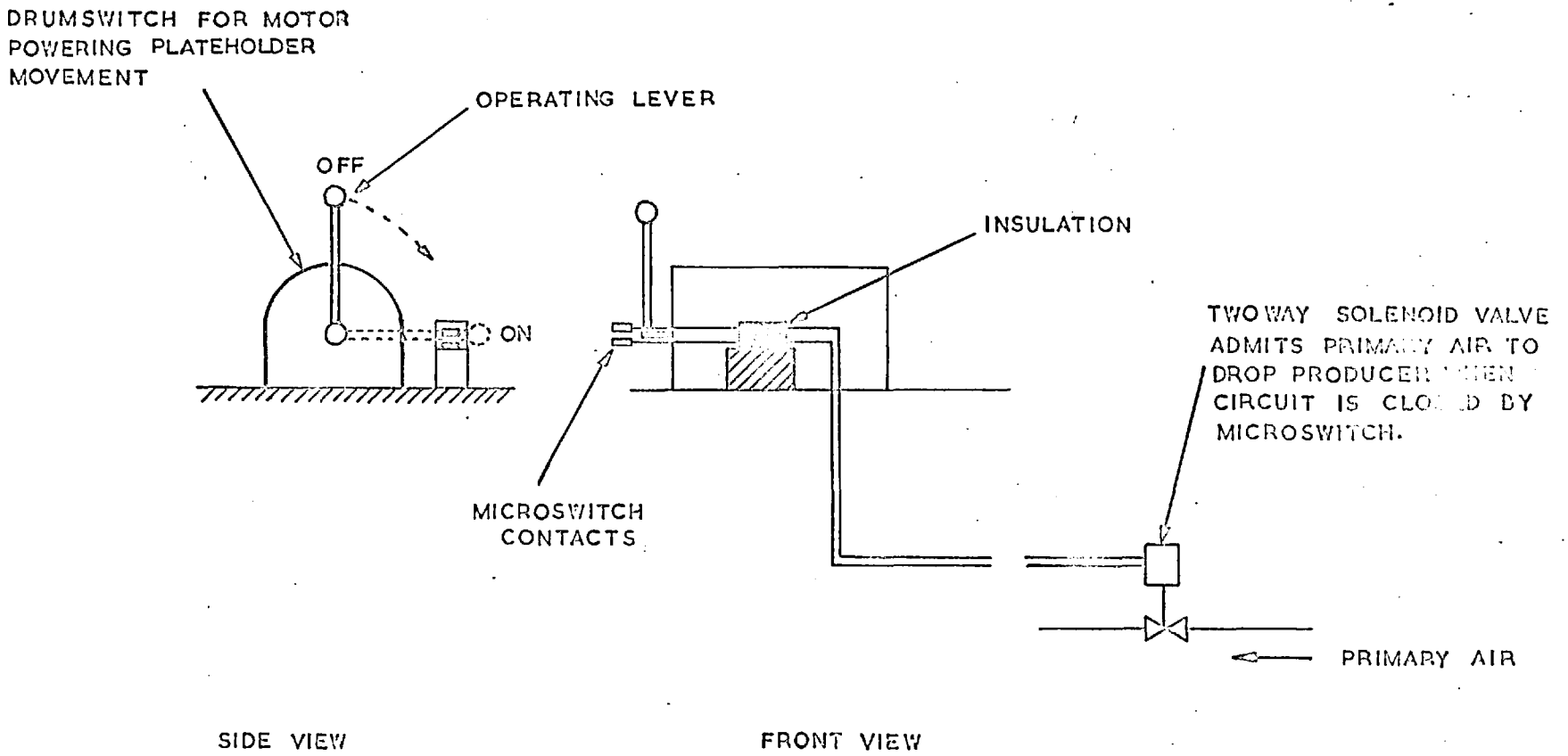
The plateholder is of the spectrographic type and can hold plates of size 10" x 4".

An 'eye' is screwed into the side of the plateholder halfway down its height. The plateholder is pulled in its guide by means of a hook engaging the eye.

A fractional Power DC motor coupled to a reduction gearing provides the motive force. The method of transmitting motion from the reduction gearing to the plateholder is shown in Fig. III.10.

The power for the motor is supplied through rheostats to control its speed. The motor was operated by a reversible drum switch. The lever of the drum switch also operated a microswitch which closed the circuit of the solonoid valve in the primary air line to the drop producer.

It was originally intended to have a mask with a vertical opening, 2 mm wide, in the rear face of the camera. But as the drop trajectories were not reproducible within the limit imposed by this width, the mask was later widened to 4 mm. With the original mask width, the maximum speed of plateholder movement would have sufficed to permit operation of the flashing unit at 3000 RPM with only a slight overlapping of exposures. With the final mask width, the maximum permissible flashing rate was of the order of 2000 RPM. This makes possible only about five images of drops with manageable sizes as they fall and, therefore, a smaller number of observations for processing, particularly in view of the use of the computer for smoothing the distance-time curves.



SCHEMATIC DIAGRAM OF SYNCHRONISATION SYSTEM

FIG. III. 12

III.2.6. Synchronization System

The camera was used in effect as a drum camera. Therefore, it was necessary to synchronize movement of the plateholder with the fall of a drop. Such synchronization could be achieved by the use of a solonoid valve operating on the primary or secondary air circuit of the drop producer. Fig. III.12shows a schematic diagram of the synchronization system. A reversing drum switch was used to start the motor which moves the plateholder. A microswitch was supported in a suitable position so that the lever operating the drum switch closed the microswitch contacts, and the microswitch operated the solonoid valve.

Initially an attempt was made to attain synchronization by using the solonoid valve in the secondary air line. The primary air pressure was to be applied for a period suitable for the accumulation of a drop of the required size at the capillary tip. Then the operation of the solonoid valve would produce a pulse of secondary air which would dislodge the drop from the capillary tip.

This method had to be discontinued as the secondary air jet jeopardised the reproducibility of drop trajectory.

The solenoid valve was then placed in the primary air line. Control over the period between application of pressure and the shedding of the drop was achieved by controlling the primary air pressure. In a number of cases, convenient synchronization also called for a time lag between the closing of the circuit of the motor operating the plateholder and actual plate holder movement. The plateholder is pulled on its runway by means of a nylon thread attached to a pulley. By arranging prior to the experiment for an appropriate amount of slack in the thread, reproducibile time delays of upto one second could be obtained between the closing of the motor circuit and the start of plateholder movement.

This method was originally developed while working with fairly large drops and, therefore, with capillaries which had a longer period of reliability. As mentioned earlier this method was not reliable for very volatile fuels like pentane. With all the fuels used, this method involved trial and error adjustment of capillary diameters, primary air pressures and lengths of slack thread in the camera drive arrangement.

The alternative would have been the adoption of an electronic system using photocell detection of the fall of a drop to initiate plateholder movement through a set of amplifiers and relays. Such an electronic system would have become elaborate, particularly in view of the fact that the flashtube which operates at voltages in excess of 2000 volts would give rise to serious interference problems. Therefore, the simpler phototransistors could not have been used. But the present synchronization system was found fairly successful with benzene at drop sizes of the order of 2000 μ. and the problems of drop producer operation at lower drop sizes could not be clearly anticipated. Therefore, the present method of synchronization system was adopted.

III.2.7 Development and measurements

The photographs were obtained with Ilford N.40 plates of dimensions 10" x 4". The photographs were developed in D.76 developer for four minutes. These conditions were chosen to obtain maximum definition.

The distance between an arbitrary datum line to the centres of drop images on the plate in a direction parallel to the long edge of the plate were measured with a 'Pye' travelling microscope correct to 0.01 mm.

The drop sizes were subsequently measured using a 'panphot' projection microscope. The magnification was of the order of 30.

III.2.8 The time monitoring system

One of the special features of the present experimental arrangement involved in the measurement of drag coefficient of drops falling in gases is the great accuracy with which time intervals between consecutive light flashes must be known.

A study of the errors in the calculated drag coefficient that could arise from a variety of errors in the performance of the experimental system is presented in Appendix (II). It is seen that the calculated drag coefficient might be incorrect to very high percentages as a consequence of quite small short term (within a range of four flashes, for example) changes in the flashing rate.

It was not possible to predict the performance of the illumination system with confidence with regard to absolute intervals in time between two light flashes and also the likely degree of variation of intervals over a period of time. The light source, the FA5 flashtube is operated by a Dawe Stroboflood unit triggered by a type 1200D Dawe Stroboflash. The reliability of the arrangement could be jeopardised at any one of these units. It can be seen from the table in Appendix (II) that a difference of 1% between the time intervals between consecutive flash pairs for drops accelerating at about 300 cms/sec could lead to the calculated drag coefficient to lie in error by 13%.

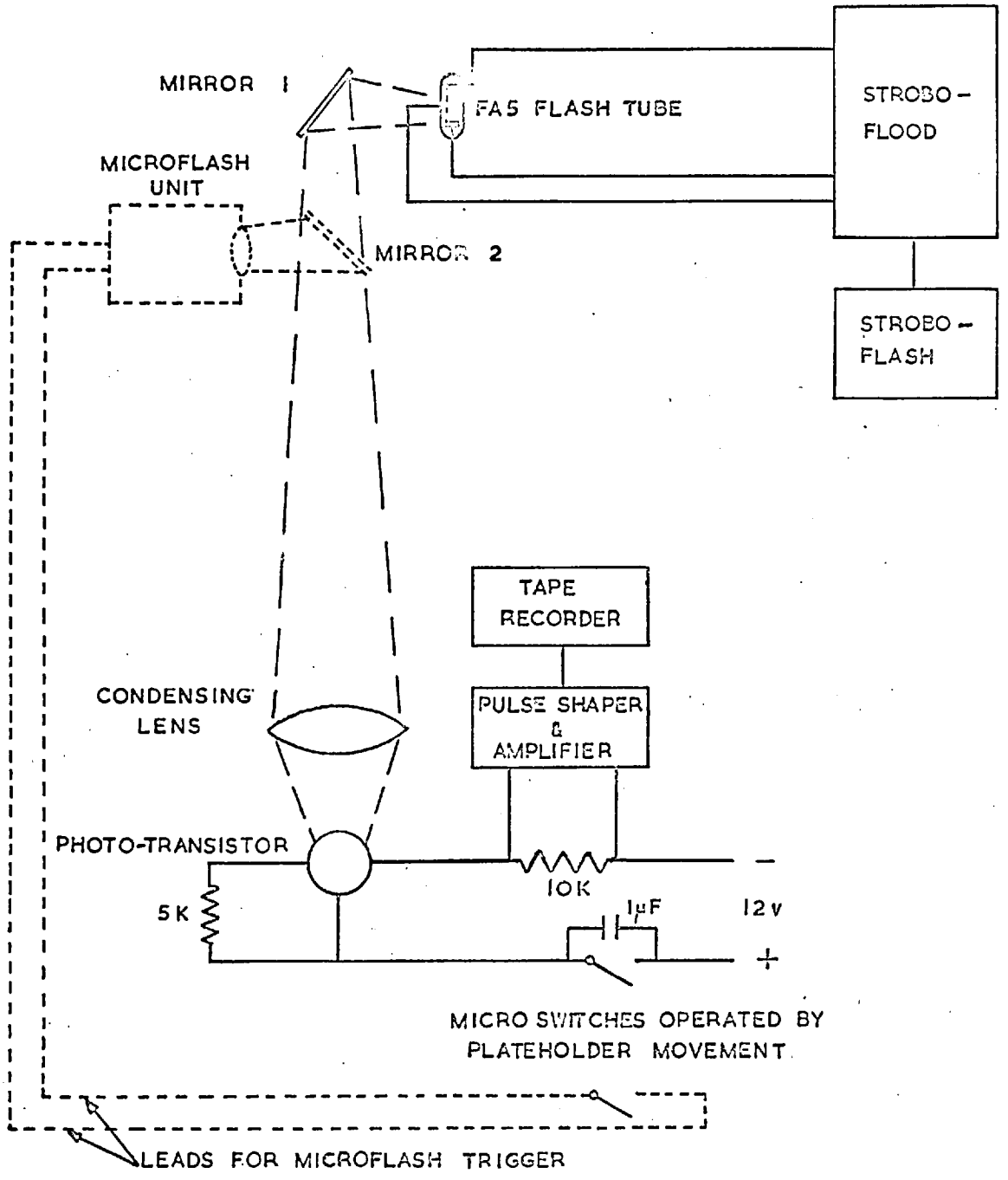
As a precaution against such errors, a technique centred on the use of a tape recorder was developed which permitted the storage of signals initiated by the light pulses from the flashtube and subsequent study of such signals to yield the time interval correct to 0.0001 secs. between a pair of flashes corresponding to any specified pair of drop images on the photographic plate.

In this technique, a twin channel tape recorder was used and signals initiated from a phototransistor by the light flashes were recorded on one track. On the other track, the output from a sine wave generator, operating at 10,000 cycle/sec are recorded. To obtain time intervals between the records of light flashes, the tape is played back and a 'cintel' counter counts the number of sine waves from the suitable track. The counter is arranged so that the signals from the track bearing the records derived from the light pulses switch the counter 'on' and 'off'. By this way, the number of sinewaves between a pair of flashes is known and, therefore, the time interval between them.

Methods of obtaining a record to accurately correspond to the light flashes and further playback and study of the tape to yield the required information are described in the following passages.

Recording

A 'Ferrograph' twin channel tape recorder was used. At first, it was attempted to record the sound produced when the flashtube discharges. It was found that the recordings revealed not a single, sharply rising pulse for each flash, but a complicated slowly decaying pattern of signals arising from echoes.



Dotted lines indicate that microflash unit and mirror 2 are at a lower level

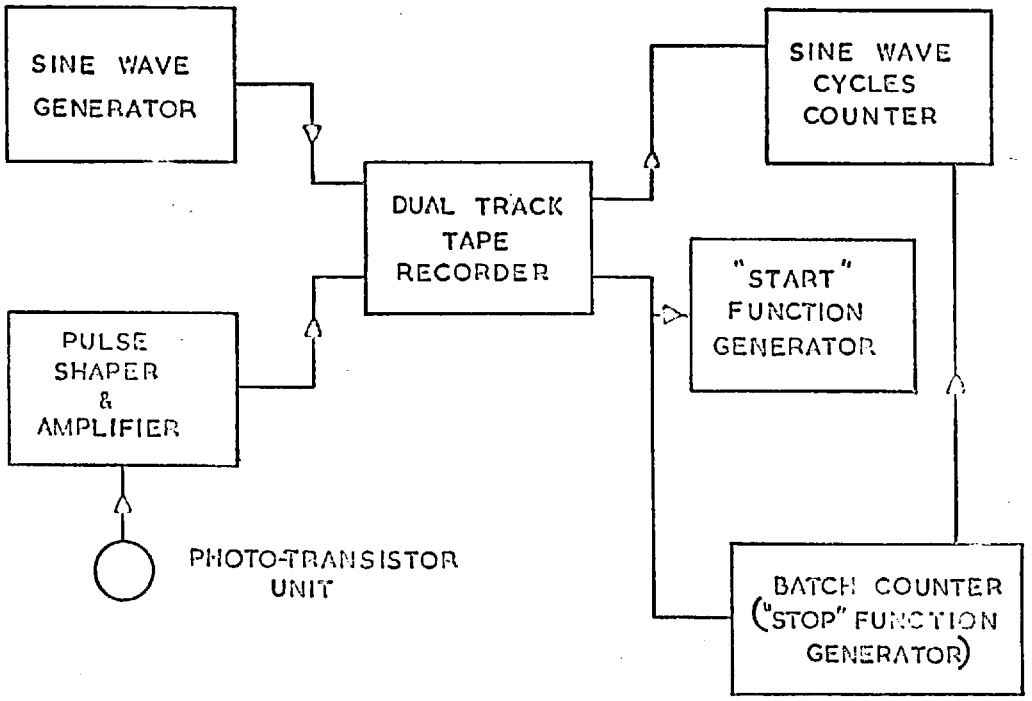
SCHEMATIC DIAGRAM OF RECORDING SYSTEM

FIG.III.13

Such signals made the task of measurement of the time interval between two flashes very difficult. Therefore, it was decided to use the light pulses from the flash-tube.

The phototransistor circuit shown in Fig. III. 13 was finally employed to provide the signal for the tape recorder.

Initially the phototransistor was placed near the light source. It was then found that the photo-transistor was highly sensitive to interference arising from the high voltage charge applied across the flashtube terminals and might lead to confusion between the signals from the light flash and those from the application of the charge to the flashtube. In fact, the transistor was even sensitive to the relatively weak triggering pulses from the Stroboflash. In case the flashtube was not functioning properly these two would not coincide. Therefore, the transistor was moved well away from the flashtube till the interference signal became negligible. The light from the flashtube was reflected by a mirror on to the sensitive surface on the transistor.



SCHEMATIC DIAGRAM OF SYSTEM FOR STORAGE AND ANALYSIS OF FLASHTUBE LIGHT PULSES.

FIG. III.14

The signals arising from the light pulses also decreased in voltage due to the decreased light intensity and had to be stepped up by using a lens to collect the light and focus it on to the sensitive area of the photocell.

It was useful all along the way to have clean and large amplitude signals. Therefore, the output from the photocell was used to trigger a pulse generator which then fed a 20 volt square wave pulse of 100 microsecond duration on to one track of the tape. The output from a sinewave generator set at 10 kc/sec was impressed on the other track and ensured accurate measurement of time intervals regardless of variations in tape speed, flutter, etc.

The accuracy with which the time between two light flashes can be measured increases with the frequency at which the sine wave generator has been set. But the tape recorded could not record frequencies higher than 10 Kc/sec reliably.

A schematic diagram of the recording system is shown in Fig. III.14.

Measurement of time intervals

On playback, the number of sine waves are counted by a 'Cintell' counter. The counter is switched on by the first signal from the track of the tape containing the signals from the light pulses after a period of run of blank tape. The signal from the tape is amplified and shaped in a pulse generator to start the counter. The 'Stop' pulse is obtained from a batch counter which counts the number of signals from the flashtube. The function of the batch counter in the present technique is to permit the calculation of time intervals between any chosen pair of flashes. The tape is played back repetitively and the batch counter setting is progressively advanced and the time intervals between flashes (1) - (2), 1 - (3), (1) - (4), (1)-(x - 1), (1)-(x) are obtained in this fashion. By subtracting the time intervals (1)-(x -1) from (1)-(x), time intervals between flasnes (x - 1) and (x) can be obtained.

In operation, the flashtube is operated for a period of about one minute in an experiment while the falling drop is under observation by the plate for perhaps 1/6 of a second.

Therefore, it is necessary to identify any particular drop image with its corresponding signal on the tape. This is achieved by using a microflash unit as a the source of a marking flash, i.e. during its movement, the plateholder is arranged to trigger the microflash unit and the light from this microflash unit is recorded on the plate and also initiates the recording of a signal on the tape. As the light pulses from the microflash and the FA5 flashtube would rarely coincide, inspection of the time intervals for a series of flashes would reveal the signal corresponding to the microflash and the subsequent time intervals could be labelled with appropriate drop image numbers.

The number of light pulses which have to be processed on tape was reduced by using the plateholder to close the photctransistor circuit.

The use of this technique first revealed that the illumination system was performing unsatisfactorily and that the variations in time intervals between pairs of flashes was of the order of 3%.

As this was worse than the most pessimistic estimates of the performance of the illumination system, the Stroboflood was checked for faults and it was found that at one of the positions of the selector switch for flashing rates, the Stroboflood was malfunctioning.

Tests with the other channels revealed that in general, the illumination system was satisfactory on the short term basis, but was still liable to drift over a long period.

In practice, it was found that the time interval between an unspecified pair of flashes, chosen at random, could be easily obtained, but the time intervals between a pair of flashes corresponding to any required pair of drop images was relatively difficult and tedius. This was due to the difficulty in obtaining the signal from the microflash unit in the correct amplitude range on the tape. At the same time, the short term performance of the flashtube was satisfactory and, therefore, the system was largely used to obtain the average flashing rate and was not used to its full potentiality.

The focussing of the light on to the minute sensitive area of the phototransistor, the tape recorder settings for each track, the pulse generator settings for recording and for playback, and batch counter setting, etc. had to be kept accurate within very narrow limits, and were all subject to drift.

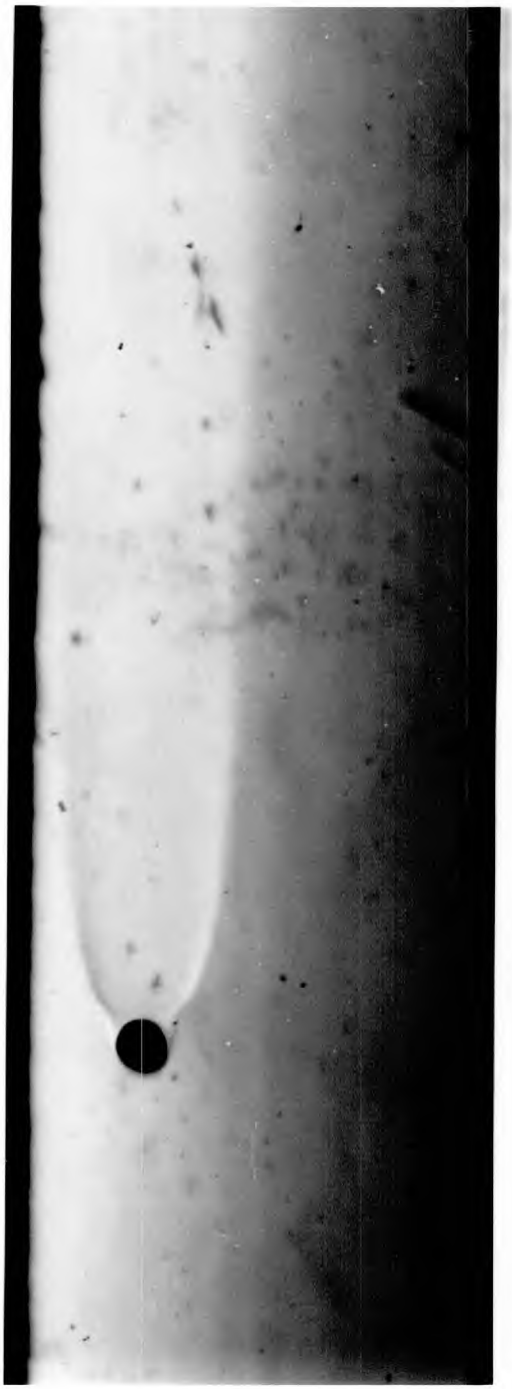
Therefore, the system was very tedious to operate in view of the large number of experiments which had to be conducted and was used to its full potentiality only for a short period. For the rest of the time, it was used to monitor the time interval between pairs of flashes chosen at random. This made it possible to obtain accurately the average flashing rate and to make sure that there were no faults in the operation of the illumination system such as inadequate warm up period, faults in the circuit such as inadequate contacts, and the end of the reliable period of operation of the flashtube, etc. The flashtube was being operated far beyond its guaranteed life of 10 hours and at flashing rates of the order of 30/sec., reliability of operation to within $\frac{1}{2}\%$ on the short term basis could only be checked by such methods of monitoring.

III.15 Photograph of a drop with a side flame

III.16 Photograph of a drop with an envelope flame.



III·16



III·15

CHAPTER IV

EXPERIMENTAL RESULTS AND DISCUSSION.

CHAPTER IV

EXPERIMENTAL RESULTS AND DISCUSSION.

Drag coefficients have been experimentally determined for drops associated with envelope flames as well as side flames.

Envelope flames and side flames have been defined in Chapter II, and the mechanism of ignition in the experimental conditions of this investigation has been described in chapter III.

Two conditions have to be met in order to obtain envelope flames in the combustion chamber. The drop must have been subjected to high temperatures and oxygen concentrations for a sufficiently long period so that the drop leaves the igniter with an envelope flame. Further, if the envelope flame is to be stable, the oxygen concentration in the combustion chamber should correspond to extinction velocities higher than the maximum drop velocity. If the drop is associated with a side flame when it leaves the igniter and if the oxygen concentration in the chamber corresponds to extinction velocities higher than the drop velocity, the flame travels upstream along the drop surface until it envelopes the drop.

The drag coefficients obtained experimentally are compared with the standard drag coefficients, i.e. the steady state drag coefficient for smooth solid spheres in an infinite medium. In all the figures showing experimental drag coefficients, curves of the standard drag coefficients are shown for comparison.

It was found that the drag coefficients were influenced profoundly by the type of flame associated with the drop, and that the greatest deviations from the standard drag coefficients were obtained for side flames. However, a systematic study of the influence of side flames on the drag coefficnts could not be pursued as such flames were in the unsteady state in the present investigation, and it would have been very difficult to stabilise them on any particular latitude on a drop.

Drag coefficients for drops under the influence of envelope flames have been obtained for isopentane, n-heptane and benzene, burning in oxygen. Iso pentane and n-heptane will be referred to below as pentane and heptane, respectively. For pentane, experiments have also been conducted in oxygen: nitrogen atmospheres containing 65% and 75% oxygen by volume. The Reynolds number range was between 100 and 400.

The drag coefficients were calculated on the basis of "approach properties", i.e. the properties of the undisturbed atmosphere in the chamber. It was found that, in general, the drag coefficients were slightly higher than, but close to, the standard values. However, the drops were burning in pure oxygen and consequently the flame temperatures were very high. Therefore the physical properties of the gas-vapour mixture in the immediate neighbourhood of the drop vary steeply. Calculations based on approach properties are therefore erroneous.

However it is very difficult to represent accurately the entire variation of the compositions of the gas vapour mixtures as well as the physical properties of the mixture in the immediate vicinity of the drop. Only approximate ways of representing the properties are feasible.

An attempt was made to use properties representative of this flow region by taking the arithmatic mean of the properties at the drop surface, the flame front and the undisturbed atmosphere. It was found that the points representing drag coefficient vs Reynolds number, calculated on this mean-property basis lay well below the curve for the standard drag coefficient. ~~standard curve.~~

Experimental Results.

IV.1.1 Envelope flames. Pentane.

It was planned to concentrate the study on pentane because this was one of the hydrocarbon fuels with a boiling point very close to atmospheric temperature and could be conveniently handled.

Thus, the change in density of the fuels, as well as the change in transfer number, which accompany the heating up of drops to their boiling point are minimised. Such changes are difficult to evaluate precisely.

Experiments were conducted in the Reynolds number range between 50 and 300 in pure oxygen. The experimental conditions which restricted study within this range of Reynolds numbers have been discussed in chapter III. Drag coefficients were also determined for pentane drops burning in oxygen-nitrogen mixtures containing 65% and 75% oxygen by volume respectively. At lower percentages of oxygen, envelope flames could not be stabilised under the drop size and velocity conditions obtained in this investigation.

The drag coefficient - Reynolds number points for pentane burning with envelope flames in 100%, 65% and 75% oxygen are shown in fig. IV.1

All the calculations in section IV.1. are based on approach properties of the medium and the properties of

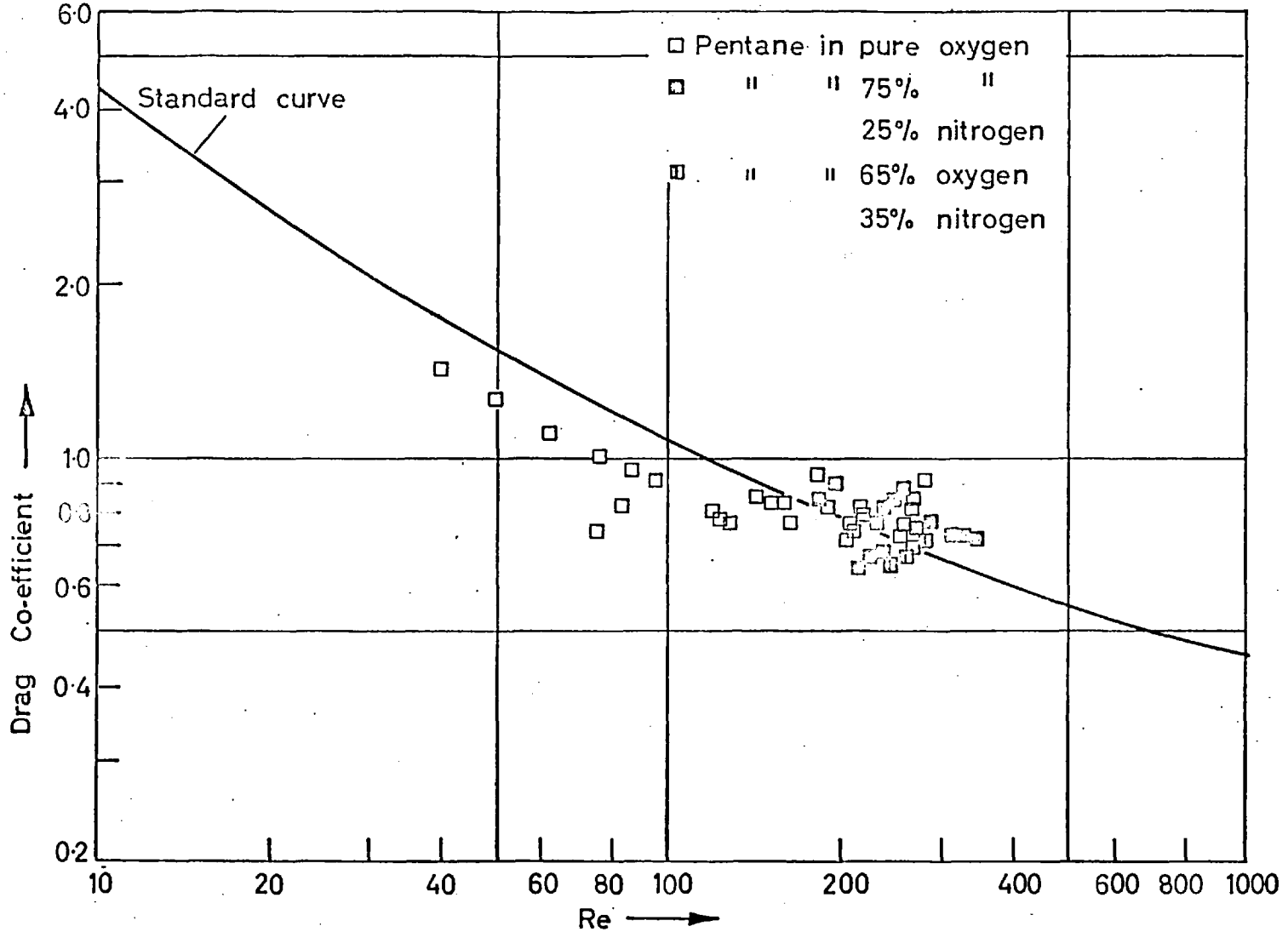


FIG. IV. 1 DRAG CO-EFFICIENT OF BURNING DROPS.

Envelope flames, Pentane.

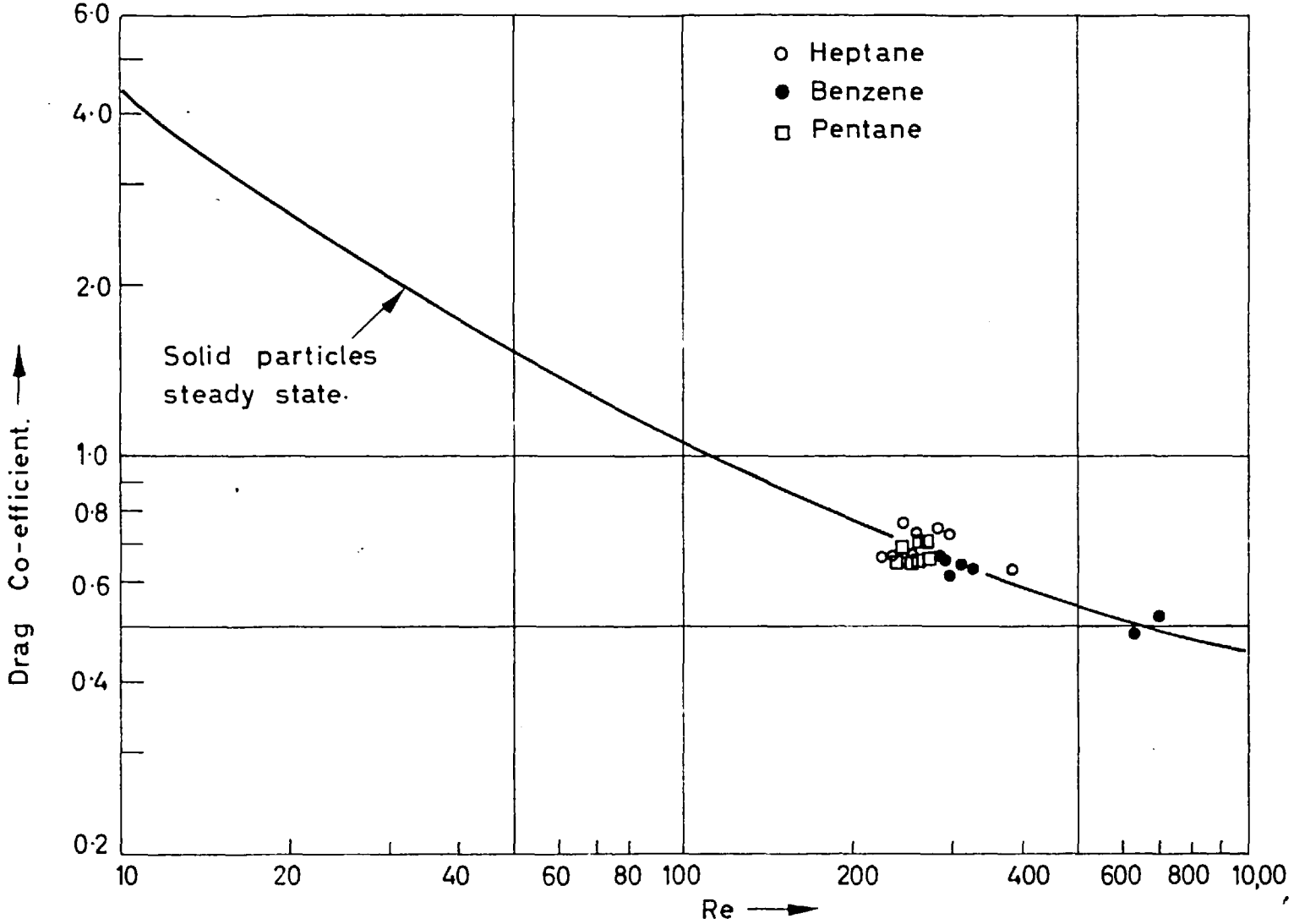


FIG IV.2 DRAG CO-EFFICIENTS OF NON BURNING DROPS.

the fuel drop at atmospheric temperatures.

As the drag coefficient curve without mass transfer is well established, experiments for non burning drops were not carried out for the entire range of Reynolds numbers. The object of experiments with non burning drops was to check on the experimental accuracy and to make sure that all the experimental parameters entering the calculations were correct by locating a few points on the standard curve. The experimental parameters were the same for all experiments.(fig.IV.2)

From fig. IV.1, it can be seen that the drag coefficient values are scattered. The scatter was larger than the expectations based on a consideration of experimental errors and also greater than that for non burning drops (fig.IV.2).

Over most of the range of Reynolds numbers studied, it was observed that the drag coefficients were quite close to the corresponding standard values, with a tendency towards a reduction of the ratio of burning drop drag coefficients to the standard drag coefficients as the Reynolds number decreases. A mean curve representing the experimental points would cross the standard drag coefficient curve at a Reynolds number of about 200.

However as the data were only obtained for a relatively narrow range of Reynolds numbers and the scatter is large, no attempt is made to use the experimental points to

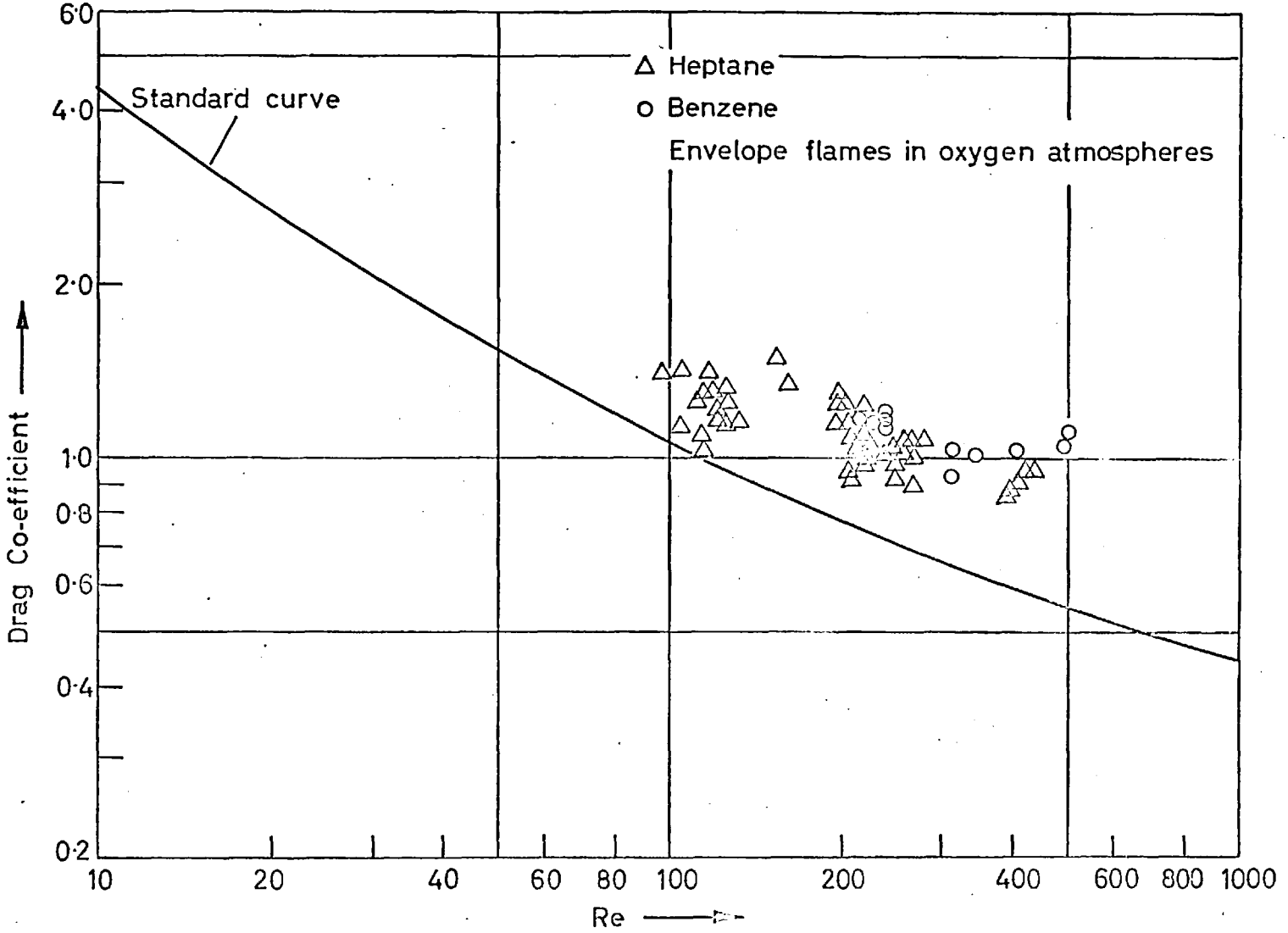


FIG. IV. 3. DRAG CO-EFFICIENT OF BURNING DROPS.

Envelope flames, Heptane & Benzene.

present an empirical relation for the drag coefficient of burning drops.

The drag coefficients of pentane drops in oxygen-nitrogen atmospheres with 65% and 75% oxygen by volume were not different from those for pure oxygen. Thus, it can be concluded that variation of oxygen percentage from 65% - 100% has little effect on the drag coefficient. The mechanism which could account for this observation will be discussed subsequently.

IV.1-2. n-Heptane and Benzene.

Experimentally determined drag coefficients for heptane and benzene, associated with envelope flames in pure oxygen are presented in fig. IV.3.

Again, the values were scattered to a greater extent than indicated by experimental errors for non-burning heptane drops. Over the entire range of Reynolds numbers indicated, the experimental points for burning heptane drops were above the standard drag coefficient curve. As with pentane, it also appears that the ratio of the drag coefficients for burning drops to those of non burning drops increases with Reynolds number. But, on extrapolating the best curve, it appears to cross the standard curve at a Reynolds number of 60.

A smaller number of experiments were carried out for benzene. The values for benzene appear to be approx-

imately the same as those for heptane.

It was stated in section IV.1 that fuel properties at atmospheric temperature are used in the calculations. The boiling point of heptane is 98deg.C and the density of heptane at this temperature is 0.6185 gms/cc while the value used in the calculations was 0.68 gms/cc. Thus, at boiling point the drag coefficients should be 9% lower. However, the temperature of the drop under the experimental conditions in this investigation could not be determined with confidence and the drop properties were calculated for atmospheric temperature.

IV.1-3 side flames.

It has been stated earlier, in chapter III and at the begining of this chapter, that under certain conditions of ignition, a drop will leave the igniter with a side flame. Depending on the oxygen concentration in the combustion chamber, such a flame will be stable or unstable. Over most of the experiments conducted in this investigation, unsteady side flames were obtained. In a few cases, such as with atmospheric air, stable side flames were obtained.

The drag coefficients for heptane, benzene and pentane under the influence of side flames are presented in fig. IV.4 It can be seen that the scatter is high. In this case, the scatter is easy to explain as the Reynolds

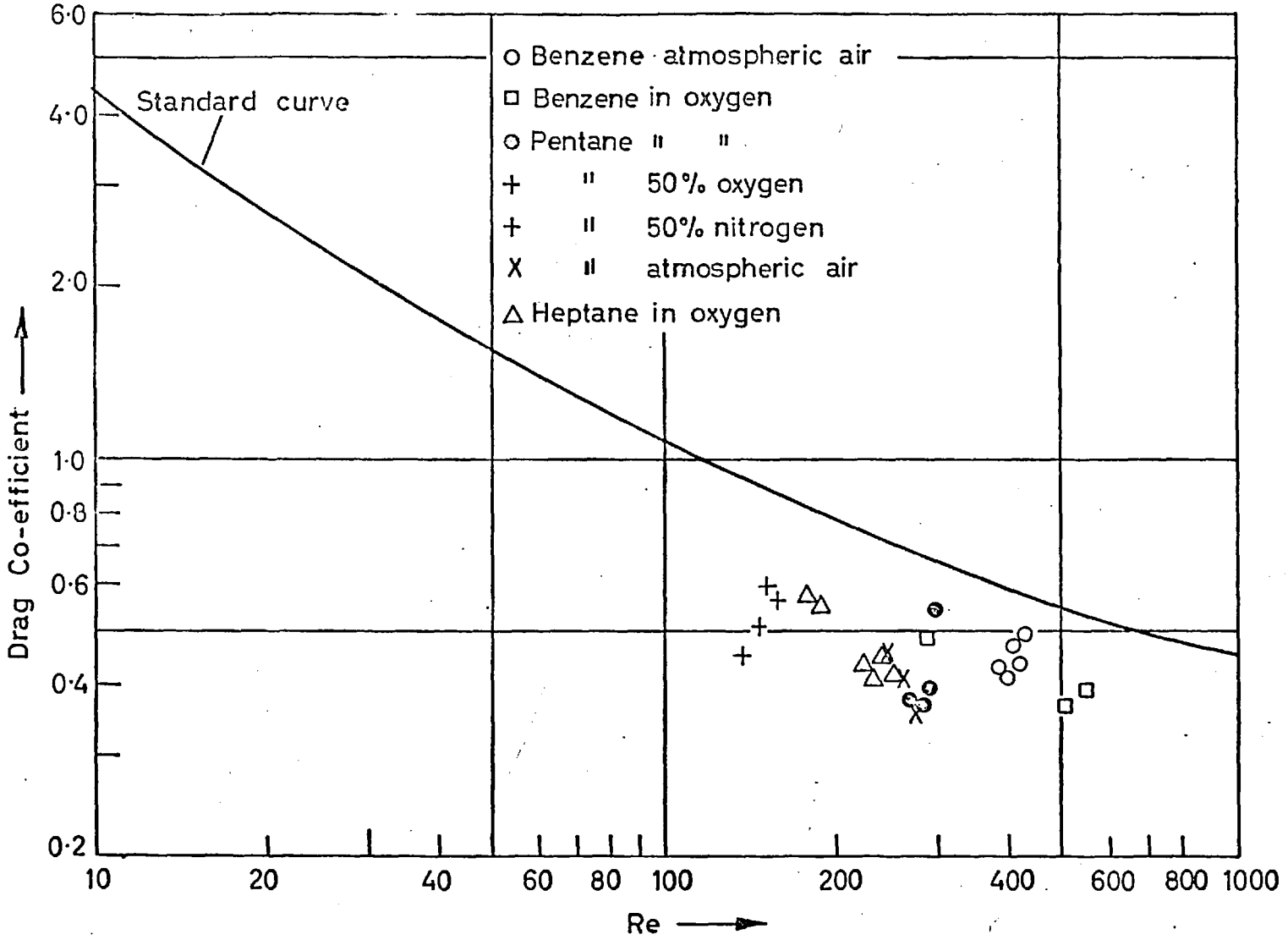


FIG. IV. 4. DRAG CO-EFFICIENT OF BURNING DROPS.

Side flames.

number is not sufficient to ensure dynamic similarity. The flame must be attached at the same ~~dimensionless~~ "latitude" to obtain dynamic similarity and further, such a flame should be stable at that latitude. Most of the experiments were conducted under conditions of flame progress from a latitude very near the rear stagnation point to a complete envelope flame in about 1/5 sec, and the drop was usually observed at 5 uniformly separated instants in this period. It would have been very difficult to match the oxygen concentration and drop size precisely in order to stabilise a side flame at a desired latitude. For this reason, no systematic study of side flames was carried out.

It is clear that the drag coefficients of drops associated with side flames are considerably lower than the standard values, often to the extent of 40% of the standard drag coefficient. Thus, the type of flame exerts a profound influence on the drag coefficients. For example, for heptane drops at a Reynolds number of about 400, which progressed from a side flame stage to an envelope flame stage, the coefficient changes from 50% to 130% of the standard values over a period of 1/5 secs.

Fig. II.10 ~~also~~ shows the results obtained by Khudyakov for side flames and fig. II.9 shows the results of Lubanski.

IV.2 Discussion of Results.

IV.2-1 Drag coefficients based on approach properties.

The initial expectation was that the flow of vapour from the drop surface, combined with the action of the flame on the wake would cause a reduction in the drag coefficient. Lubanski[5], Spalding 3 and Khydyakov[4] have reported reductions with spheres of kerosine, paraffin, etc., burning in atmospheric air. All these authors used supported spheres at high Reynolds numbers. Their measurements were for steady flow and with a steady flame configuration. As pure oxygen was used in most of the experiments in this investigation, it was expected that the much higher transfer numbers would cause greater reductions in drag. Subsequently, it was found that the drag coefficients in the presence of side flames were different from those corresponding to envelope flames and the authors quoted above [5,3,4] obtained mainly side flames.

Except for certain results obtained by Bolt [47], there have appeared no reports on the drag coefficients of unsupported drops associated with envelope flames. Bolts results are shown in fig. II.11.

A number of theoretical investigations of the effect of intense mass transfer on drag coefficients in certain idealised systems have been mentioned in chapter II. [33,34,38,2]. All these publications indicate that the

effect of evaporation would be to reduce the drag coefficient. The results of the present investigation, however, show that over a certain range of Reynolds numbers, the drag coefficients with envelope flames are higher than the corresponding standard drag coefficients.

The explanation lies in the fact that while combustion causes intense evaporation, it also causes steep property gradients in the immediate neighbourhood of the drop. The rise in temperature causes a decrease in density and an increase in viscosity. Therefore, the viscous forces near the drop surface would be considerably higher than those indicated by calculations which are based on approach properties. An idea of the magnitude of such differences can be obtained when one notes that for heptane drops of 0.11cm dia., travelling at 300 cms/sec, calculations based on atmospheric temperatures indicated a Reynolds number of 218, while Bolt obtained a Reynolds number of 17 on the basis of approach properties in his experimental chamber which was at a temperature of 800 deg.C. It was felt that the mean temperatures to be used for the combustion of heptane in oxygen could well be in excess of 800 deg.C and therefore correlation of drag coefficients against Reynolds numbers on this basis would be considerably different from the one drawn on the bases of approach properties.

IV. 2-2 Study of the drag coefficients of burning drops on the basis of mean properties

The physical properties of the fluid and the conventional dimensionless groups are not uniquely defined in the presence of large temperature differences. Jakob[56] has pointed out that for complete dynamic similarity between two non-isothermal systems, the same ratios must exist between physical properties at geometrically equivalent points. Deisler[57] has derived expressions in a complex manner. However, his calculated results were reasonably well represented when the arithmatic mean temperatures were used to evaluate the Nusselt and Reynolds numbers. Douglas and Churchill[58] have stated that the rigorous introduction of the temperature gradients to yield heat transfer information was beyond the methods of analysis available to them and therefore they used the properties at the arithmetic mean temperatures. A number of other workers have also used mean properties for heat transfer correlations in the presence of large temperature gradients.

In combustion work too, the burning rate relations presented by various authors involve the assumption of constant properties. Rasbash and Stark[59] have used the properties of gases at the arithmatic mean temperature to

calculate the Nusselt and Reynolds numbers for the evaporation of water drops in a bunsen flame.

The physical models generally used in the study of the combustion of fuel drops are highly idealised and particularly for an envelope flame of the shape obtained in this investigation, no theoretical model is available. Therefore, the use of accurately integrated mean properties is not feasible. The correct evaluation of mean properties to be used in this investigation becomes further complicated as the compositions of gases vary greatly over small distances and cannot be easily evaluated quantitatively, particularly since direct data on the transport properties of gases at temperatures far in excess of 1500^{o}K are not available.

IV.2-3 Calculation of Mean Properties.

As mass transfer and chemical reactions occur in the neighbourhood of the drop, the composition of the gas vapour mixture varies greatly from point to point and therefore, the use of properties at a mean temperature is not convenient as this will have to be related to a representative composition. Therefore, it was decided to use the arithmetic mean of the properties of the gas-vapour mixtures corresponding to (a) the drop surface, (b) the flame front, and (c) the undistubed atmosphere, at temperatures corresponding to each location.

The flame temperatures and the composition of the gases at the flame front were calculated according to the method presented by Rosin.[60] This method enables one to calculate the adiabatic flame temperature and takes dissociation into account. It has been pointed out in chapter II that the flame temperature of a burning drop is different from the adiabatic flame temperature. However, calculations of flame temperatures for hydrocarbon drops burning in pure oxygen are not available even for spherically symmetric envelope flames. The use of such calculations involves the assumption that the effect of radiation is negligible.

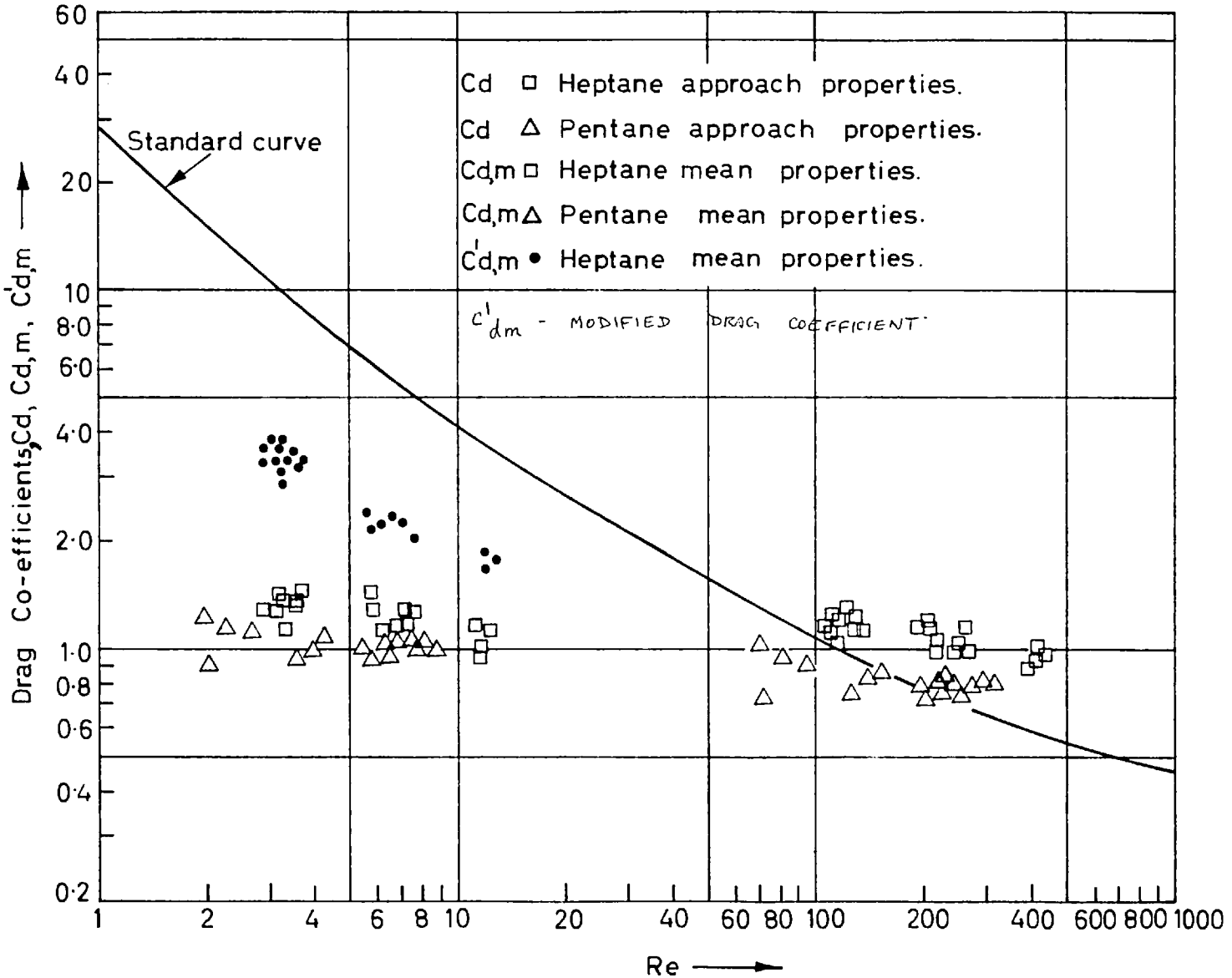


FIG. IV. 5. DRAG CO-EFFICIENT OF BURNING DROPS

Further, the heat and mass transfer relations for drops with relative velocities of the order of 300cm$/sec would be different from those for spherical flames. Therefore, it was decided to adopt the simpler calculations proposed by Rossin. Experimentally determined values of the physical properties of gases are available upto temperatures of the order of 1500 K. The properties of various gases at the flame front with a temperature far in excess of 1500° K were calculated by graphical extrapolation of property- temperature curves. The gas composition at the flame front, according to the calculation procedure of Rossin, is known. The mean of the properties of various gases, weighted according to the composition of the mixture, is used to represent the properties of the mixture at the flame front.

It was found that for pentane drops burning in pure oxygen, the Reynolds numbers, calculated on the mean property basis, were 1/35 times and the drag coefficients were 1.25 times ~~of~~ those calculated on the basis of approach properties. (Ref. Page A1-10)

The drag coefficient-Reynolds number points for pentane and heptane drops are shown in fig, IV.5 as indicated by both mean and approach properties. It can be seen that the drag coefficients, calculated on the mean property basis are approximately 80% lower than the corresponding standard drag coefficient. Thus, when the effect of evaporation

alone is isolated by making an approximate allowance for the changed physical properties due to combustion in the medium surrounding the drop, the drag coefficient is seen to be reduced in accordance with expectations. It can also be noticed that the points for heptane and pentane are closer when plotted on the mean property basis. This is due to the difference in density between heptane and pentane vapour which lowers the ratio for heptane of drag coefficients on the mean properties basis to those on the approach properties basis. If one further lowers the drag coefficients for heptane by assuming the density for heptane at its boiling point, the drag coefficients on the mean properties basis for heptane and pentane would coincide. This seems largely to explain the discrepency between the drag coefficients of pentane and heptane on the approach properties basis.

IV.2-4 Comparison with theory.

Spalding has suggested that for a flat plate in laminar flow at moderate Reynolds numbers, the ratio of drags with and without mass transfer is of the order of $\frac{\ln(1+B)}{B}$. In the absence of any similar solutions for spheres at Reynolds numbers comparable with those of this

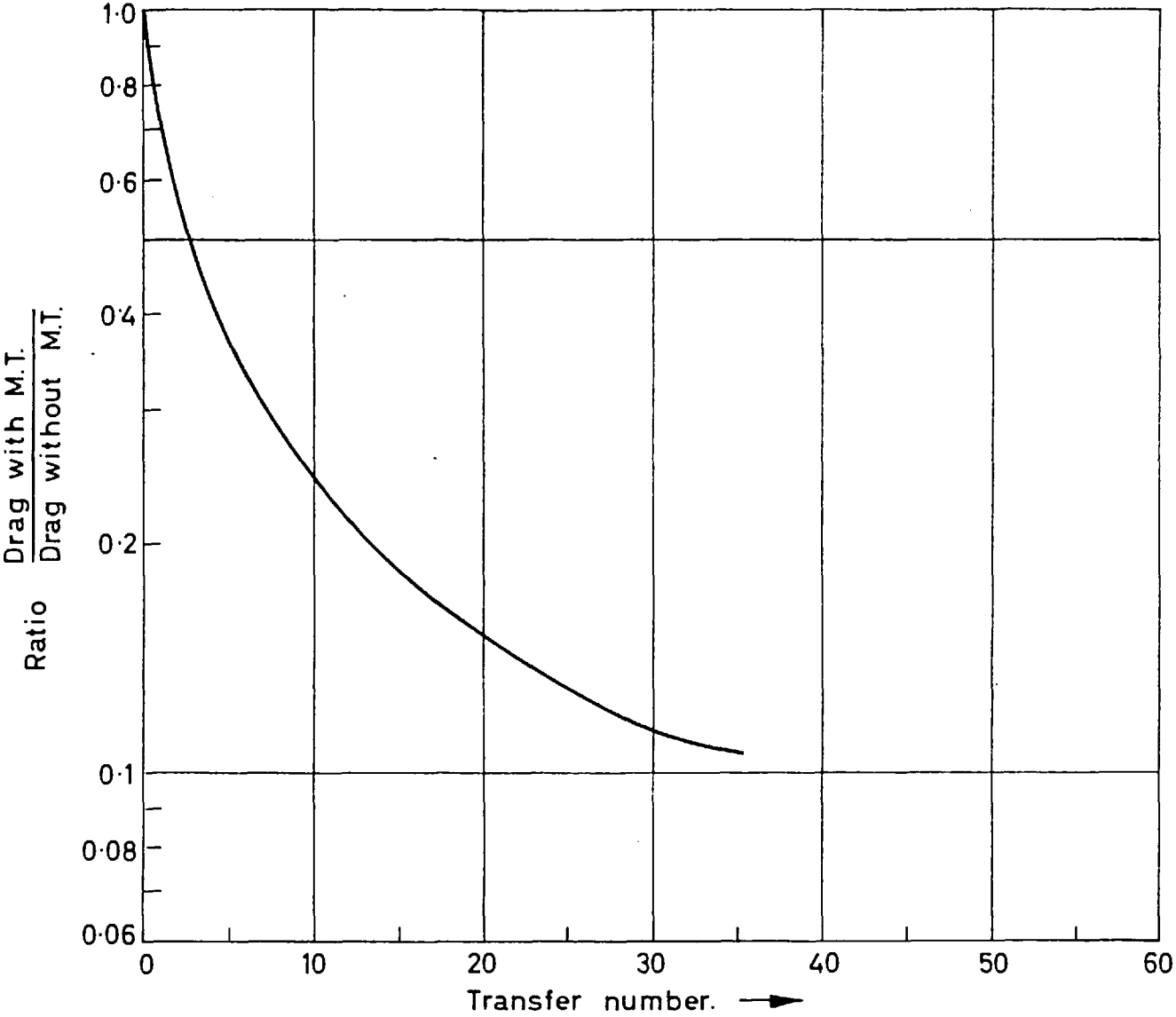


FIG. IV 6 PREDICTED EFFECT OF EVAPORATION ON THE DRAG CO-EFFICIENT. (Spalding ref: 50.)
FLAT PLATE IN LAMINAR FLOW.

investigation (mean properties basis) the experimental results of this investigation will be compared with the predictions of Spalding. Fig.IV.6 shows a curve of $\frac{\ln(1+B)}{B}$ for a range of transfer numbers. From table I, the transfer number for pentane drops burning in a pure oxygen atmosphere is found to be 34. For this transfer number, fig. IV.6 indicates that the drag coefficient would be reduced by about 90%. This agrees surprisingly well with the value for the reduction in drag coefficient of about 80% indicated by fig IV.5.

The conclusion emerges therefore that the apparent lack of influence of combustion on the drag coefficient-Reynolds number points based on approach properties was due to the fact that evaporation reduces the drag resistance, while the high temperatures in the neighbourhood of the flame increase it through increased kinematic viscosity. These two effects nearly cancel each other out.

Similar calculation of mean properties could not be carried out for side flames as only a part of the sphere was subjected to the influence of the flame and the drag coefficient values refer to unsteady side flames.

The work of Muggia[38] has been discussed in chapter II. It was attempted to compare the results of this invest-

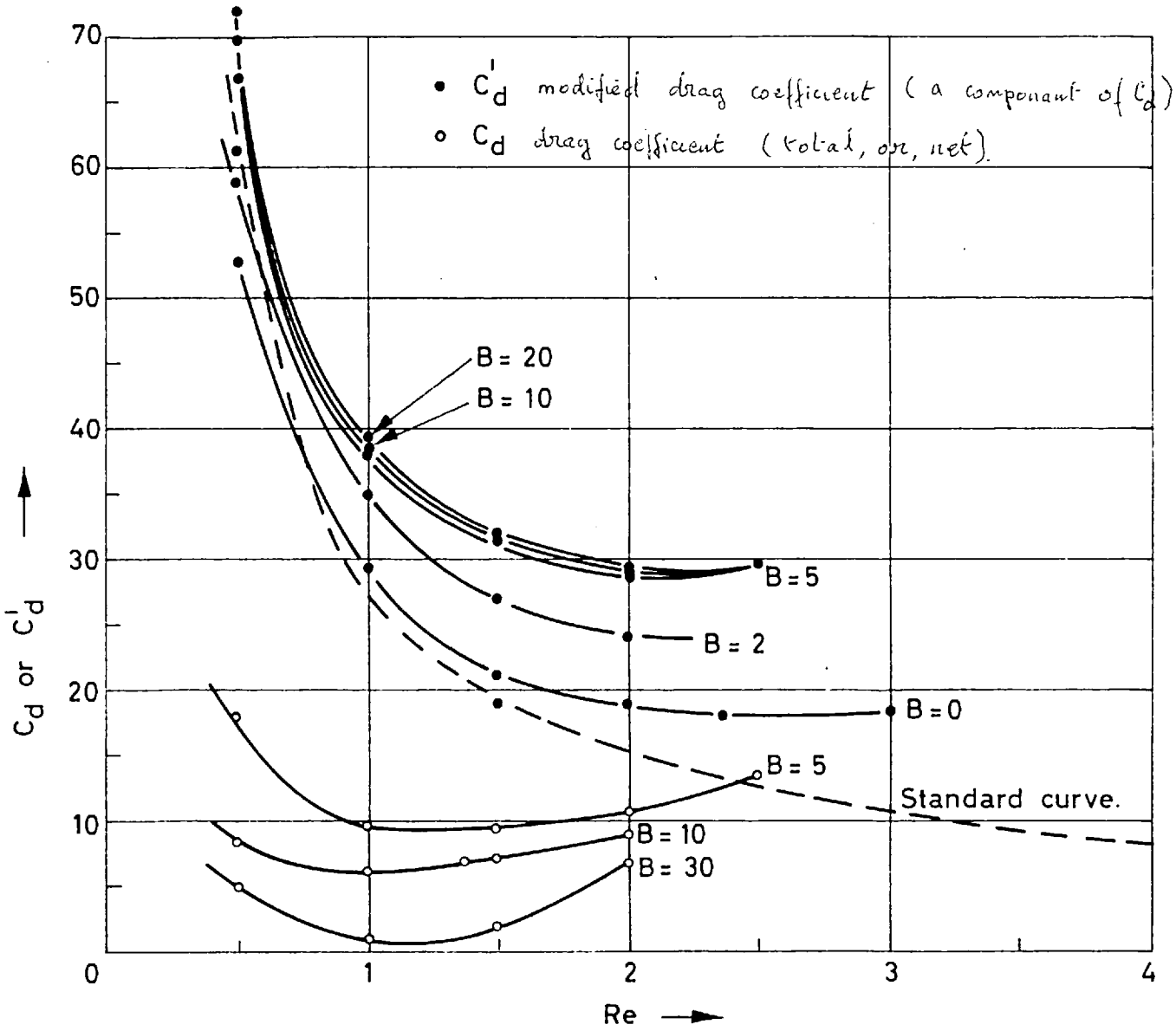


FIG. IV 7. DRAG CO-EFFICIENT OF EVAPORATING DROPS.

Muggia ref: 38.

igation with those of Muggia as the Reynolds numbers with reference to the mean properties lay between 2 and 10 in this investigation.

The drag coefficients predicted by Muggia as given by the equation 2.2.12 were calculated and are shown in fig. IV.7. The drag coefficient values change very steeply over small ranges of Reynolds numbers and increase to a high figure near a Reynolds number of about 3. Equation 2.2.12 indicates that the drag coefficient becomes ∞ at a Reynolds number of 16/3. This is due to the approximations used in his theoretical developements. Thus, Muggia's work is inapplicable except at very low Reynolds numbers.

IV.2-5 Slope of the drag coefficient - Reynolds number curve for burning drops.

The drag coefficient values based on mean properties have been found to be approximately constant within a range of Reynolds numbers of 2 - 10, whilst the standard drag coefficient decreases steadily within this range of Reynolds numbers. As the experiments were done with freely falling drops, low Reynolds numbers were associated with small drop sizes. It is suggested below that the lower drag, on mean properties basis, observed for small drops can be explained by the fact that the evaporation rate per unit mass of drop increases with a decrease in drop size.

Muggia[38] equated the resultant of the pressure and viscous forces acting on the drop to the time derivative of the momentum of the drop, which is part liquid and part already transformed to vapour. He calculated the momentum transfer rate to the drop from the difference between the integral of the forces on the drop and the flow of momentum from the drop. As the flow was steady, the same expression can be calculated on any closed surface which contains the drop within it, rather than on the surface of the drop. The resulting relation is:

$$m\,a = 6\pi\mu r v \frac{2 + B}{2 + \tfrac{1}{4}B - 3/16\ Re(2+B)} + v\frac{dm}{dt} \qquad 4\ ..1$$

The drag coefficient is obtained by dividing this expression by $\tfrac{1}{2}\rho_g \pi r^2 v^2$. The term $v\frac{dm}{dt}$ is the rate at which momentum leaves the control surface due to vapour flow. Muggia's drag coefficient can be visualised as the difference between two coefficients C_d' and C_d''.

$$C_d = C_d' - C_d'' \qquad 4.\ .2.$$

C_d' being the coefficient due to the integral of pressure and viscous forces on the control surface and C_d'' corresponding to vapour momentum leaving the drop. Values of C_d' were calculted for Muggia's drag relation (2.2.12) and are shown in fig. IV.7. It can be observed that, over the range of applicability of his equation to non-burning drops (i.e. $Re < 1$), the difference between C_d' and the standard drag coefficient is quite small in comparison with the difference of the total drag coefficient he calculated for evaporating drops from the standard one.

Calculations of $C_{d,m}''$ were made from the drop size and vapour velocity data obtained in this investigation

for heptane drops by assuming an evaporation constant of 0.025 cm^2/sec quoted by Penner[61] and mean properties. The use of suffix 'm' indicates that mean properties were used. $\mathcal{C}_{d',m}$ was obtained from $\mathcal{C}_{d,m} + C_{d'',m}$. These values are plotted in Fig. IV-5. It can be seen that the C_d' points follow a curve of a similar form to the standard curve, i.e. they decrease with increasing Reynolds number, but they lie well below the standard curve. The evaporation constant chosen relates to supported drops and for the conditions of this investigation, the constant could well be higher. There is further uncertainty regarding the choice of mean properties and the location of the $\mathcal{C}_{d,m}$ curve is therefore only approximate.

It therefore appears that the great drag reduction for small drops is caused by the larger evaporation rate per unit mass.

IV.2-6. Comparison of burning rates.

Penner[61] reports an evaporation constant of 25×10^{-3} cm^2/sec for heptane drops in 100% oxygen atmospheres. It was observed in most of the experiments in this investigation that a clear dropsize decrease could not be noticed over the period of drop life recorded on the photographic plates. This corresponds to a period of 1/6 sec. The decrease in drop diameter as indicated by Penner was calculated to establish whether the failure to observe a drop size decrease is in line with available information of burning rates.

$$d^2 = d_o^2 - \lambda t$$

where

d = drop dia. at time t

d_o = initial drop diameter.

t = time

For an initial dropsize of 2 mm., the drop size after 1/6 sec is

$$d^2 = \left\{(.2)^2 - 0.025 \times 1/6\right\}$$

$$d = \sqrt{0.036} = 0.1925 \text{ cms.}$$

This would correspond on the microscope projection screen to a reduction of approximately 1 small division of the scale on the screen and would not be noticed with the available sharpness of drop images. Thus, the burning rates prevalent in this investigation were not demonstrably low.

IV.2.7 Extrapolation of data to steady state conditions.

The drops studied in this investigation were travelling in the unsteady state. It is known that acceleration affects the drag coefficient.

The work of Keim[21], Ingebo[22] and Gilliland[23] on the effect of acceleration have been reviewed in chapter II. The results of these authors show that the ratio C_d/C_{do} increases with increase in the dimensionless groups ρ_g/ρ_l and ad/v^2. In the experimental conditions of this investigation, it appeared that the groups ρ_g/ρ_l and ad/v^2 were too small to cause a significant departure of C_d/C_{do} from unity. However, there was no direct evidence reported in literature for the specific conditions of drop size and ballistics encountered in this investigation. Therefore, an attempt was made to extrapolate the acceleration - time points for some of the experiments to zero acceleration and obtain the terminal velocity and calculate the drag coefficient on the basis of the terminal velocity.

The terminal velocities were calculated in the following manner. The acceleration values obtained from computer calculations were plotted with acceleration and time as the coordinates. The curve obtained was then extrapolated to zero acceleration in accordance with the

expectation that acceleration decays with time at a diminishing rate. Thus, the total acceleration was found. As the datum velocity was known, the terminal velocity could be calculated. The drag coefficients calculated for the terminal velocity condition, along with the corresponding points pertaining to the experimental condition are shown in fig. IV.8. It can be seen that no significant reduction of scatter is discernible. Thus it appears that for the ρ_g/ρ_l and velocity conditions of this investigation, the accelerations were low enough for drop movement to be considered quasi-steady.

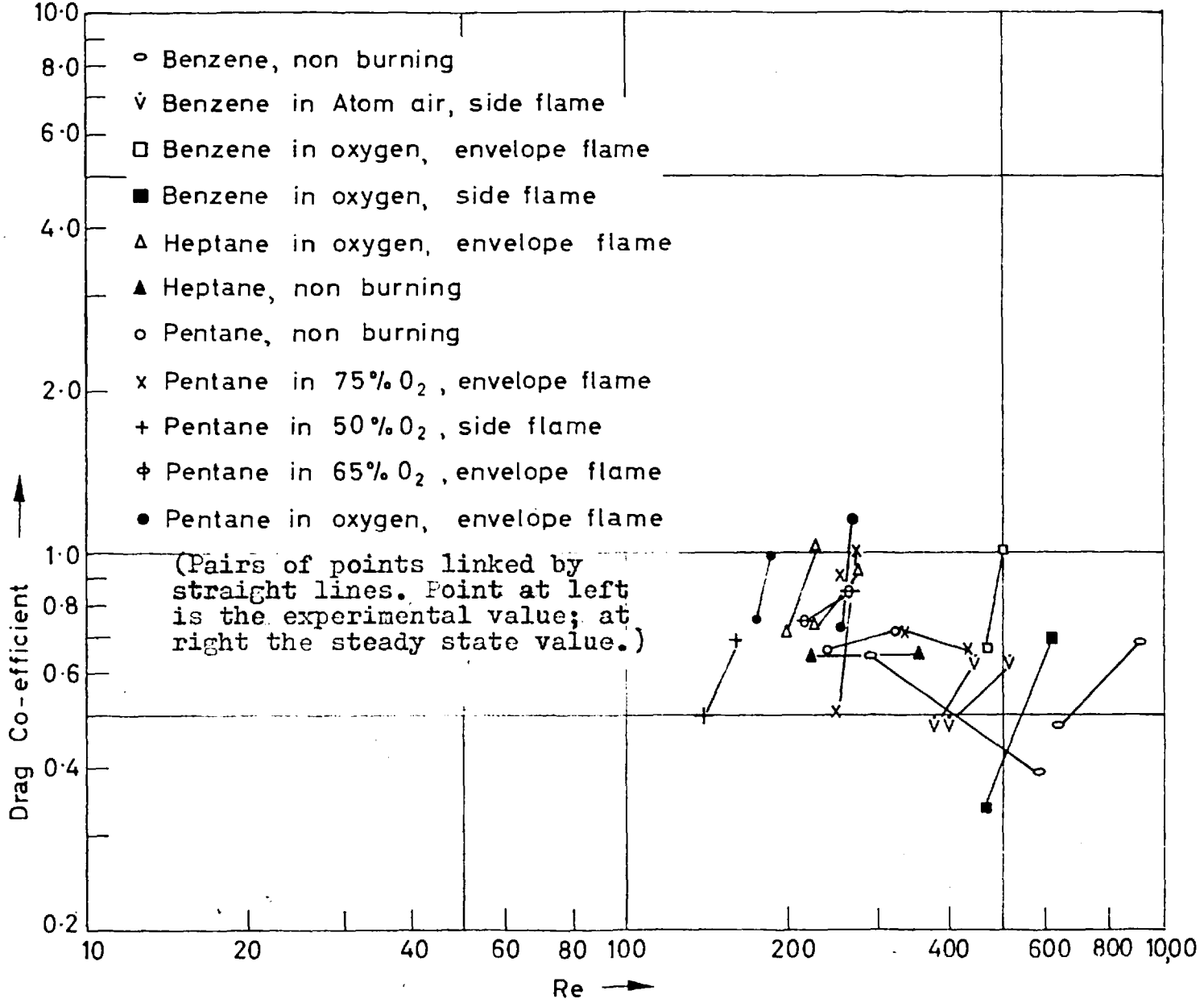


FIG. IV 8. DRAG CO-EFFICIENT OF DROPS. Steady state.

CONCLUSIONS

The drag on a drop is affected by mass transfer, the distribution of which over the sphere is influenced by the type of flame associated with the drop. In this investigation, drag coefficients have been obtained for both envelope and side flames.

The drag coefficients have been calculated on the basis of approach as well as mean properties. The following conclusions emerge from this investigation.

1) The coefficients for drops with side flames downstream of the equator were always lower than the corresponding standard values, often by about 50%, and the degree of reduction depended on the lattitude at which the flame was attached to the drop.

2) As to envelope flames and coefficients based on approach properties, the conclusions are:

(a) The coefficients for all fuels were higher than the standard values over most of the experimental range, i.e., $90 < Re < 400$.

(b) Heptane drops had coefficients higher by about 20% compared to pentane drops.

(c) For all fuels, the ratio of coefficients with and without combustion decreased with decreasing Reynolds numbers. This finding is consistant with

the relatively larger evaporation rates for small drops.

3) The conclusions from the calculations based on mean properties for drops with envelope flames are:

(a) The coefficients for heptane and pentane drops are only slightly different from each other (compare 2.b)

(b) The coefficients were lower than the standard values by about 80%.

4) It is believed that, for burning drops, the effect of evaporation, which tends to lower the drag coefficient and the effect of increased temperatures, which increase the viscous forces, nearly cancel each other out over the experimental region studied.

5) The experimental points exhibited large scatter and did not warrant the presentation of empirical equations. They were difficult to obtain experimentally because of the following reasons:

(a) The low surface tension of the fuels.

(b) The transient nature of the experimental system.

(c) The need for great accuracy in the time intervals between successive light flashes.

6) The experimental results could not be quantitatively interpreted on a theoretical basis since a satisfactory theory which would represent the complex drop-flame system

over the flow regime studied has not yet been developed. However, the results have been explained in comparison with a theory relevant to highly simplified systems.

APPENDIX I

CALCULATION OF THE DRAG COEFFICIENT AND REYNOLDS NUMBER.

Appendix I.

A1.1 Calculation of drag coefficient and Reynolds number; approach properties. A1.1

A1.2 Calculation of drag coefficient and Reynolds number; mean properties A1.7

A1.3 Calculation of C''_{dm} A1.11

calculation of drag coefficient and Reynolds number. Approach properties.

The relation describing the movement of a drop, falling under gravity and subjected to aerodynamic resistance is as follows:-

$$mg\left(\frac{\rho_l - \rho_g}{\rho_l}\right) - ma = \tfrac{1}{2} C_d \rho_g v^2 A \qquad 5.1.1.$$

where the suffixes refer to the liquid and gas states.

$$mg\left(\frac{\rho_l - \rho_g}{\rho_l}\right)$$

is the downward force experienced by the drop due to gravity and the buoyancy of the medium, and $\tfrac{1}{2} C_d \rho_g v^2 A$ is the aerodynamic drag resistance and, 'ma' is the resulting gain in drop momentum.

For spherical drops,

$$m = \tfrac{1}{6} \pi d^3 \rho_l$$

and $$A = \frac{\pi}{4} d^2$$

Eqn. 5.1.1 can now be rewritten as follows:

$$\tfrac{1}{6} \pi d^3 \rho_l g \left(1 - \frac{\rho_g}{\rho_l}\right) - \tfrac{1}{6} \pi d^3 \rho_l a$$

$$= \frac{\pi}{8} d^2 C_d \rho_g v^2$$

therefore, $$C_d = \frac{4}{3} \frac{\rho_l}{\rho_g} d \frac{\left[g\left(1 - \frac{\rho_g}{\rho_l}\right) - a\right]}{v^2} \qquad 5.1.2.$$

The Reynolds number is given by $\frac{dv\rho}{\mu}$.

The results of an experiment consist of a series of drop images on a plate progressively farther away from the short edge of the plate. These images represent the successive positions of the drop in the chamber, each position corresponding in time to one flash discharge in the flashtube. The times elapsed between successive lightflashes are obtained through the time monitoring system.

The distances of successive drop images from an arbitrary datum on the photographic plate are measured in the direction of the major axis of the plate using a Pye travelling microscope.

The density of the drop liquid, and the viscosity and density of the medium are known at atmospheric temperature. The data required to be derived from the photographs are - the drop diameters, velocities and accelerations.

velocity and acceleration:

The travelling microscope, and the time monitoring system yield distance - time records for the drop images on the plate. It is necessary to obtain the instantaneous velocities and accelerations from

these data. The first and second differentials of the function of distance with respect to time would give velocities and accelerations. It is therefore necessary to represent each set of distance - time data by means of a function which is accurate enough to yield velocities and accelerations within an acceptable margin of error. Because the drops were burning, there was no prior knowledge regarding the form of the equation which would be obeyed by the ballistics of the drop. It was felt that the simplest solution would be to fit the distance - time data to a least squares polynomial. In this connection a theorum by Weirstrass states that "if a function f(x) is single valued and continuous in the closed interval, (a_1 to a_2) and if ϵ is any preassigned positive number, then there exists at least one polynomial p(x) such that $(f(x) - px) < \epsilon$ for all the x's in the interval."[62].

However in this investigation, a set of only 4 or 5 s - t points were usually obtained. Therefore it was not possible to fit polynomials of a degree higher than 3 to the experimental data, and there was a limit to the accuracy of the s - t polynomial. However, the drag coefficients calculated from accelerations and velocities obtained from 3rd and 4th order polynomials for a few sets of data were not very different, and thus, approximations

to 3rd order polynomials were not seriously in error.

Least squares polynomials of degree 3 were fitted to the s - t data using the University of London 'Atlas' computer. The programme employed was the programme 1000 from the CHLF 3 Autocode library of the University of London Computer Unit. Polynomials of the form

$$s = b_1 + b_2 t + b_3 t^2 + b_4 t^3 \ldots\ldots \qquad 5.1.3$$

were obtained where b_1, b_2, b_3 and b_4 are the coefficients of the polynomial. The velocity is given by, $v_p = b_2 + 2b_3 t + 3b_4 t^2$ 5.1.4

and the acceleration by $a_p = 2b_3 + 6b_4 t$ 5.1.5

v and a are the velocities and accelerations of the drop image on the plate. To obtain the velocities and accelerations of the drop, v_p and a_p are multiplied by K', which is the ratio of size of object to the size of its image on the photographic plate.

A projection microscope was used to enlarge the drop image. The size of the drop image on the projection microscope screen was measured. The ratio of the drop image size ~~in mm.~~ on the plate to the drop image size on the screen is K". If 'D_1' is the diameter of the drop image on the screen, the drop ~~image~~ size is given by

$$K' K'' D_1 = d \text{ cms.}$$

Therefore, in terms of v, a and D_1, eqn. 5.1.2 becomes,

$$C_d = \frac{4}{3} \frac{\rho_1}{\rho_g} \frac{K' K'' D_1 \left[g(1 - \frac{\rho_g}{\rho_1}) - K' a_p \right]}{(K' v_p)^2} \quad ..5.1.6.$$

For heptane drops falling through oxygen at atmospheric pressure and at 15°C, $\frac{\rho_g}{\rho_1} = \frac{1}{505}$. Therefore, eqn. 5.1.6 can be simplified by approximating $(1 - \frac{\rho_g}{\rho_1})$ to 1 and,

$$C_d = \frac{4}{3} \frac{K' K'' D_1 (g - K' a_p)}{(K' v_p)^2} \quad 5.1.7.$$

Similarly the Reynolds number becomes,

$$Re = \frac{dv}{\nu} = \frac{(K')^2 K'' D v_p}{\nu} \quad 5.1.8.$$

Example: Plate 115.

Fuel: heptane; density 0.684 gms/cc.

medium: oxygen; Temperature = 15°C. density of oxygen at 15°C = $1.429 \times \frac{273}{288} \times 10$ gms/cc. Kinimatic viscosity of oxygen at 15°C = 0.152 stokes. Interflash period. 0.0308 secs: uniform flashing rate.

magnification K' = 2.

magnification K'' = 0.0256.

t, secs.	s, in mm. on plate.
0.0000	36.58
0.0308	69.00
0.0616	102.35
0.0924	135.90
0.1232	169.20

D_1 = 1.6 units on the projection screen of the microscope.

The polynomial with the least square deviation which was fitted to this set of s-t data is

$$s = 3.657 + 103.27\ t + 76.952\ t^2 - 336.5\ t^3 \text{ cms}$$

$$v_p = \frac{ds}{dt} = 103.27 + 153.90t - 1009.6\ t^2 \text{ cms/sec}$$

For t = 0.0308 secs

v_p = 107.05 cms/sec.

$$a_p = \frac{dv}{dt} = 153.90 - 2019.3\ t$$

For t = 0.0308 secs

a_p = 91.9 cms/sec^2.

Therefore,

$$C_d = \frac{2}{3} \times 0.684 \times \frac{298}{1.429 \times 273 \times 10} \times 2 \times 0.0256 \times \frac{1.6(981 - 2 \times 91.9)}{10 \times (2 \times 107.5)^2}$$

$$= \underline{0.995}$$

$$\text{Reynolds number} = \frac{(K')^2\ K'Dv_p}{\nu}$$

$$= (2)^2 \times 0.0256 \times \frac{1.6}{10} \times 107.5 \times \left(\frac{1}{0.152}\right)$$

$$= \underline{116}$$

A.1.2. Calculation of drag coefficients and Reynolds numbers on the basis of mean properties.

The mean properties used were calculated using the relations.

$$\rho_m = \frac{\rho_s + 2\rho_f + \rho_g}{4}$$

$$\mu_m = \frac{\mu_s + 2\mu_f + \mu_g}{4}$$

where suffixes m, s, f and g refer to the mean, the drop surface, flame front and the ambient gas respectively. At each point the properties calculated correspond to the composition at that point.

Flame temperature:

As described in IV.2.3., the adiabatic flame temperature was calculated using tables presented by Rossin[60]. The flame temperatures for pentane in oxygen, taking dissociation into account, was 2810°C. Inspection of the calculation procedure reveals that the flame temperature of heptane could not differ from that of pentane by more than 1%.

Composition:

The composition at the drop surface is taken to be 100% fuel vapour, and the ambient gas is oxygen.

Rossin's tables could be used to calculate the

composition of dissociated products up to a temperature of 2500°C. This temperature corresponds to a 40% oxygen atmosphere. At this temperature, 40% of the carbon was present as carbon monoxide and 25% of the hydrogen as OH. At higher temperatures, the proportions of these components will be larger. As no concise calculation procedures are available and in view of the approximate nature of the calculations of mean properties, it is assumed that, at the flame front the gas mixture is composed of CO and OH only.

Densities:

For heptane vapour at boiling point, (98.5°C) ignoring deviation from perfect gas laws,

$$\rho_s = 32.8 \times 10^{-4} \text{ gms/cc.}$$

for pentane vapour, on a similar basis,

$$\rho_s = 28.4 \times 10^{-4} \text{ gms./cc.}$$

At the flame front, the density of products of reaction of pentane, assumed to consist of CO and OH alone is

$$\rho_f = 0.72 \times 10^{-4} \text{ gms/cc.}$$

the density of oxygen at 15°C is

$$\rho_g = 13.5 \times 10^{-4} \text{ gms/cc.}$$

Viscosities:

ν_g = 0.152 stokes.

Data on the viscosities of hydrocarbon vapours is meagre. Therefore, for pentane and heptane, the viscosity values quoted for benzene are used[65].

$$\mu_s = 750 \times 10^{-7} \text{ poises.}$$

viscosity data are not available for the flame temperatures relevant to this investigation. High temperature viscosity data has been presented in the form of tables[66] of μ/μ_o vs. T where μ_o is the viscosity at 273°K. Such tables are available for temperatures up to 1800°K. Therefore, to obtain the values corresponding to 2810°C, the values were plotted and graphically extrapolated. For the approximate conditions representing the flame after making allowance for the viscosity properties of water vapour, the viscosity value chosen 7810×10^{-7} poises.

Mean properties. Burning pentane drops.

$$\rho_m = \tfrac{1}{4} (28.4 + 2 \times 0.72 + 13.5) \times 10^{-4} \text{ gms/cc}$$

$$= 11.23 \times 10^{-4} \text{ gms./cc.}$$

similarly ν_m = 5.49 stokes.

for calculations based on approach properties, the values used were

$$\rho_g = 13.5 \times 10^{-4} \text{ gms/cc.}$$

$$\nu_g = 0.152 \text{ stokes.}$$

Therefore, $C_{dm} = \frac{13.5}{11.23} C_d = 1.25 \; C_d.$

$$Re_m = \frac{0.152}{5.49} Re = \frac{Re}{35}$$

Mean properties. Burning heptane drops.

All data except the density of vapour at drop surface are similar to those for pentane. Therefore, for heptane, using $\rho_s = 32.8 \times 10^{-4}$ gms/cc.

$$\rho_m = \tfrac{1}{4} (32.8 + 2 \times 0.72 + 13.53) \times 10^{-4} \text{ gms/cc}$$

$$= 12.33 \times 10^{-4} \text{ gms/cc.}$$

$$C_{dm} = \frac{13.5}{12.33} Cd = 1.11 \; C_d \quad \text{(note difference from pentane.)}$$

A.1.3 Calculation of $C''_{d,m}$

In section IV.2.5., the slope of the drag coefficient - Reynolds number curve was explained as a consequence of the greater ratio of evaporation rate to drop mass, and the drag coefficient was visualised as consisting of two componants, $C'_{d,m}$ representing the integral of forces on a surface enclosing the drop, and $C''_{d,m}$, representing the flow of momentum out of the surface due to vapour flow from the drop.

In this section, the calculation of $C''_{d,m}$ is described.

$$C''_{d,m} = -\left(\frac{dm}{dt}\right) v \frac{1}{\frac{1}{2} \rho_m A v^2}$$

In the absence of direct knowledge of dm/dt, the evaporation constant quoted by Penner,[61] $\lambda = 0.025$ cm^2/sec for heptane drops in oxygen atmospheres is used.

$$d^2 = d_o^2 - \lambda t$$

$$dd/dt = - \lambda/2d \qquad 5.2.1$$

$$dm/dt = \frac{d}{dt} \left(\rho_l \frac{4}{3} \pi r^3\right)$$

using 5.2.1,

$$dm/dt = - \pi/2 \quad \rho_l \lambda r$$

therefore,

$$C''_{d,m} = \frac{\rho_l}{\rho_g} \frac{\lambda}{rv} \qquad 5.2.2$$

In terms of experimental observations,

$$r = \tfrac{1}{2} K''' D_l \quad \text{cms., where } K''' = K'K''$$

$$v = K' v_p \quad \text{cms.}$$

therefore,

$$C''_{d,m} = 2 \frac{\rho_l}{\rho_g} \frac{\lambda}{K''' K' D_l v_p} \qquad 5.2.3.$$

Example:

Heptane in oxygen.

$\rho_l = 0.684$ gms/cc

$\rho_g = 12.13 \times 10^{-4}$ gms/cc

$K' = 2, \quad K''' = 0.0516.$

$D_l = 3, \quad v_p = 130.4$ cm/sec.

$$C''_{d,m} = \frac{0.684 \times 0.025 \times 10}{12.13 \times 10^{-4} \times 2 \times 0.516 \times 3 \times 130.4}$$

$$= .66$$

APPENDIX II.

STUDY OF SOURCES OF ERROR IN THE EXPERIMENTAL TECHNIQUE.

I) Errors due to short term change in the interflash period.

2) Errors from movement of the drop in the transverse direction.

3) Errors in drop size estimation.

4) Errors due to local air currents.

5) Wall correction.

1) Errors due to short term change in the interflash period.

Errors arising from a change in the interflash duration over a very small number of flashes, will be considered in this appendix when no time monitoring system (one which gives the exact time interval between any required pair of flashes in a series of flashes) is used. The flashing frequency, ~~time~~ is obtained from the indicator on the stroboflash unit. Therefore, any changes in the time intervals between consecutive flashes will not be noticed. All calculations will be made on the basis of the stroboflash setting and so the periods used in the calculations could be incorrect.

It is assumed that no polynomial curve fitting involving the minimising of the variance is used. A simple divided difference method can be used to obtain the velocities and accelerations, and one value of the drag coefficient can be obtained from 3 consecutive drop images. Assuming that the velocity rises linearly in the period between two successive light flashes, the vertical distance between two drop images on the plate indicates the mean velocity of the drop at the midpoint of the corresponding time interval. The distance-time data actually obey a curvilinear equation and instantaneous

velocities and accelerations should be used for accurate estimations of the drag coefficient. However, it is desired to locate only large sources of error in the calculation of drag coefficients and Reynolds numbers and simplified relations will be used to indicate the magnitude of errors involved.

Let the distance between two consecutive drop images be v_x and that between the next pair of images be v_{x+1}. Using the notation of Appendix I,

$$a = (v_{x+1} - v_x) K'N^2$$

where N = flashing frequency/sec.

As 3 drop images are considered for each acceleration figure, the mean velocity should be used for calculating the drag coefficient.

$$v = \frac{1}{2} (v_{x+1} + v_x) K'N$$

$$d = K'K''D$$

Therefore, ~~from equ 5.7~~, the drag coefficient, in terms of v_{x+1}, v_x, D_1 and N, is:

$$C_d = \frac{4\rho_l K'K''D_1 \left\{g - (v_{x+1} - v_x)K'N^2\right\}}{3\rho_g \left[\frac{1}{2}(v_{x+1} + v_x)K'N\right]^2}$$

If we substitute k' for $\frac{4}{3}\frac{\rho_l}{\rho_g}\frac{K'K''}{[\frac{1}{2}K']^2}$,

we have, $$C_d = k'D_l \frac{1}{g} \frac{\left[981 - K'(v_{x+1} - v_x) N^2\right]}{(v_{x+1} - v_x)^2 N^2} \quad .. 6.1$$

Let us now suppose that the flashing rate changed from N/sec for v_x to N' for v_{x+1}, and, v_{x+1} and v_x remain the vertical distances between consecutive pairs of drop images on the plate. The actual drag coefficient would then be:

$$C_d''' = k'D_l \frac{\left[981 - K'(N'v_{x+1} - Nv_x) \frac{N' + N}{2}\right]}{(Nv_x + N'v_{x+1})^2} \quad 6.2$$

If the drag coefficient is calculated according to eqn. 6.1. the error would be

$$100 \frac{C_d - C_d'''}{C_d}$$

It was known that the flashing rate, N, does not vary by more than 2% and an error of this order could be rejected. Therefore, error calculations will be carried out only for flashing rate variations of 2% and less. In this appendix, only errors in the experimental variables

which would cause errors in the calculated drag coefficients of 5% and more are studied. Hence, the denominator in equation 6.3 could be approximated to $(v_{x+1} + v_x)^2 N^2$, and the error in drag coefficient becomes:

$$100 \frac{C_d - C_d'''}{C_d} = 100K' \frac{\left[\frac{1}{2}(N'v_{x+1} - Nv_x)(N+N') - (v_{x+1} - v_x)N^2\right]}{981 - K'(v_{x+1} - v_x) N^2} \quad ..6.3$$

The errors in drag coefficient calculated for $100 (\frac{N - N'}{N}) = \frac{1}{2}$, 1 and 2% and for values of $(v_{x+1} - v_x)$ in the range 0.1 to 0.36 cms. are presented in table III. It is assumed that v_x is 3 cms., K' = 3 and N = 30 flashes/sec.

TABLE III - TABLE OF ERRORS IN CALCULATED DRAG COEFFICIENT

$100 \frac{N' - N}{N'}$	½%	1%	2%
$v_{x+1} - v_x$			
0.1 cms.	7%	13%	25%
0.2 cms.		20%	45%
0.3 cms.		55%	
0.36 cms.		2300%	

An inspection of the table reveals that errors in drag coefficient increase with (i) increase in the short term errors in the flashing frequency, and (ii) increase in the acceleration rate.

For a difference between v_{x+1} and v_x of 1 mm, even a change in flashing rate of ½% causes an error in the calculated drag coefficient of 7%.

2) Movement of the drop in the transverse direction.

If the drop drifts in the direction of the camera axis, the distance from the drop plane to the lens plane changes and therefore, the magnification K' changes. This would cause an error in the drag coefficient calculation.

$f_\ell = 14"$ where f_ℓ = focal length of lens.

$m_1 = 57"$, distance from lens plane to drop plane

$n = 18.6"$ where n = distance from lens plane to plate.

$K' = 3.06$

If m_1 changes to 56", the new $K' = \frac{56}{18.6} = 3.01$.

Therefore, the error in Reynold's Number calculated on the basis K" = 3.01 would be

$$100\left(1 - \frac{Re'}{Re}\right) = 100\left\{1 - \frac{3.01^2}{3.06}\right\} = 3\%$$

The error in calculated acceleration would be proporionate to the error in K'. The error in calculated drag coefficient would also be of the same order as that in Reynold's Number.

This is the case if the drop travelled parallel to the plate plane and perpendicular to camera axis. But, if the drop travelled 1" towards the camera between successive pairs of flashes; the error would be very much greater. The magnification changes by 2% and therefore v_{x+1} also changes by 2%. Therefore, the error in v_{x+1} would be reflected in a magnified error in acceleration. It would result in an error in C_d of roughly the same magnitude as with a 2% error in flashing rate as $\alpha_x = K'N v_{px}$. But the drop generally travels vertically over 3" in the chamber between two flashes (30 RPS) and a transverse movement of 1" in 3" is very unlikely. At the most, the drop would travel $\frac{1}{2}$ - 1" over 3 ft. and thus the error would be reduced considerably. For 1" transverse movement in 3 ft., the drop would travel $\frac{1"}{12}$ in 3" and the magnification changes by, say, $\frac{1}{6}$%. This would hardly result in a big error in C_d calculations.

3) Error in drop size estimation.

This error could be caused by the drop being

(i) slightly out of focus and also, when using a travelling microscope for size determination, (ii) due to the inherent error of the microscope. The Pye travelling microscope is accurate to $\pm$ 0.02 mm. and is not capable of very crisp focusing. Thus, a drop measuring 0.4 mm. could be read with an error of 5% and must be measured with the panphot projection microscope. Errors in drop size measurement result in proportional errors in C_d as well as Re.

4) Local Air currents.

The velocity of the drop is usually of the order of 250 cms/sec. Thus a local air velocity of 25 cms/sec would cause an error in Re of 10% and as v^2 is the divisor in the C_d formula, it would cause in the drag coefficient an error of:

$$\frac{100\left\{ C_d - C_d/(1.1)^2 \right\}}{C_d} = 17.5\%$$

This is the error from the movement of the drop in a steady 25 cms/sec air stream. If the drop should be falling through a velocity gradient in the air stream, the error would be greater. But such velocities are considered to be unlikely.

5) Errors due to Natural Convection.

Natural convection due to combustion would tend to lift the drop up. Hence the drag coefficient obtained from burning drops, uncorrected for the convection velocity would be higher than the real drag coefficient.

6) Wall Correction.

It has been reported that v/v_t where v is drop velocity in a confined space and v_t is drop terminal velocity in free space approaches 1 for $d/D_c = 0.1$ where d/D_c is the ratio of drop/vessel diameter at Reynolds numbers above 10. Therefore, in the present ivestigation, the wall correction should not be significant.

Conclusions.

(1) It was found that the potential source of largest magnitudes of error were the short term changes in the frequency of flashing of the light source. This lead to the decision to develop a time monitoring system.

(2) In practice, even after developing a time monitoring system, it was found that errors in drop size determination gave rise to large errors in the calculated drag coefficients and Reynolds numbers. Due to the deterioration in the reproducibility of drop trajectory

with decrease in the size of the drop and the resulting deterioration in sharpness of focus, such errors are higher for small drop sizes.

APPENDIX III

TABLES OF RESULTS

Only plates which corresponded to uniform flashing rates are reported in this appendix. The existance of uniform flashing rates was verified either from detailed tape recorded data using the 'marker' flash and the batch counter, or, after failure of the batch counter, by random sampling of the interflash frequencies both immediately before an experiment and subsequently on play-back.

TABLE IV

Properties of fuels and gases.

Fuel	Density.	Boiling Point.
Pentane[64]	0.626 gms/cc	32°C
Heptane[64]	0.684 gms/cc	98.4°C
Benzene[64]	0.879 gms/cc	80°C.

Viscosity of benzene vapour[65] at 90°C = 75 x 10^{-6} poises.

Density of oxygen at 15°C = 1.35 x 10^{-3} gms/cc.

Kinematic viscosity of oxygen[60] at 15°C = 0.152 Stokes.

TABLE V

POSITION - TIME HISTORIES;

NONBURNING DROPS

Heptane

$K^1 = 2$
$K'' = 0.254$
$t = 0.0307$ secs.

Plate

	S (mm)	D_1
(1)	21.34	
	59.66	3.1
	100.66	
	143.84	
(2)	28.02	
	62.61	
	105.45	2.65
	146.46	
	184.93	
(3)	55.54	
	95.57	4.2
	138.92	

$K^1 = 3.1$
$K'' = 0.29$
$t = 0.0343$ secs.

	S mm	D_1
(4)	46.19	
	74.15	
	103.84	1.4
	135.00	
	167.44	

Benzene

(5)	44.93	
	74.04	1.7
	105.42	
	138.94	
(6)	38.34	
	66.42	1.7
	96.86	
	129.58	
(7)	6.38	
	53.50	
	98.50	2.7
	141.11	

TABLE VI

POSITION - TIME HISTORIES; HEPTANE, BENZENE; ENVELOPE FLAMES, HEPTANE, 100% OXYGEN ATMOSPHERE

$K' = 2$
$K'' = 0.254$
$t = 0.0307$ secs.

Plate	S (mm)	D_1
(8)	12.85	
	55.34	
	96.56	3
	136.07	
	173.75	
(9)	54.11	
	92.70	
	132.56	2.9
	174.26	
(10)	32.71	
	74.16	
	114.34	2.9
	152.79	
	189.41	
(11)	44.19	
	83.11	2.9
	123.47	
(12)	44.22	
	86.16	4
	131.02	
	177.54	
(13)	29.42	
	76.86	4
	121.40	
(14)	28.74	1.9
	62.10	
	96.09	1.7
	130.08	
	163.61	
	196.08	1.4

Plate	S (mm)	D_1
(15)	25.00	1.8
	56.01	
	87.56	
	119.34	1.6
	150.53	
	180.89	1.3
(16)	16.39	1.8
	48.94	
	82.13	
	115.50	
	149.18	
	182.20	1.5
(17)	82.25	
	53.97	1.8
	86.26	
(18)	36.58	1.7
	69.00	
	102.35	
	135.90	
	169.20	1.3
(19)	42.75	2.5
	79.71	
	117.65	
	156.33	
	195.30	2.3

	S (mm)	D_1
(20)	18.26	
	53.95	2.5
	90.59	
(21)	36.25	
	72.55	
	110.02	
	148.23	
	187.08	2.3
(22)	15.53	2.5
	90.22	
	129.44	
	169.70	2.4
(23)	81.44	2.3
	114.50	
	146.45	
	177.36	2.1
(24)	61.69	2.4
	102.91	
	142.99	
	182.05	2.2
(25)	24.51	2.8
	67.28	
	109.00	
	149.19	
	187.84	
(26)	17.63	
	65.08	4.2
	110.56	
	153.70	
	194.15	
(27)	8.39	
	56.34	
	102.33	4.2
	146.13	
	187.39	

$K' = 3.1$
$K'' = 0.29$
$t = 0.0344$ secs.

	S	D_1
(28)	46.19	
	74.15	1.35
	103.84	
	135.00	
	167.44	

Benzene, 100% oxygen atmosphere

$K^1 = 2$
$K'' = 0.254$
$t = 0.0307$ secs.

	S	D_1
(29)	43.27	
	85.59	2.55
	126.73	
	166.33	
(30)	68.16	
	109.58	
	149.47	2.5
	187.60	
(31)	46.09	
	86.11	2.6
	127.56	
	170.28	

$K^1 = 3.1$
$K'' = 0.29$
$t = 0.0344$

(32)	108.78	
	142.12	1.7
	176.26	
(33)	96.05	
	129.62	1.8
	164.25	
(34)	102.45	
	135.94	1.7
	170.46	
(35)	96.42	
	130.32	1.65
	165.30	
(36)	65.85	
	107.16	2.4
	149.24	
(36)	64.36	
	102.99	
	142.44	2.2
	182.43	

TABLE VII

POSITION - TIME HISTORIES; PENTANE, ENVELOPE FLAMES

$K' = 3.1$
$K'' = 0.292$
$t = 0.0343$ secs
Atmosphere 75% oxygen, 25% nitrogen

	S	D_1
(37)	34.91	
	57.11	
	80.46	1.5
	104.51	
	129.23	
	154.39	
(38)	35.26	
	58.46	
	83.02	1.8
	108.42	
	134.91	
	162.33	
(39)	37.57	
	58.71	1.3
	80.68	
	103.25	

Atmosphere 65% oxygen, 35% nitrogen

(40)	42.20	
	64.11	
	87.10	1.5
	110.79	
	134.85	
	159.28	
(41)	49.32	
	71.90	1.4
	95.42	
	119.56	

Atmosphere: oxygen

	S	D_1
(42)	46.06	
	73.97	
	103.15	1.45
	133.24	
(43)	45.04	
	71.49	
	99.08	1.2
	127.38	
	155.81	

$t = 0.0277$ secs.

(44)	40.45	0.85
	60.16	
	79.68	0.70
	98.63	
	116.84	0.55
	133.76	
	149.26	
	162.95	0.40

$K'' = 1$

(45)	44.74	0.38
	67.44	
	91.26	
	115.42	0.36
	140.17	
	165.16	0.35
(46)	42.21	0.27
	62.22	
	82.84	
	103.81	0.24
	124.96	
	146.08	0.24

	S	D_1
(47)	30.99	0.26
	51.79	
	73.07	
	94.71	0.24
	116.65	
	138.63	0.23
(48)	47.01	
	69.04	0.37
	91.78	
(49)	32.09	
	53.83	0.4
	76.44	
(50)	33.73	
	55.64	0.35
	78.27	
(51)	44.31	
	65.74	
	88.15	0.35
	111.17	
	134.48	
(52)	38.18	
	59.29	0.34
	80.89	

$K^1 = 3.1$
$K'' = 0.292$
$t = 0.0343$

(53)	67.81	
	97.35	
	128.14	1.6
	159.53	
	191.48	
(54)	104.95	
	139.15	1.6
	173.70	

TABLE VIII

POSITION - TIME HISTORIES; DROP WITH SIDE FLAMES

	S	D_1
Pentane, 100% oxygen atmosphere		
(55)	45.55	
	75.47	
	107.72	1.5
	142.01	
(56)	41.85	
	72.24	
	104.95	1.6
	139.15	
Pentane, atmospheric air		
(57)	34.41	
	63.33	
	94.59	1.5
	128.27	
	164.13	
Pentane 50% oxygen 50% nitrogen		
(58)	51.75	
	73.57	
	96.56	0.95
	120.44	
	144.83	
	169.70	
Heptane, 100% oxygen Atmosphere		
(59)	31.22	
	59.16	1.4
	89.43	
	121.70	
(61)	27.77	
	53.78	
	81.67	1.2
	111.24	
Benzene, 100% oxygen atmosphere		
(62)	21.23	
	60.27	2.2
	101.88	
(63)	45.24	
	85.92	2.4
	129.06	
Benzene, atmospheric air		
(64)	39.39	
	79.39	
	121.30	1.8
	164.87	
(65)	18.08	
	57.45	1.8
	98.87	
(66)	24.77	
	64.09	1.7
	105.45	
	148.56	

SYMBOLS*

a	acceleration of the drop	L/t^2
a_p	acceleration rate of the drop image on the plate	L/t^2
A	projected area of the drop	L^2
B	transfer number	-
b_i	coefficients of polynomial	-
c	specific heat of the medium, constant pressure	L^2/t^2T
C_d	drag coefficient	-
C_{do}	drag coefficient, steady state	-
C_{dm}	drag coefficient, mean properties basis	-
C'_d, C''_d	components of the drag coefficient (C'_d : modified drag coefficient)	-
$C_{d,loc}$	drag coefficient, local	-
C_d^*	drag coefficient for rapid mass transfer	-
C'''_d	corrected drag coefficient	-
D	diffusion coefficient	L^2/t
D_l	drop image size on panphot projection screen	L
D_c	diameter of vessel	L
$\vec{F}$	body force vector	ML/t^2
F_l	drag force	ML/t^2
g	acceleration due to gravity	L/t^2
h	heat transfer coefficient	M/t^3T
h_m	mass transfer coefficient	M/tL^2
h'	enthalpy per unit mass	L^2/t^2

* Dimensions are given in terms of Mass (M), Length (L), time (t), and temperature (T)

H	Heat of combustion	L^2/t^2
i	rate factor	-
K'	magnification: field/plate	-
K"	magnification: plate/screen	-
K"'	magnification: field/screen	-
K_b	mass flux, dimensionless	-
k	conductivity of medium	ML/t^3T
k'	a constant	-
L	latent heat of evaporation	L^2/t^2
m	mass of drop	M
m'	mass concentration (suffixes s, g, and O_2 g refer to drop surface, the medium and the concentration of oxygen in the medium respectively.)	M/L^3
M_A	Molecular weight of component A	M/mole
N_A	molal flux of component A across the interphase	moles/L^2t
N	flashing frequency, average .	-
N'	flashing frequency, short term	-
Nu_H	Nusselt number	-
Nu_m	Nusselt number for mass transfer	-
P	Pressure	M/Lt^2
Pr	Prandtl number	-
p_{O_2}	partial pressure of oxygen in the medium	M/Lt^2
r	drop radius	L

r_s	drop radius (eqns. 2-3.2-4)	L
r_f	flame radius (eqns. 2.3.2 -4)	L
r'	stoichiometric ratio	-
R	radial distance from drop centre	L
R_j	universal gas constant	L^2/t^2T
Re	Reynolds number	-
s	distance of drop image from an arbitrary datum on the plate	L
t	time	t
T	temperature (suffixes g, f and s refer to ambiant gas, the flame and drop surface respectively)	T
v	velocity	L/T
v	relative velocity between drop surface and the medium at infinite distance to it	L/T
v_{yo}	normal velocity of vapour at drop surface	L/T
v_t	terminal velocity	L/T
v_p	velocity of drop image in the plate	L/T
x	position coordinate, x direction	L
θ	Correction factor for high intensity mass transfer case. (suffixes v, T and AB indicate corrections for momentum, heat and mass transfer coefficients).	-
ρ	density (suffixes l, g, O_2, i and o refer to the liquid, the medium, oxygen, inner and outer phases respectively.	M/L^3

λ	evaporation constant	L^2/t
Λ	diffusivity ratio	-
τ	surface tension	-
μ	viscosity	M/Lt
ν	kinematic viscosity	L^2/t

REFERENCES

(1) Priem, R.J. and Heidman, M.F. "Propellant vaporisation as a criterion for rocket engine combustion chambers". NASA T.R. R - 67, 1960.

(2) Spalding, D.B. "Mass transfer in laminar flow". Proc.Roy.Soc., A. vol 221, 1954,79.

(3) Spalding, D.B. Proceedings of the General Discussion on Heat Transfer. The Inst. of Mech.Engrs. The American Society of Mech.Engrs. 1951, 345.

(4) Khudyakov, G.N. Bull.Akad.Nank. VRSS (Tech.Sci. section) April, 508, 1949.

(5) Lubanski, R. D.I.C. thesis. City and Guilds 1946.

(6) Ingebo, R.D. "Heat transfer rates and drag coefficients for ethanol drops in a rocket motor". 8th Symposium on Combustion, 1961.

(7) Langmuir, and Blodgett, S.R., Tech.rept.5418, 1946, Air Matl. command, Wright patterson Airforce Base.

(8) Goldstein, S. "Steady flow of viscous fluid past a fixed spherical obstacle." Proc.Roy.Soc.A., 123, 1929, 225.

(9) Proudman, I., and Pearson, J.R.A., Journal of Fluid Mechanics. 2, 1957, 237.

(10) Kawaguti, M., Jl. Physical Society of Japan 10, 1955, 694.

(11) Macdonald, I.S., "Thesis digest, University of Birmingham, Department of Chemical Engineering, 1958.

(12) Torobin, L.B., and Gauvin, W.J., "The sphere wake in steady laminar fluids". Canadian Jl. of Chemical Engineering. 37, 1959, 167.

(13) "Injection and combustion of liquid fuels". W.A.D.C. T.R. 56-344. March, 1957. ASTIA Document AD 118142.

(14) Garner, F.H., and Grafton, R.W. "Mass transfer in fluid flow from a solid sphere". Proc.Roy.Soc.A., 224, 1954.

(15) Taneda, S., Rep.Res.Inst.Appl.Mech.Japan 1956, 99.

(16) Lewis, B. and Von Elbe, G., "Stability and structure of burner flames, Jl. Chem.Physics, vol.II 1943,75.

(17) Williams, G.C., Hottel, H.C. and Scurlock, A.C., "Flame stabilisation and propagation in high velocity gas streams, 3rd symposium on Combustion 1949.

(18) Torobin, L.B. and Ganvin, W.H. "Accelerated motion of a particle in a fluid" Canadian Jl. of Chemical Engineering, 37, 1959,224.

(19) Schmidt, F.S., Ann Physik. 1920,633.

(20) Lunnon, R.G., Proc.Roy.Soc.A. 118,1928,630.

(21) Keim, S.R. Proc.American.Soc.Civil Engineers 82. Hy 6 (Jl. hydr. division) paper 1113, 1956.

(22) Ingebro, R.D. "Drag coefficients for droplets and solids accelerating in airstreams". NACA.TN3762.

(23) Gilliland, E.R. and Hughes, R.R. Chem.Eng.Prog. 48, 1952, 497.

(24) Bassett. A.B. Quart. Jl. of Mathamatics. 41, 1910, 369

(25) See ref. 14.

(26) Fuks, N.A. "Evaporation and droplet growth in gaseous media". Pergamon Press, 1959.

(27) "Basic considerations in the combustion of hydrocarbon fuels with air". NACA Rep.1300.1957.

(28) Fuchs, N. "Mechanics of Aerosols". Acad.Nauk. SSSR,45.1955.

(29) Ranze, W.E., Marshal, W.R. Chem.Eng.Prog. 48,3,1952. 141-146 and 48,41952, 173-180.

(30) Lewis and Chang. Trans A.I.Ch.E. 21,1928, 127-136.

(31) Ackerman, G. Forshungshaft 382,1937, 1-16.

(32) Colburn, A.P. and Drew, T.B. Trans A.I.Ch.E. 33, 1937, 197-212.

(33) Mickley, H.S. and Ross, R.C. NACA TN 3208.

(34) Higby, R. Trans. A.I.Ch.E. 31, 1935, 365-389.

(35) Fröessling. N. Beitnage zur Geophysic. 52, 1938, 173-180

(36) Bird, R.B., Stewart, W.E. and Lightfoot, E.N. "Transport Phenomena". John Wiley & Sons, Inc.

(37) See ref. 2.

(38) Muggia, A. Aeroteknica, 36, 1956, 127-131. RAE Transl. 679.

(39) Spalding, D.B. Fuel, 29, 1950, 2-7.

(40) Graves, C.E. "Burning rate of single fuel drops and their application to gas turbine combustion problems". NACA. R.M. E53E22, 1953.

(41) Spalding, D.B. Fuel, 30, 1951, 121.

(42) Kohlman, D.L. "Experiments on cylinder drag, sphere drag and stability in rectilinear couette flow". Ph.D. thesis, M.I.T., March, 1963.

(43) Godsave, G.A.E. "Combustion of drops in a fuel spray". 4th international symposium on combustion, 1953, 818.

(44) Spalding, D.B. "The combustion of liquid fuels". 4th international symposium on combustion. 1953, 847.

(45) Kumagai, S. and Kimura, I. 3, 1951, 431.

(46) Kumagai, S. and Isoda, H. 4, 1952, 337.

(47) Bolt, J.A. and Saad, M.A. 6th International symposium on combustion. 1958.

(48) See ref. 27.

(49) Saad, M.A. Ph.D. Thesis. University of Michigan, 1956.

(50) Spalding, D.B. "Some fundamentals of combustion". Butterworths Scientific Publications, London, 1955.

(51) See ref. 2.

(52) Torobin, L.B., and Gauvin, W.H. Canadian of Chemical Engineering, 37, 1959, 129.

(53) Abberton, J. Unpublished document. 1961. Chemical Defense Research Establishment. Porton.

(54) Lane, W.R. "A microburette apparatus for the production of small drops". J. Sci. Instruments. 1953, 98.

(55) Harkins, K. and Brown, T.A., J. of the American Chem. Soc., 41, 1919, 599.

(56) Jakob, M. "Heat Transfer". 1. John Wiley & Sons, New York (1949).

(57) Deisler, R.G., N.A.C.A. TN2242. December 1950.

(58) Douglass, W.J.M. and Churchill, S.W., Chem. Eng. Prog. series - Heat transfer, 52, 1956, 23.

(59) Rashbash, K. and Stark, I. "On the evaporation of water drops in a bunsen flame". D.S.I.R. Fire officers committee, F.R. Note 26/1951. Aug. 1952.

(60) ~~Rossin~~ Spiers, Technical Data on Fuel. 5th Edition, 1952.

(61) Penner, S.S., Chemical reactions in flow systems. Pergamon Press.

(62) Singer, J. Elements of Numerical Analysis. Academic Press. 1964.

(63) CHLF3 Autocode library. 2nd edition. August 1963. University of London.

(64) Handbook of Chemistry and physics. 31st edition. 1948.

(65) Craven, P.M. and Lambert, J.D., Proc. Roy. Soc. A.205, 1951, 439.

(66) National Bureau of Standards circular 564, 1955.